THE FARADAY'S LAW MACHINES LABORATORY

By Claude M. Summers

RENSSELAER POLYTECHNIC INSTITUTE

E E 481 .S4.25 K1

THE FARADAY'S LAW MACHINES LABORATORY

By

Claude M. Summers
Consulting Professor of Electric Power Engineering
Rensselaer Polytechnic Institute

With An Introduction By

Eric T. B. Gross
Philip Sporn Professor of Engineering
Chairman, Electric Power Engineering
Rensselaer Polytechnic Institute

1972

The Rensselaer Bookstore - Troy, N. Y. 12181

The Rensselaer Bookstore - Troy, N. Y. 12181

First Printing 1971

Second Printing 1974

Copyrighted © 1974 by Claude M. Summers

Not to be reproduced in any manner whatsoever
without written permission of the author.

Library of Congress Catalog Card Number: 74-83455

PRINTED IN THE UNITED STATES OF AMERICA

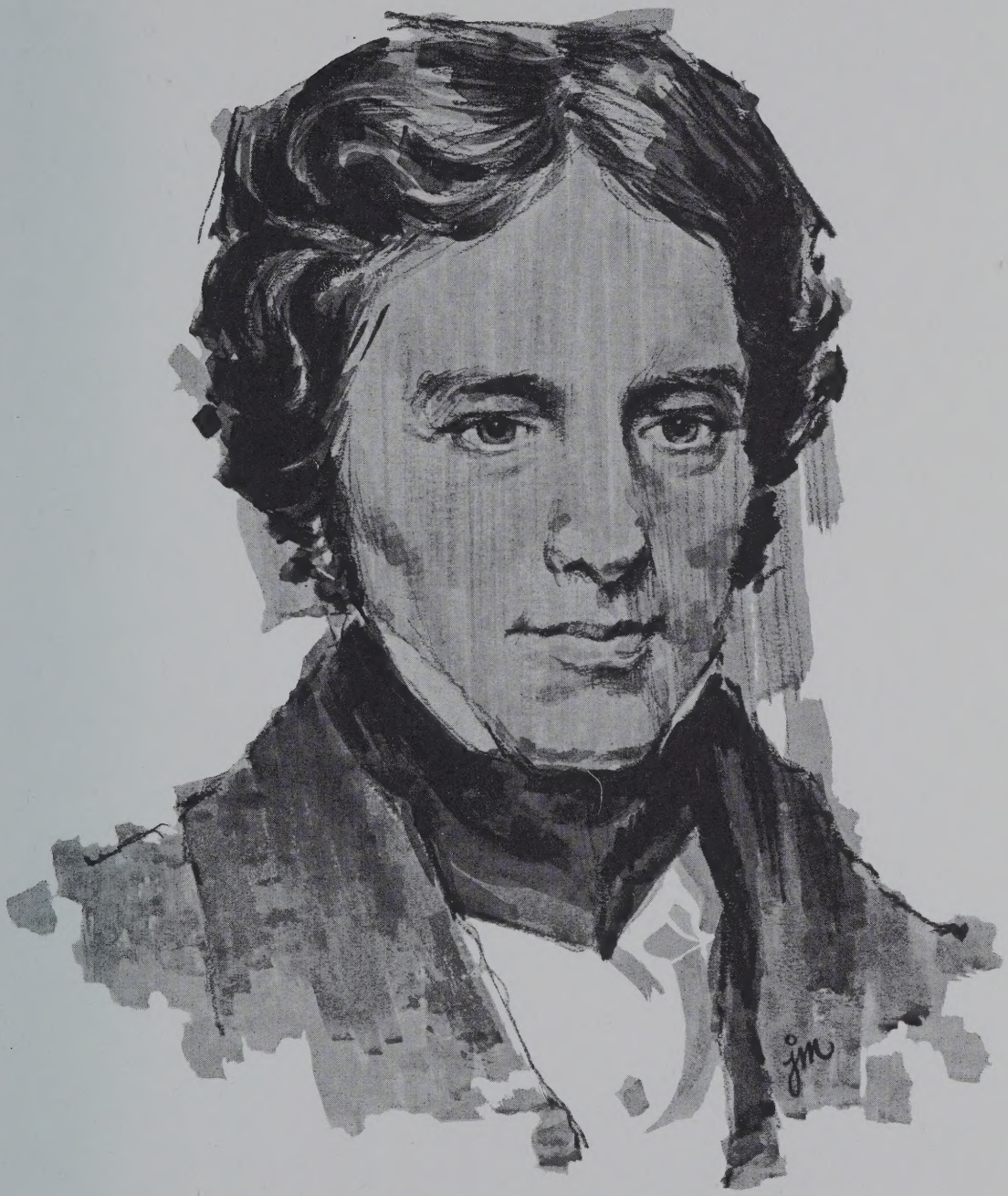

Michael Faraday
1791-1867

THE FARADAY'S LAW MACHINES LABORATORY

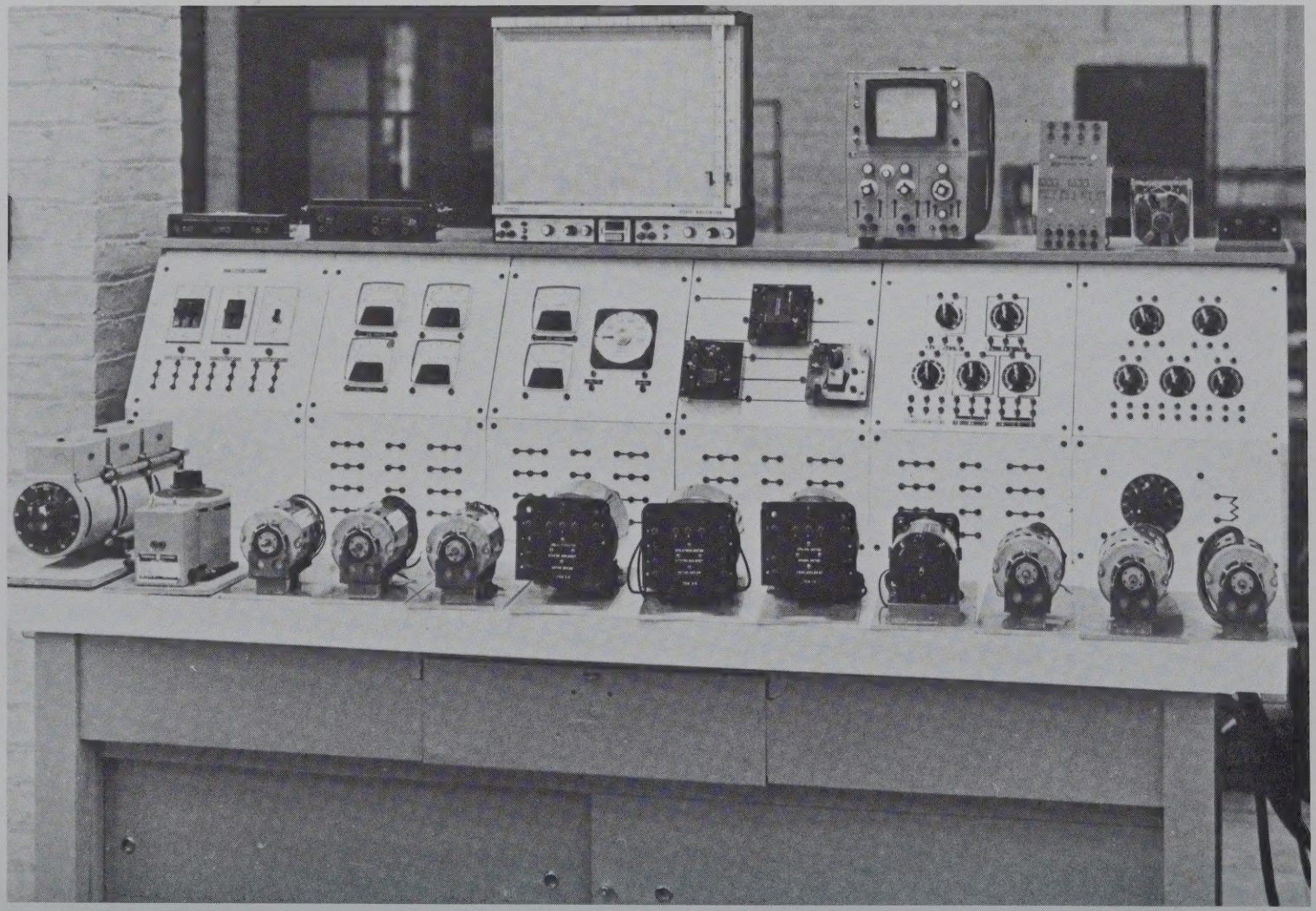

Laboratory Bench with its complete array of Motors, Generators, Transformers and Instruments

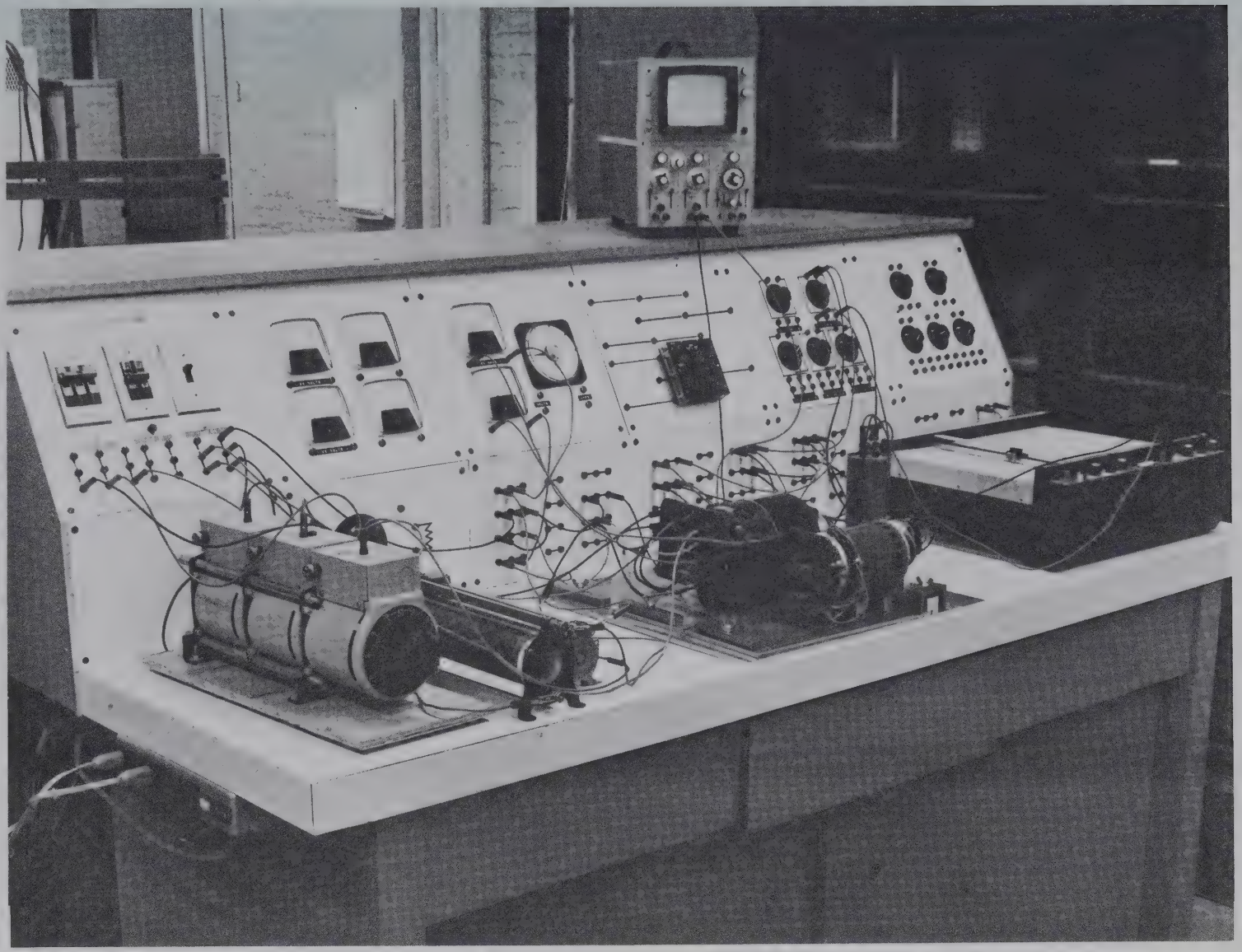

Laboratory set up for observing the Transient Behavior of a Synchronous Machine

INTRODUCTION

In the early days and even until the beginning of the forty's, when electrical machinery laboratories at our colleges were newly built or modernized, it was thought that laboratory machines should duplicate the electrical characteristics of machines as they are used in industry, where the machines were usually very much larger in size than suited for a university laboratory. A very few instructors joined me in feeling, even then, that much smaller machines, rated perhaps a few hundred watts, could do equally well what really was the purpose of any college laboratory, that is, to acquaint the students with the way basic phenomena are applied in equipment for use in commercial applications. However, any such "revolutionary" suggestions were considered taboo, and set aside.

In the middle forties, when new areas of electrical engineering subjects required attention, machinery laboratories were recognized as occupying more than their proper share of floor space. An ill-conceived, but quite logical suggestion proposed the elimination of these machinery laboratories altogether. However, it is difficult to understand how anyone acquainted with the electrical technology of our times would ever make such a suggestion! As an alternate suggestion, it was proposed to replace the old machinery laboratories by a few "generalized" machines, which like toys had their elements so designed that by a predetermined connection any type of electrical machine could be represented. A number of such generalized machines were developed, and highly analytical supplementary texts written. Neither proved suitable for the required level of undergraduate education, for which these earlier machine laboratories had served well. One type of "generalized" machine was made freely available in this country by its manufacturer, supposedly in support of electric power engineering education. In most colleges, these machines were quickly found unusable in the way they were intended; one can still see them today in some laboratories sitting in a corner and collecting dust.

It has been our thinking for many years that the reduction of college laboratory machine size is desirable in order to give every student better access to his machine. Such machines may have their own "standard" characteristics, not being analogs to much larger standard machines, but this is not at all a significant factor. With smaller units, more machines can be made available, and it would be possible to have not more than two, possibly only one student experiment with this equipment. The total cost of many small machines can certainly be made much lower than the total cost of a few large ones. The time has now finally become ripe for this development which expresses the thinking of the Rensselaer School of Electric Power Engineering, which in turn is greatly influenced by the thinking of a faculty composed entirely of professors backed up by many years of permanent full-time work in engineering with industry.

Immediately after Claude M. Summers terminated his distinguished career as an engineer in industry, and his position of being in charge of the

laboratory operation at the General Electric Fort Wayne works, he accepted an appointment as Professor of Electrical Engineering at the Oklahoma State University. Soon thereafter he decided to develop a flexible machinery laboratory using small fractional horsepower motors of standard design. He presented the success of his endeavors in 1962 at the Denver Summer Meeting of the AIEE, in a well received conference paper (CP62-1308) entitled "The Unitized Machines Laboratory".

An equipment grant to Rensselaer by the General Electric Company for the strengthening of the electric power engineering program gave us the machines to build this new laboratory called "Faraday Machinery Laboratory". The purpose of the laboratory is to emphasize the approach based on the application of fundamental laws in contrast with sets of analytical expressions, very helpful in advanced studies, but not so well suited to the average undergraduate student. A subsequent very substantial grant in support of the same activity by the ESSO Education Foundation gave us the basis to start the full scale development of a new machinery laboratory which would use many of the mature ideas accumulated in our minds over the last twenty years.

It was fortunate that Professor Summers' services became available at the proper time. He has been with us as Professor and Consultant since the beginning of the Spring semester 1969, spending two full Spring semesters (1969 and 1970) in residence at Rensselaer and acting in a consulting capacity in between and until the present time. We are very grateful to Claude Summers for his participation in this work and proud of its success.

This new laboratory became ready for operation in February 1971, at the beginning of the Spring semester. The first group of students started work and studies in the laboratory at that time, showing much enthusiasm for the new way of experimenting, and even volunteering additional time for extended investigations. Experiences during this pilot operation are incorporated in this volume, a revised edition of the earlier draft made available to the students as supplementary text. The students are usually seniors who have completed the standard course on electrical machines during the semester which precedes their taking this laboratory course.

We plan to make available all design details and equipment specifications to anyone desiring them, in the conviction that many would want to essentially duplicate what has been accomplished here at Rensselaer. Such activity will also help American industry enormously by bringing back to the college senior emphasis on the important role which electric power engineering plays in American technology. It is unthinkable that anyone graduating from a four year college course emphasizing electrical engineering would not have the basic knowledge and understanding of the rudiments of electrical machines in the broadest sense. Since it has become known, through announcement of these grants, that we are engaging in developing this laboratory, we have received many inquiries. The information to be supplied to others who wish to develop a similar laboratory will provide helpful answers to most of their questions.

I can not close these remarks without thanking the ESSO Education Foundation and the General Electric Company for the encouragement given us to pursue this project and for their generous grants without which this Faraday Laboratory would not have become a reality.

December 1971 Eric T. B. Gross

THE FARADAY'S LAW MACHINES LABORATORY

Preface

This text was developed as background material for a new electrical machines laboratory for seniors in Electrical Engineering. The laboratory was developed to teach the physical comprehension of the internal behavior of rotating machines and transformers. This text is necessary because the background required here is not found in present day American texts.

Most electrical engineering curricula are oriented toward "circuits" and "systems" with the associated mathematics not well suited to convey a thorough physical understanding of machines. The L di/dt approach does not consider such important design factors as flux density, area, permeability, or turns, whereas the N $d\phi/dt$ approach is directly related to these significant physical factors. The new American texts deal with more abstract mathematical generalizations which tend to obscure the fundamental physical concepts of machine behavior. The foundation for the laboratory and for this text, therefore, is Faraday's Law, Lenz's Law, and the Theorem of Constant Flux Linkages.

The text and laboratory are intimately related; hence a discussion of the laboratory is appropriate. Small machines ranging from 1/12 to 1/4 hp and transformers rated 1/2 kva are used. The machines are conventional except for added information windings placed internally at strategic locations during manufacture. These windings supply data regarding the internal behavior. No attempt is made to obtain a scaled-down model of a larger machine. For our purpose, the underlying fundamentals such as the rotating magnetic field; armature reaction; transient build-up of speed or flux; neutralizing MMF's due to load currents in the primary and secondary windings of transformer; or the nature of leakage flux, are essentially the same regardless of the size of the machine. Great flexibility is achieved with small machines because of the ease in handling and the rapidity with which a set-up may be made or modified. Thus, a large number of observations or measurements may be made quickly on a variety of machines and the student therefore, spends a minimum of time in non-productive activity.

Conventional indicating meters may be used, but a different philosophy of measurements called "Shape Measurements" is stressed throughout. These measurements may be defined as the fast qualitative recording or display of one quantity with respect to another. Typical examples are the display of the hysteresis loop, the cycling flux-time relations in a machine, the flux-time build-up of a field, the speed-time build-up in a motor, or the speed-torque curve. In all cases, emphasis is placed on the physical reasons for the observed shape. Shape measurements are enhanced by the use of analog computing elements during the measuring process. With these facilities it is possible to observe the instantaneous reluctance torque (expressed by the equation $T = \phi^2 dR/d\theta$) in a reluctance synchronous motor during one revolution of the rotor.

Only simple equations are used in the text, and no attempt is made to equate machine behavior to a mathematical expression. Rigorous mathematical treatment is avoided in favor of physical understanding of the basic laws, and the application of these laws to realistic conditions. Transients are treated by applying an increment of a parameter and determining the initial rate of change from the application of known laws. The increment is traced through the machine for the effect of the next applied increment of the original parameter. In this way the exponential shape is developed without the use of exponential equations, and it is expected that the student will achieve a better understanding of the causes for the developed shape of the transient.

Chapter 1 deals with a changing flux linking a coil of wire - a subject that may be found in any elementary college physics text. However, heavy emphasis is placed on Faraday's Law and its importance to many fundamentals of electric machines, and the invariable integral-differential relation between flux and induced voltage. Experiments are available in the laboratory to give the student a "feel" for the fundamentals discussed.

Chapter 2 covers in detail the flux, current, and induced voltage in a transformer. The high-reactance transformer with its exaggerated internal characteristics is discussed. This type of transformer is an excellent educational device.

Chapter 3 deals with a transformer with rotating secondary and shows how it can become a motor, thus uniting the fundamentals of transformers and rotating machines.

Chapter 4 covers the rotating magnetic field and the torque it exerts on the bars of a squirrel cage rotor. The general shapes of the transient build-up of speed at no load and with load are developed.

In Chapter 5, the major emphasis is placed on the phenomena of armature reaction and degree of excitation in synchronous machines.

The dynamic behavior of d-c machines is discussed in the final chapter.

It should be recognized that this is not intended as a classroon text. It covers only a small portion of the overall machine theory. It does include, however, the major fundamentals which are compatible with experimentation. The student should associate the text material with what he can do experimentally in the laboratory. If the student can develop a sufficient curiosity to say "I wonder what will happen if..." and proceeds with an experiment to find the answer, this text and laboratory will have been successful.

The author wishes to express his appreciation to the electric power engineering faculty at Rensselaer Polytechnic Institute for suggestions and assistance in developing the laboratory and in preparing the text, in particular to P. L. Alger, H. Frankel, M. H. Hesse and L. P. Winsor. William

Mischler and Charles Wilson, graduate students in the department, were helpful in developing experiments and equipment. But above all, the author expresses his most sincere appreciation to Eric T. B. Gross for his overall direction and continued stimulation for the development of the new laboratory and text.

This work was made possible by grants from the ESSO Education Foundation and from the General Electric Company.

December 1971
Troy, N.Y.

Claude M. Summers

C O N T E N T S

Chapter 1. POWER ENGINEERING FUNDAMENTALS

Nomenclature for Chapter 1. . . . . N 1.1
1.1 Faraday's Law, Lenz's Law and the Constant Flux Linkage Theorem . 1.1
1.2 Application of Laws to Coil Linked with Permanent Magnet Flux . . 1.2
1.3 Application of Laws in a Coil Linked with Electromagnetic Flux. . 1.4
1.4 The Magnetic Circuit and Magnetic Units 1.6
1.5 Energy in the Magnetic Field. 1.7
1.6 Faraday's Law and Inductance. 1.9
1.7 Faraday's Law and Mutual Inductance 1.11
1.8 Magnetic Forces 1.12
1.9 Experiments 1.14
Figures for Chapter 1 . . . . . F 1.1

Chapter 2. TRANSFORMERS

Nomenclature for Chapter 2. . . . . N 2.1
2.1 Leakage Flux, Magnetizing Flux and Total Flux 2.1
2.2 Magnetizing Reactance and Leakage Reactance 2.2
2.3 The Transformer Equation. 2.3
2.4 The Saturation Curve and the Graphical Determination of the Magnetizing Current Wave 2.5
2.5 The Hysteresis Loop and the Graphical Determination of Total Excitation Current 2.6
2.6 The Transformer Equivalent Circuit. 2.6
2.7 The Transformer Phasor Diagram. 2.8
2.8 The No-Load Block Diagram 2.9
2.9 Flux Reactions Under Load and the Load Block Diagram. 2.10
2.10 The High Reactance Transformer. 2.11
2.11 Transformers for Experimental Work. 2.13
2.12 Induced Voltage, Flux and the Integrating Circuit 2.13
2.13 Predicting the Behavior of Ferroresonant Systems. 2.15
2.14 Experiments 2.21
Figures for Chapter 2 . . . . . F 2.1

Chapter 3. THE TRANSFORMER WITH A ROTATING SECONDARY AND THE RELUCTANCE MOTOR

Nomenclature for Chapter 3. . . . . N 3.1
3.1 Description of Equipment for Experimental Work. 3.1
3.2 Output Voltage as a Function of Rotor Position - The Induction Regulator. 3.1
3.3 Magnetizing Flux and Excitation Current 3.2
3.4 Torque as a Function of the Rotor Position. 3.2
3.5 Analysis of Instantaneous and Average Torque at Synchronous Speed. 3.3
3.6 Starting and Synchronizing the Reluctance Synchronous Motor . . . 3.5
3.7 Experimental Studies. 3.6
Figures for Chapter 3 . . . . . F 3.1

Chapter 4. SINGLE PHASE INDUCTION MOTORS

	Nomenclature for Chapter 4.	N 4.1
4.1	The Rotating Magnetic Field	4.1
4.2	Balanced Two Phase Rotating Field	4.1
4.3	Unbalanced Two Phase Rotating Field	4.2
4.4	Split Phase Rotating Field With Two Equal Fluxes.	4.2
4.5	Split Phase Rotating Field With Unequal Fluxes.	4.3
4.6	Sinusoidal Distribution of a Rotating Magnetic Field.	4.3
4.7	Torque Exerted on Two Diametrically Opposite Stationary Rotor Bars	4.4
4.8	Multiple Stationary Rotor Bars Having No Inductance	4.5
4.9	Squirrel Cage Rotor Free to Rotate.	4.5
4.10	Rotor Reactance	4.6
4.11	Inertia Torque.	4.8
4.12	Speed Build-Up at No Load	4.8
4.13	Speed Build-Up with Load.	4.10
4.14	Measurement of Torque by the Inertia Method - Experiment 4.1. .	4.10
	Figures for Chapter 4	F 4.1

Chapter 5. SYNCHRONOUS MACHINES

	Nomenclature for Chapter 5.	N 5.1
5.1	The Generation of Three-Phase Voltage	5.1
5.2	Armature Reaction: Generator with Unity Power Factor	5.2
5.3	Armature Reaction: Generator with 90° Lagging Power Factor . .	5.3
5.4	Armature Reaction: Generator with 90° Leading Power Factor . .	5.3
5.5	Voltage Regulation and Phasor Diagram	5.4
5.6	Synchronous Motor with No-Load and with Normal, Under and Over Excitation.	5.6
5.7	Behavior of Synchronous Motor with Load - Instability	5.7
5.8	Synchronous Motor with Load and with Normal, Under and Over Excitation.	5.8
5.9	Transient Behavior of Synchronous Machines.	5.8
5.10	Transient Power in a Synchronous Motor.	5.10
5.11	Effect of Rotor Excitation.	5.10
5.12	Experiments	5.10
	Figures for Chapter 5	F 5.1

Chapter 6. DC MACHINES

	Nomenclature for Chapter 6.	N 6.1
6.1	The Field Circuit and the Transient Build-Up of Flux.	6.1
6.2	Transient Induced Voltages in Field	6.5
6.3	The Armature Circuit and the Transient Build-Up of Voltage at No-Load in a Generator.	6.6
6.4	Transient Build-Up of Speed in Motor at No-Load	6.7
6.5	Steady State Load on DC Motor	6.9
6.6	Sudden Application of Constant Load	6.11
	Figures for Chapter 6	F 6.1

NOMENCLATURE FOR CHAPTER ONE

ϕ - General symbol representing flux

$\Delta\phi$ - Increment of flux

ϕ_o - Initial flux

ϕ_1 - Final steady state flux

ϕ_{12} - Initial flux in coil No. 1 linking with coil No. 2

ϕ^1 - Leakage flux

ψ_1 - Initial flux change

ψ_2 - Induced flux

ψ_r - Net flux change

ψ_{12} - Initial change of flux linking coil No. 2

ψ_{21} - Induced flux in coil No. 2 linking with coil No. 1

E_o - Initial applied voltage

E_1 - Final steady state voltage

E_c - Initial change in input voltage

e - General symbol representing induced voltage

e_1 - Induced voltage in a single coil system by ψ_r also
Induced voltage in coil 1 of a two coil system by ψ_{21}

e_2 - Induced voltage in a single coil system by ψ_2 also
Induced voltage in coil 2 of a two coil system by ψ_{12}

e_r - Net change in voltage

continued

I_o - Initial current in coil No. 1

I_1 - Final steady state current

i_1 - Initial current change in coil No. 1

i_2 - Induced current

i_r - Net change in current

W_e - Electrical energy

W_f - Energy in the magnetic field

W_L - Energy dissipated in heat

R - Circuit resistance

t - Time in seconds

Δt - Increment of time

N - Number of turns

G - Length of magnetic flux path

A - Cross sectional area of flux path

μ - Permeability of magnetic flux path

μ_o - Permeability of free space

μ_r - Relative permeability of a magnetic material

H - Magnetic field intensity

$\mathfrak{R}$ - Reluctance of magnetic flux path

CHAPTER 1

POWER ENGINEERING FUNDAMENTALS

1.1 Faraday's Law, Lenz's Law and the Constant Flux Linkage Theorem

Power engineering is based on the voltages, forces and stored energies of magnetic fields, that are governed by laws first announced by Faraday and Lenz. The equation:

$$e = - N \, d\phi/dt \quad \text{volts} \qquad 1.1$$

due to Faraday, states that any change, $d\phi$, in the magnetic flux linking an electric circuit induces a voltage, e, that is proportional to the number of turns, N, that link the flux, and to the rate of change of flux, $d\phi/dt$. Flux ϕ, is usually measured in webers, e in volts, and t in seconds; the units being so chosen that Eq. 1.1 is numerically true when these units are used.

Lenz's law states that the current produced by a flux-induced voltage in a closed electric circuit is always in a direction to create a flux opposite to the initial change. That is, the current created by the induced voltage produces a flux change, ψ_2, that attempts to cancel the flux change, ψ_1, that caused the voltage. This explains the - sign in Eq. 1.1, which is in accord with the conservation of energy principle.

These two laws lead to the Constant Flux Linkage Theorem, which states that, if a closed electric circuit has zero resistance, the magnetic flux linking it cannot change. If the resistance, R, is zero, the current due to a voltage e, equal to -e/R, will be so large that the opposing flux change it creates, $-\psi_2$, will be just equal to the initial change, ψ_1, so reducing the net flux change, and voltage, to zero. Of course, the resistance can never be zero (except at temperatures close to absolute zero, where some metals become superconducting), so in practice the theorem is only an approximation.

For example, if a field coil carrying a current I_o amperes is suddenly short-circuited, the energy required to sustain the current must come from the stored energy of the magnetic field, instead of from the external power supply. Therefore, the flux begins at once to decrease, at such a rate that the induced voltage is always equal to the IR drop. Both flux and current decay asymptotically, and reach zero when all the magnetic energy has been dissipated in I^2R loss.

The theorem is very useful in making short-circuit calculations, because the flux linking the circuit is the same the instant after short-circuit as it was before, and the initial current must be enough to produce the initial flux. This principle enables the current to be calculated at the instant after short-circuit.

These three concepts are considered basic fundamentals in Power Engineering, and the most important of the three is Faraday's Law. It should be thoroughly understood; therefore we will investigate a few applications.

1.2 Application of Laws to Coil Linked with Permanent Magnet Flux

Consider first a permanent magnet in the vicinity of a coil in air connected to a resistor as in Fig. 1.1. Let the North Pole of the magnet P be a distance x away from the center of the coil with a flux ϕ_o linking the coil. Some flux lines link with only a part of the turns, therefore the flux ϕ_o is considered as an equivalent flux linking with all of the turns. Let us now move the magnet closer to the coil by a distance Δx in the time Δt. There will be an increase in flux ψ_1, thus the total flux linking the coil from the permanent magnet is now $\phi_o + \psi_1$. According to Lenz's Law, a current is induced in the coil, creating an opposing flux ψ_2 that will tend to keep the net flux linking the coil at a constant value. If the resistance is zero, then the net flux change

$$\psi_r = \psi_1 + \psi_2 = 0$$

and

$$\psi_1 = -\psi_2 \qquad 1.2$$

The action of ψ_1 and the reaction of ψ_2 are rigidly related. Any change in flux linking the coil instantly induces a voltage according to Faraday's Law. This causes a current to flow in the direction shown in Fig. 1.1 which, in turn, produces the counteracting flux ψ_2. Let the permanent magnet be moved the distance Δx in zero time, and held at the new position. The flux increase ψ_1 from the magnet linking the coil is instantaneous. The shapes of all of the flux-time relations are shown in Fig. 1.2(a), where ψ_1 is shown superposed on ϕ_o. When the circuit resistance is zero flux ψ_2 is equal and opposite to ψ_1 at every instant of time. The induced current-time curve, not shown under these conditions has the same shape as the ψ_2 curve. The resultant flux curve ϕ_1 is the sum of all the separate fluxes linking the coil. Thus,

$$\phi_1 = \phi_o + \psi_1 + \psi_2 = \phi_o \qquad 1.3$$

In reality the magnet can not be moved in zero time. The more realistic shape of the flux-time curves, for zero resistance, is shown in Fig. 1.2(b). The flux ψ_1 is shown gradually increasing over a finite period of time, but at every instant, the counteracting flux ψ_2 remains equal and opposite to ψ_1. Equations 1.2 and 1.3 therefore remain valid.

Now let us assume for the moment, that the magnet can be moved in zero time but let us introduce resistance into the circuit. The current produced by the induced voltage dissipates some energy as heat in the resistance. It can not therefore retain its initial value indefinitely and soon decays to zero. The counteracting flux produced by and proportional to the current likewise decays to zero as shown in Fig. 1.3. The resultant flux gradually builds up to the value $\phi_1 = \phi_o + \psi_1$ as ψ_2 decays to zero in Eq. 1.3. The shape of the flux-time curve is shown in Fig. 1.3. Even though the magnet was moved the distance Δx in zero time, the resultant flux linking the coil will change over a finite period depending on the decay time of ψ_2. This

gradual change in flux ψ_r linking the coil induces a voltage according to equation 1.4 below

$$e_1 = - N \frac{d\psi_r}{dt} \qquad 1.4$$

The Constant Flux Linkage Theorem is frequently applied to resistive circuits as an approximation, particularly if the resistance is low. In this case the initial value of ψ_2 is equal and opposite to ψ_1, but it begins at once to decay asymptotically toward zero. The shapes of the induced voltage, current, and counteracting flux are also shown in Fig. 1.3. During the period of flux change, Eq. 1.4 is more adequately expressed as

$$e = - N \frac{d(\psi_1 + \psi_2)}{dt} = - N \frac{d(\psi_1 + \frac{Ni_2}{\mathcal{R}})}{dt} \qquad 1.5$$

The flux ψ_2 produced by the induced current i_2 depends on the number of turns and on the reluctance of the path through which ψ_2 must pass. The inter-relations between current, voltage and flux are well illustrated by Eq. 1.5. In effect, the induced voltage must produce a current which will create the flux ψ_2 such that the required value of e_1 from Eq. 1.5 will occur.

Finally let us consider the fully realistic case where the magnet is moved in a finite time toward a coil that has a finite resistance. The initial flux increase ψ_1 follows a time-shape similar to that shown in Fig. 1.2 (b). The opposing flux ψ_2 gradually becomes less than the ideal curve and eventually decays asymptotically to zero as in Fig. 1.4.

The flux ψ_2 curve has zero values at t_o and at t_1 and obviously has a peak value between the two time values. The induced current curve i_2 has the same shape as the flux curve because the latter is proportional to the current, for an air flux path. The induced voltage curve, e_1 has the same shape as the current curve because in a resistance circuit the current is proportional to the voltage. Therefore the flux ψ_2, the induced current i_2 and the induced voltage e_1 all have the same shape over the period of time t_o to t_1. When the fluxes are combined as in Eq. 1.3 the resultant flux linkage curve is shown in Fig. 1.4 and when this curve is differentiated graphically, or by Eq. 1.5, the induced voltage curve e_1 must be derived.

The product of the induced voltage e and the current i_2, gives the power. The area under the power curve is the energy W_e dissipated as heat during the interval from t_o to t_1. This energy is obtained from the magnetic field W_f and from the mechanical energy necessary to move the permanent against the opposing field ψ_2. These relations can be expressed by the equation

$$W_f = W_e = \int_{t_o}^{t_1} e_1 i_2 dt = \int_{t_o}^{t_1} i_2^2 \; R \; dt \quad \text{watt seconds} \qquad 1.6$$

Thus far we have considered a motion of the magnet which increases the flux linking the coil. Now, let us reverse the motion and return the magnet to its original position x in Fig. 1.1. The flux change ψ_1 now is reversed in direction so that it diminishes the flux. The flux ψ_2 also is reversed and thereby creates an attractive force with the magnet. Mechanical energy must be expended in overcoming this attractive force while returning to its original position.

In Fig. 1.5 the shapes of the various quantities versus time are shown for the reverse motion of the magnet during the time interval t_2 to t_3. A portion of Fig. 1.4 for the time period t_o to t_1 is included for comparison. The curves for the induced voltage e and the current it produces i_2 are both reversed from that of Fig. 1.4. The reversed current creates the required counteracting flux ψ_2. The product of the e_1 and i_2 curves gives another positive pulse of power similar to that in Fig. 1.4. The energy, likewise is the area under the power curve, or expressed as an equation

$$W_e = \int_{t_2}^{t_3} e_1 i_2 \, dt \qquad 1.7$$

The shape of the flux curve between t_2 and t_3, except reversed, is identical to that from t_o to t_1. The energies represented by Eq. 1.6 and 1.7 are identical.

We have gone through a complete cycle of energy transformation. We have exerted mechanical energy to move the magnet against an induced magnetic field. The increased energy in the magnetic field was converted to electrical energy which was dissipated as heat. The same underlying laws apply to transformers and to rotating electrical machines.

1.3 Application of Laws in a Coil Linked with Electromagnetic Flux

In this section we will study the behavior of a coil similar to that in Fig. 1.1, except without the permanent magnet. The flux is supplied by a current from a dc source E_c connected to the terminals of the coil as in Fig. 1.6. Let the current I_o flow through the coil in the direction indicated to produce the initial flux ϕ_o. Then let the voltage be increased by E_c so that the current flowing through the windings increases by the small amount i_1. This increase in current creates an increase of flux ψ_1. In accordance with Faraday's and Lenz's Laws, this change in flux generates a voltage in the coil, the polarity of which is such that the current it causes produces a flux ψ_2 in opposition to ψ_1. Thus the induced voltage directly opposes the initial increase in voltage.

Let us assume that the increase in voltage E_c can be applied instantly. This situation is essentially realistic. If the circuit were purely resistive, the current increase i_1 and the flux increase ψ_1 would occur simultaneously with E_c. The net flux change ψ_r induces a voltage e_2, with the resulting flow of current i_2 and generation of flux ψ_2.

Again, let us assume that the resistance is low enough to apply the Constant Flux Linkage Theorem with reasonable approximation. Thus, at the instant ψ_1 is initiated, ψ_2 is established equal and opposite to ψ_1. Therefore at t_o

$$\psi_1 = - \psi_2 \qquad 1.8$$

Since the fluxes ψ_1 and ψ_2 are in the same magnetic path, the currents producing them are equal and opposite. Likewise the induced voltage directly opposes the increase in voltage E_c. Expressed by equations these relations, at t_o are:

$$i_1 = - i_2 \qquad 1.9$$

$$E_c = - e_2 \qquad 1.10$$

The relations of the several components are shown by arrows in Fig. 1.6. The circuit through which the currents flow contains resistance. Therefore i_2 and its flux ψ_2 can not be maintained at their initial values. They both immediately begin to decay asymptotically to zero. The shapes of the flux-, voltage-, and current-time curves are illustrated in Fig. 1.7(a), (b), and (c) respectively. During the decay period from t_o to t_1, the net change of flux through the coil is

$$\psi_r (t) = \psi_1 + \psi_2 (t) \qquad 1.11$$

The final steady state flux ϕ_1 is attained when ψ_2 decays to zero. Thus,

$$\phi_1 (t) = \phi_o + \psi_1 + \psi_2 (t)$$

$$= \phi_o + \psi_1 \quad (\text{when } \psi_2 = 0) \qquad 1.12$$

A voltage is induced by each component of flux. Let us assume that the high spike of voltage induced by the instantaneous rise of flux ψ_1, at t_o, is cancelled by an equal spike induced by the sudden rise of ψ_2. No further voltage is induced by the flux ψ_1 because it remains constant after the initial sudden rise. The only voltage of importance is $e_2 = - N_2 \, d\psi_2/dt$. Neglecting the initial spike and starting from the time t_o+, the voltage can be expressed as:

$$e_2 = - N \frac{d\psi_r}{dt} = - N \frac{d\psi_2}{dt} \qquad (\text{for } t > t_o \text{ only}) \qquad 1.13$$

As previously stated this induced voltage is equal and opposite to E_c at t_o but e_2 decays as the derivative of the flux ψ_2 decays. The change of voltage during the decay period is

$$e_r = E_c + e_2 \qquad 1.14$$

The final steady state voltage is

$$E_1 = E_o + e_r$$

$$= E_o + E_c \quad (\text{when } e_2 = 0) \qquad 1.15$$

The initial current $I_o = E_o/R$ would instantly increase to its full value I_1 if it were not opposed by the induced current $i_2 = e_2/R$. The net change of current flowing in the coil is

$$i_r(t) = i_1 + i_2(t) \qquad 1.16$$

where $i_1 = E_c/R$, is the input current change. The actual input current that would be read on an ammeter is

$$I_1(t) = I_o + i_r(t)$$

$$= I_o + i_1 \quad (\text{when } i_2 = 0) \qquad 1.17$$

All of these relations are shown on Fig. 1.7.

1.4 The Magnetic Circuit and Magnetic Units

The magnetic path is quite similar in theory to the dc electric circuit. The magnetomotive force, which drives the flux through the path, is analogous to voltage, the flux is analogous to current, and the reluctance of the path takes the place of resistance. A list of the analogous terms and equations is given below.

DC Circuit	Magnetic Circuit	
Electromotive Force Voltage E	Magnetomotive Force MMF of Ampere-turns Ni	
Current I	Flux ϕ	
Resistance R $R = G/A\rho$	Reluctance $\mathcal{R}$ $\mathcal{R} = G/A\mu$	1.18
G-Length of conductor A-Cross sectional area of conductor ρ-Conductivity of material	G-Length of Path A-Cross sectional area of flux path μ -Permeability of material	
Current = E/R $I = EA\rho/G$	Flux = MMF/$\mathcal{R}$ $\phi = NIA\mu/G$	1.19
Electric Field Intensity (ε) $(\varepsilon) = E/G$	Magnetic Field Intensity (H) $H = NI/G$	1.20

The magnetomotive force is measured in ampere-turns or gilberts where one ampere-turn = 0.4π gilberts.

The permeability of free space μ_o, or air, is $4\pi\ (10^{-7})$ henries per meter. Thus Eq. 1.20 for any magnetic path of permeability μ_r becomes

$$\text{Flux } \phi = 4\pi\ \mu_r NI(10^{-7})\ A/G \quad \text{webers} \tag{1.21}$$

In this equation NI is expressed in ampere-turns, A in square meters, G in meters, and μ_r is the relative permeability of the material in the magnetic path compared to its value in air.

Flux density B is the flux per unit of area, or $B = \phi/A$. Dividing Eq. 1.20 by the area gives

$$B = 4\pi\mu_r NI\ (10^{-7})/G \quad \text{webers per sq. meter} \tag{1.22}$$

If the length G is expressed in centimeters

$$B = 1.258\ \mu_r NI\ (10^{-8})/G \quad \text{webers per sq. centimeter}$$

If the length is in inches

$$B = 3.19\ \mu_r Ni\ (10^{-8})/G \quad \text{webers per sq. inch} \tag{1.23}$$

Substituting Eq. 1.20 in Eq. 1.23 gives

$$B = 3.19\ \mu_r H \times 10^{-8} \quad \text{webers per sq. inch} \tag{1.24}$$

The saturation curve for magnetic core materials is usually plotted as B vs H. Substituting Eq. 1.21 in Eq. 1.1, we obtain

$$e = -N\ d\phi/dt = -(4\pi\mu_r N^2 A\ 10^{-7}/G)\ di/dt \quad \text{volts} \tag{1.25}$$

The quantity $4\pi\mu_r N^2 A\ 10^{-7}/G$ is called the inductance, L. Substituting for this quantity in Eq. 1.25, we get the familiar relation

$$e = -N\ d\phi/dt = -L\ di/dt \quad \text{volts} \tag{1.26}$$

Compatible units are obtained when A and G in Eq. 1.25 are expressed in sq. meters and meters respectively.

1.5 Energy in the Magnetic Field

When the voltage applied to the coil in Fig. 1.6 is increased, the electrical energy input is increased. The amount of energy increase is due to the increase in voltage and current. It is

$$dW_e = E_c\ i_r\ dt \tag{1.27}$$

There are additional losses in the circuit also

$$dW_L = i_r^2 \, R \, dt \qquad 1.28$$

The difference between the additional energy input and the additional losses must go into increasing the energy in the magnetic field. Thus

$$dW_f = dW_e - dW_L$$

$$= E_c \, i_r \, dt - i_r^2 \, R \, dt \qquad 1.29$$

From Eq. 1.16 and the discussion relating thereto we have

$$i_r = E_c/R - e_2/R \qquad 1.30$$

After substituting Eq. 1.30 and 1.29 and simplifying we get the important equation

$$dW_f = e_2 \, i_r \, dt \qquad 1.31$$

or

$$W_f = \int_{t_o}^{t_1} e_2 \, i_r \, dt \qquad 1.32$$

The energy in the magnetic field, or the increase in field energy in the present case, is the area under the power curve obtained by multiplying the induced voltage by the net current flowing in the coil. The shape of the power curve is shown in Fig. 1.8.

The energy in the field can be represented in another way. If the permeability of the path through which the flux passes is constant, then ψ_r is proportional to i_r. That is

$$i_r = k \, \psi_r \qquad 1.33$$

This can be substituted in Eq. 1.32. Remembering that $e_2 = - N \, d\psi_r/dt$, Eq. 1.32 becomes, after changing the limits of integration;

$$W_f = \int_o^{\psi_r} Nk\psi_r \, d\psi_r$$

$$= Nk \, \psi_r^2/2$$

But $k\psi_r = i_r$. Therefore

$$W_f = \tfrac{1}{2} \, N \, i_r \, \psi_r \qquad 1.34$$

In Fig. 1.9 the current is plotted against the flux. The energy in the field shaded areas is one half the area of the rectangle $N i_r \psi_r$.

For a flux density of one weber per square meter, which is of the order of magnitude found in the air gaps of motors and generators, the stored energy in air is $10/8\pi$, or 0.398 watt-second, per cubic centimeter. (see sect. 1.8) This is 4.81 ft lb/cu in. This value is 10,000 times the energy density in the electrostatic field of an air capacitor at its limiting permissible electric stress; which explains why magnetic rather then electrostatic forces are relied on in power engineering.

For a given flux density, the energy density is inversely proportional to the permeability. Since μ_r is of the order of 100 or more for steel at usual flux densities, the stored energy in the steel is small, and the magnetic energy in electrical apparatus is almost all in the air paths of the magnetic flux.

1.6 Faraday's Law and Inductance

Ohm's Law of Magnetic circuits as expressed in Eq. 1.19 is

$$\phi = NiA\mu/G$$

and Faraday's Law from Eq. 1.1 is

$$e = - N \, d\phi/dt$$

Substituting the value of flux into Faraday's Law gives:

$$e = - N \, d(NiA\mu/G)/dt$$

When A, μ, and G are constant

$$e = - N^2 A \mu /G \, (di/dt) \qquad 1.35$$

This is similar to Eq. 1.25 except the latter includes conversion factors for consistent units. Inductance is defined, without conversion factors, by the group of terms in Eq. 1.35 as

$$L = N^2 A \mu /G \qquad 1.36$$

This equation contains the physical quantities of turns, dimensions, and material (permeability) necessary for the design of an inductance.

Substituting Eq. 1.36 in Eq. 1.35 we obtain

$$L \, di/dt = N \, d\phi/dt \qquad 1.37$$

Faraday's Law can now be stated in terms of the time rate of change of current as well as the time rate change of flux. The L di/dt approach is useful in circuit analysis, while the N $d\phi/dt$ is more useful in the understanding and design of electrical machines.

When the quantities representing inductance in Eq. 1.36 are constant, the geometry of the magnetic circuit is fixed, and therefore L is constant. This is the case throughout Chapters 1 and 2. In some motors however, one or more of the factors A, μ, and G are continuously changing as the rotor turns, and an appropiate treatment of Faraday's Law must be applied. With the flux linkage λ expressed as $\lambda = N\phi$.

We now have

$$e = \frac{d(N\phi)}{dt} = \frac{d\lambda}{dt} = \frac{d(Li)}{dt}$$

and

$$e = i\frac{dL}{dt} + L\frac{di}{dt}$$

This is the generalized expression of Faraday's Law. The first term is proportional to the rate of change of inductance which is usually proportional to the speed of the rotor. This term is therefore called the speed voltage. The second term is the transformed or induced voltage with which we have been dealing before. The general form of Faraday's Law is useful in the analysis of rotating machines and the treatment is fully covered in most textbooks on rotating machines.

We can modify Eq. 1.37 as follows:

$$L\,di = N\,d\phi$$

$$L\int_{I_o}^{I_o + i_r} di = N\int_{\phi_o}^{\phi_o + \psi_r} d\phi$$

From which

$$L = N\psi_r/i_r \qquad 1.38$$

Eq. 1.38 gives the definition of inductance as the flux linkage per unit of current. The saturation curve for a magnetic material can be plotted as flux linkages versus current, as in Fig. 1.10. It is obvious that the ratio $N\phi/I$ is not constant and varies with the degree of saturation. Another definition called Incremental Inductance is the ratio of a small change in flux linkages to a correspondingly small change in current. Thus

$$\Delta L = \Delta N\,\phi/\Delta i \qquad 1.39$$

Some of the incremental values are shown in Fig. 1.10 and from these the nonlinear inductance curve can be plotted.

All electrical machines contain magnetic circuits operating at some degree of saturation. The saturation and inductance curves of Fig. 1.10 are not easily expressed by equations. It is frequently more expedient to use graphical methods when analytical procedures require the use of these nonlinear curves.

From these definitions it is obvious that the phenomenon of inductance is present whenever flux links a conductor carrying a current. In some cases there may be several components of flux, and each component will have associated with it a specific inductance. For example, mutual flux is responsible for mutual inductance, and total flux for self inductance. Mutual flux and mutual inductance are present when there are two adjacent coils linked with a common flux. This subject is considered in the next section.

1.7 Faraday's Law and Mutual Inductance

Refer to Fig. 1.11 where two coils are linked with a common flux. Coil No. 1 is supplied from a dc source, and coil No. 2 is connected to a resistance. The initial voltage E_o establishes a flux ϕ_{12} which links both coils. An additional flux in coil No. 1 established by E_o links only with the turns in that coil and it is called Leakage Flux ϕ^1. The mutual flux and its inductance are discussed below. Leakage flux is covered in Chapter 2.

Let there be an increase in voltage E_c above the initial voltage E_o. It causes an increase in current i_1 and this in turn produces a flux increase ψ_{12} above the initial mutual flux ϕ_{12}, linking both coils. During the period of time while ψ_{12} is changing, a voltage is induced in Coil No. 2

$$e_2 = - N_2 d\psi_{12}/dt \qquad 1.40$$

This voltage causes the induced current i_2 to flow in coil No. 2 and through the resistor R_2. A flux ψ_{21}, produced by i_2, directly oppose the initial flux change ψ_{12}. Let this flux also completely link with all turns in coil No. 1, whereby another voltage e_1 is induced

$$e_1 = - N_1 d\psi_{21}/dt \qquad 1.41$$

Again according to Lenz's Law the voltage e_1 directly opposes the initial change in voltage E_c. This reaction, of course, occurs only during the period of changing flux. Eventually the voltage, current and flux in coil No. 1 reach a final steady state value at which time the induced voltage, current and flux in coil No. 2 will have decayed to zero.

The flux ψ_{12} in coil No. 1 depends on the MMF and the reluctance of the path through which the flux must pass, as expressed in Eq. 1.19

$$\psi_{12} = + N_1 \, i_1 \, A\mu/G \qquad 1.42$$

Substituting this value of flux in Faraday's Law Eq. 1.40 we have

$$e_2 = - N_1 \, N_2 \, A\mu/G \, (di_1/dt) \qquad 1.43$$

The quantity $N_1 N_2 A\mu/G$ is called Mutual Inductance M. Substituting M in Eq.

1.43 and equating it to Eq. 1.40 we have:

$$e_2 = - M \, di_1/dt = - N_2 \, d\psi_{12}/dt$$

and

$$M \int_{I_o}^{I_o + i_1} di_1 = N_2 \int_{\phi_{12}}^{\phi_{12} + \psi_{12}} d\psi_{12}$$

and

$$Mi_1 = N_2 \psi_{12}$$

and finally

$$M = N_2 \psi_{12}/i_1 \qquad 1.44$$

Mutual inductance is defined therefore as the flux linkage in one coil per unit of current in another. If there is a complete coupling between the two coils such that $\psi_{12} = \psi_{21}$ we can divide Eq. 1.41 by Eq. 1.40 and obtain one of the basic transformer relations:

$$e_1/e_2 = N_1/N_2 \qquad 1.45$$

From the definition of mutual inductance in Eq. 1.43 or from the substitution of Eq. 1.42 in Eq. 1.44, we have the equation:

$$M = N_1 N_2 A\mu/G \qquad 1.46$$

This equation is the basis for a design formula since it contains the physical quantities of turns, dimensions and material (μ). This is the basis for the final size, shape, cost and performance of the design.

1.8 Magnetic Forces

In Section 1.5 it was shown that the energy in the magnetic field in (Eq. 1.32 but using symbols for general nomenclature)

$$W_f = \int_{t_o}^{t_1} eidt$$

Substituting for the induced voltage its equivalent e = L di/dt we have:

$$W_f = \int_o^I Lidt \; di/dt = LI^2/2 \quad \text{watt-seconds} \qquad 1.47$$

From this equation we can calculate the energy stored in an air path in terms of flux density. The value of i^2 from Eq. 1.22 is

$$i^2 = B^2 G^2 (10^{+7})^2 / (4\pi\mu_r N)^2 \qquad 1.48$$

Now substitute this equation and the value of L as defined in Eq. 1.25 in Eq. 1.47, we get:

$$W_f = Li^2/2 = [B^2 10^7/8\pi\mu_r] (AG) \text{ watt-seconds} \qquad 1.49$$

In this equation B is expressed in webers per sq. meter; A in sq. meters; and G in meters. Note also that the quantity AG is the volume of the magnetic path.

As shown by Eq. 1.49 the magnetic energy of a field in air is $B^2 10^7/8\pi$ watt-seconds per cubic meter. If the density B is maintained constant over a given area, A, while the length of gap is changed from G to G + g, the magnetic energy will increase by the amount $AgB^2 10^7/8\pi$. This must be equal to the work done in overcoming the attractive magnetic force, F. Since B remains constant, there is no voltage induced in the circuit, and therefore there is no power supplied to, or taken from the line during the motion. The force is then given by the equation:

$$W_f = Fg = AgB^2 10^7/8\pi \qquad \text{newton meters} \qquad 1.50$$

whence the force per unit area exerted by a flux density of B webers/sq m is equal to $B^2 10^7/8\pi$ newtons/sq m. In more familiar terms, this is 39.8 newtons/sq cm, or 57.8 lb/sq in, for a density of one weber per square meter.

If, instead of holding B constant while the air gap was increased from G to G + g, we held the mmf constant, the value of B would have decreased to BG/(G + g) during the motion, while the current needed to create the density remained constant, equal to $BG10^7/4\pi N$. Therefore, the energy supplied to the line is:

$$W_e = \int eIdt = \int NId\phi = (BG\ 10^7/4\pi)\ (BA)\ (1-G/(G+g))$$

$$= AgB^2\ 10^7/4\pi = 2\ W_f \qquad \text{watt seconds} \qquad 1.51$$

In this case, the magnetic energy decreased by the same amount that it increased when B was held constant, while the power supplied to the line is twice the work done and also twice the energy taken from the field. Assuming g very small in comparison with G, the force F to be overcome in increasing the air gap is the same in both cases, so that the work done is also the same. With constant current, all the work went into increasing the magnetic energy of the field. With constant B, the energy of the field decreased by the same amount as the work done, and both the released energy and the work energy were returned to the line. These relations give the general rule, due to Lord Kelvin, that:

When, in a singly-excited electric circuit, without saturation, a deformation takes place at a constant current, one half of the energy taken from the line is used to do mechanical work and the other half to increase the energy of the magnetic field.

1.9 Experiments

Experiment No. 1.1

The physical behavior of these fundamental laws should be thoroughly understood. A "feel" for these laws can be obtained by experimenting with a coil and a permanent magnet. A sensitive ammeter (a microammeter) can be placed in series with the resistance R, or a sensitive voltmeter (or microvoltmeter) can replace the resistance. By moving the magnet in various ways, and at different speeds, and observing the reaction of the ammeter or voltmeter, a clear understanding of the behavior of the laws can be obtained. In all cases the current in a closed circuit must produce a flux such that its rate of change will induce, in accordance with Eq. 1.1, a voltage required to produce the current. It is instructive also to sense how the force varies with the position and speed of motion of the magnet, although the small forces may be difficult to detect.

Experiment No. 1.2

To appreciate these concepts, experiment No. 2 may be performed. Take two similar rectangular permanent magnets, and sense the force between them when they are moved in various ways. Each magnet maintains nearly a constant flux, and its associated magnetic energy stored in the air around it. When the magnets are pushed together, with like poles in contact, a strong repulsive force is exerted. The work done in pushing them together is stored up in increasing the field energy, as the fixed amount of flux has to flow through a smaller area. Since the energy is B^2 times the volume, the increase of B when the area is decreased more than offsets the smaller volume of the field. Conversely, if unlike poles of the magnets are brought together, there is a strong attractive force, that does work when the poles move toward each other. This work is supplied by the field energy, so the total field energy is reduced to match the smaller field volume. In effect the energy of two of the four magnet poles has been wiped out, and this has gone into the work of restraining the attractive force as the magnets come together, or into the kenetic energy of impact. Since the magnetic force is proportional to the rate of change of stored energy in the direction of the motion, moving the magnets around and sensing the changes in the force gives an understanding of how the magnetic energy is distributed. The magnetic force always acts in a direction to decrease the reluctance, or increase the inductance, of the flux path.

Compare the forces between the two magnets with those between a magnet and a piece of iron. Also try the effect of moving a strip of copper or aluminum past a magnet pole, at first slowly and then rapidly. The motion induces currents in the strip, which exert forces opposing the motion.

A current flowing in a wire in air creates a circular magnetic field around the wire, whose flux density is inversely proportional to its radius.

When two current-carrying wires are placed side by side, their magnetic fields add. If the currents are in the same direction, the fields between the wires are opposite, so the net field is small, while the fields outside the two wires are in the same direction, making the net field large.

As each current flows across the field of the other, there is a force exerted in the direction that will increase the inductance. Thus, with the currents in the same direction, the wires are pulled together--with opposite directions of currents the wires are repelled. This means that if a rectangular coil carries a current, the forces between wires try to make the coil circular. These forces vary as the square of the current, so become very large under short-circuit conditions. For this reason, high-voltage transformer coils are usually made circular, to prevent their being wrecked by high currents. Also, if large cables lie on the floor, in irregular positions, and if the currents in them suddenly become very large, the cables will whip about and may very easily knock a man down, or wreck adjacent equipment. It is essential, therefore, that such cables be arranged in positions of maximum inductance, or securely tied down. It is essential, also, that the end windings of machines be securely braced and tied in ways to resist motion due to short-circuit forces.

Experiment No. 1.3

Obtain a considerable length of flexible copper wire, arranged in the form of a loosely wound coil, and place it on a smooth or polished table. Then, pass a direct current through the coil and see if you can detect any force tending to make the coil a circular shape. One way to do this is to put a fuse or a circuit breaker in series with the wire and then apply a considerable voltage, causing a high current to flow, and the fuse to blow. The coil ought to jump and take a circular shape.

Next, take a permanent magnet and move it across the wire when the current is flowing. See if you can detect the force between the magnet and the magnetic field of the wire, and move the magnet into different positions, so that you can sense the relative magnitudes and directions of the forces that are exerted. Then, place the coil around one leg of a C- or E-shaped laminated core, and again note the forces when the permanent magnet is moved into different positions with respect to the open end of the core.

This experiment demonstrates the fact that an electromagnet, consisting of a laminated core surrounded by a coil carrying a current, has properties similar to those of a permanent magent.

Experiment No. 1.4

In this experiment, we use a coil carrying a direct current, forming an electromagnet, instead of the permanent magnet used in experiment No. 1. Here the motion induces voltages in both coils, which create currents that oppose any changes in flux linkages. The experiment is illustrated by Fig. 1.11. Coil 1, with N_1 turns carrying a current I_1 supplied by a battery, has a resistance R_1, and coil 2, with N_2 turns is closed through a resistance R_2. The flux linking coil 1 has two components, ϕ_1 that links coil 1 but not coil 2, and ϕ_{12} that links both coils. Likewise, any current, I_2, in coil 2,

creates a leakage flux, ϕ^{11}, that links only coil 2 and a mutual flux, ϕ_{21}, that links both coils.

If the current in coil 1 in changed by an amount ΔI_1, both ϕ^1 and ϕ_{12} will change correspondingly, and these changes will induce voltages in coil 1 equal to $L_1 \Delta I_1/dt$ and $L_{12} \Delta I_1/dt$, where L_1 and L_{12} are the inductances given by Eq. 1.25 for the respective flux paths, each proportional to N^2. However, the flux change $\Delta\phi_{12}$ will also induce a voltage in coil 2, and this is proportional to $N_1 N_2$, since it is caused by its linkage with N_2 turns of coil 2 instead of the N_1 turns in coil 1. In the same way, the current ΔI_2 induced in coil 2 by $\Delta\phi_{12}$ creates a change in the leakage flux of coil 2, $\Delta\phi_2$, and also a change in the mutual flux linking both coils, $\Delta\phi_{21}$. Therefore, the voltages induced in the two coils by their relative motion are:

$$E_1 = - N_1 \Delta\phi^1/dt - N_1 \Delta\phi_{12}/dt - N_1 \Delta\phi_{21}/dt \qquad \text{volts} \qquad 1.52$$

$$E_2 = - N_2 \Delta\phi^1/dt - N_2 \Delta\phi_{21}/dt - N_2 \Delta\phi_{12}/dt \qquad \text{volts} \qquad 1.53$$

Since ϕ_{12} is proportional to N_1, and ϕ_{21} is proportional to N_2 (Eq. 1.19) and as both these fluxes share the same path, the mutual inductance, which represents them, is the same; and is given by Eq. 1.25 with the factor $N_1 N_2$ instead of the N_1^2 or N_2^2 which occur in the self inductances.

Thus, when two windings link a common flux path, the inductance of each winding must be considered as made up of two parts, one due to the leakage flux and the other due to the mutual flux. The sum of these two gives the self-inductance, proportional to N^2, while the mutual flux gives the mutual inductance, M, proportional to $N_1 N_2$, that induces a voltage in each winding.

As in experiment No. 1, it is desirable to observe the induced currents, voltages, and forces when the positions and speed of relative motion of the two coils are varied.

Experiment No. 1.5

Display of Transient flux induced voltage for Fig. 1.11.

Figure 1.12 shows the detailed circuit for displaying the transient shapes of flux and induced voltage in a coil shown in Fig. 1.6. In order to isolate the measuring circuit from the power supply, two magnetically coupled coils are used as in Fig. 1.12. The coupling is made more effective by inserting 10 laminations of steel into the center of the two coils. Thus the changes of flux and the induced voltage in coil 2 can represent the corresponding quanties in coil 1. The transients displayed will therefore have a shape similar to those in Fig. 1.7.

An example of the transient induced voltage and flux is shown in Fig. 1.13. These were taken with one opening and one closing of the swith S. Note the different time constants of both induced voltage and flux for the decay and build-up conditions. The student should explain this difference.

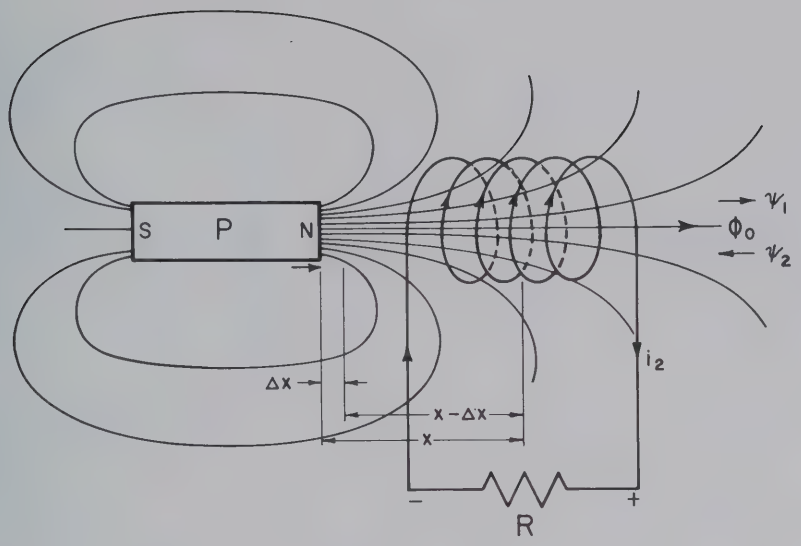

Fig. 1.1 Flux from a permanent magnet linking a coil.

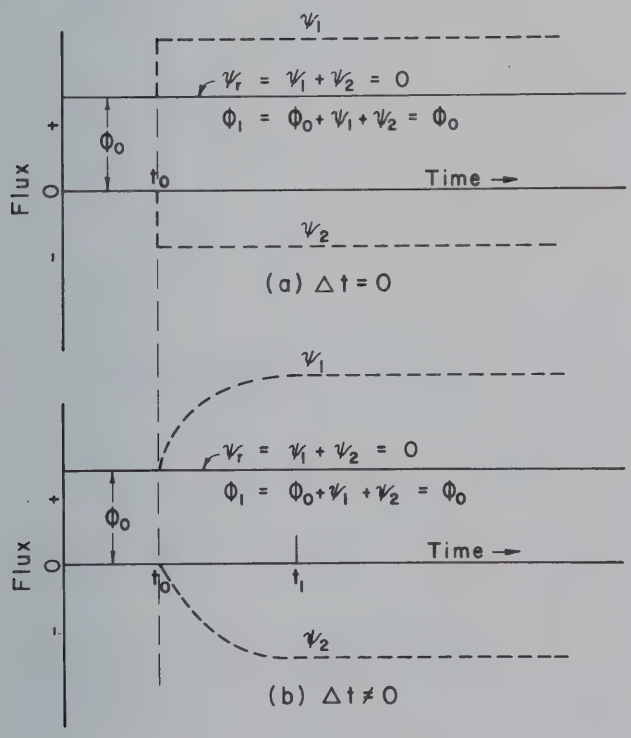

Fig. 1.2 Time varying flux relations in coil with zero resistance linked with flux from a permanent magnet.
(a) Magnet moved in zero time.
(b) Magnet moved gradually.

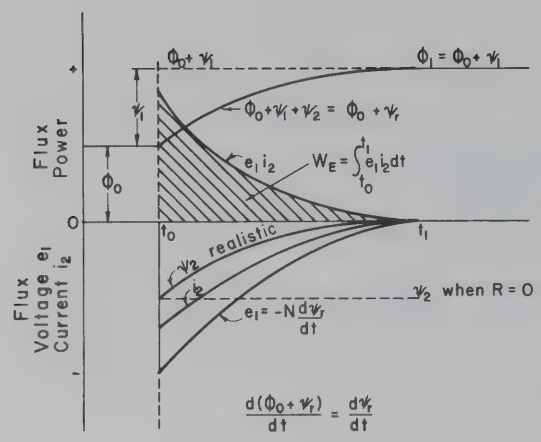

Fig. 1.3 Shapes of time varying quantities in coil linked with permanent magnet flux.

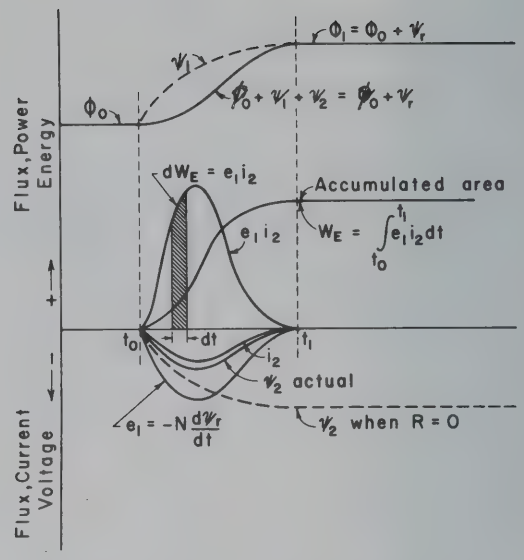

Fig. 1.4 Shape of time varying quantities when permanent magnet is moved forward in a finite time.

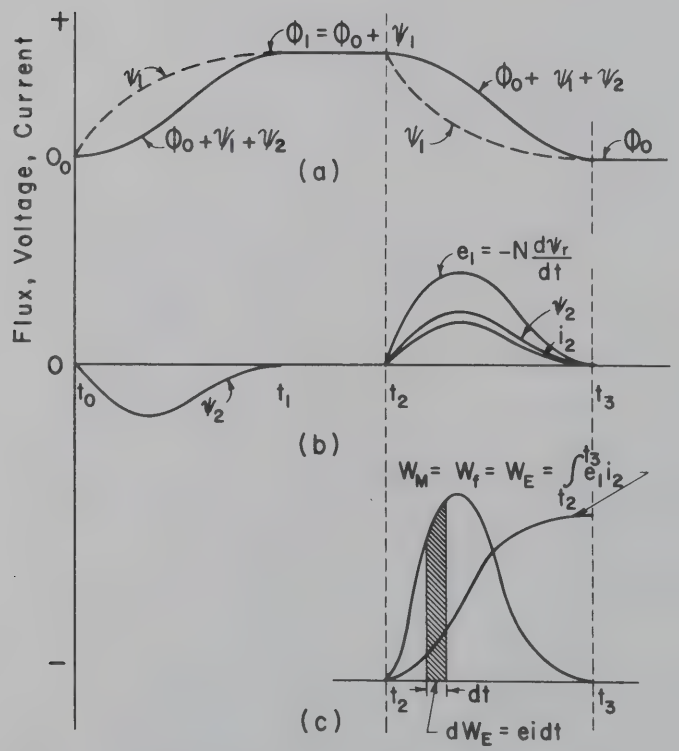

Fig. 1.5 Shapes of time varying quantities when permanent magnet is withdrawn.

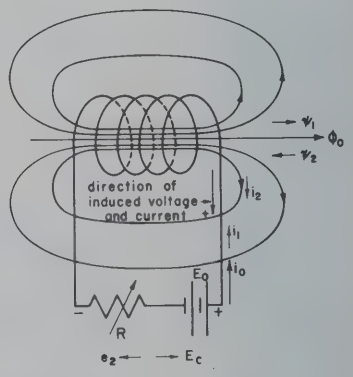

Fig. 1.6 Coil supplied by an external dc source, linked by its own flux.

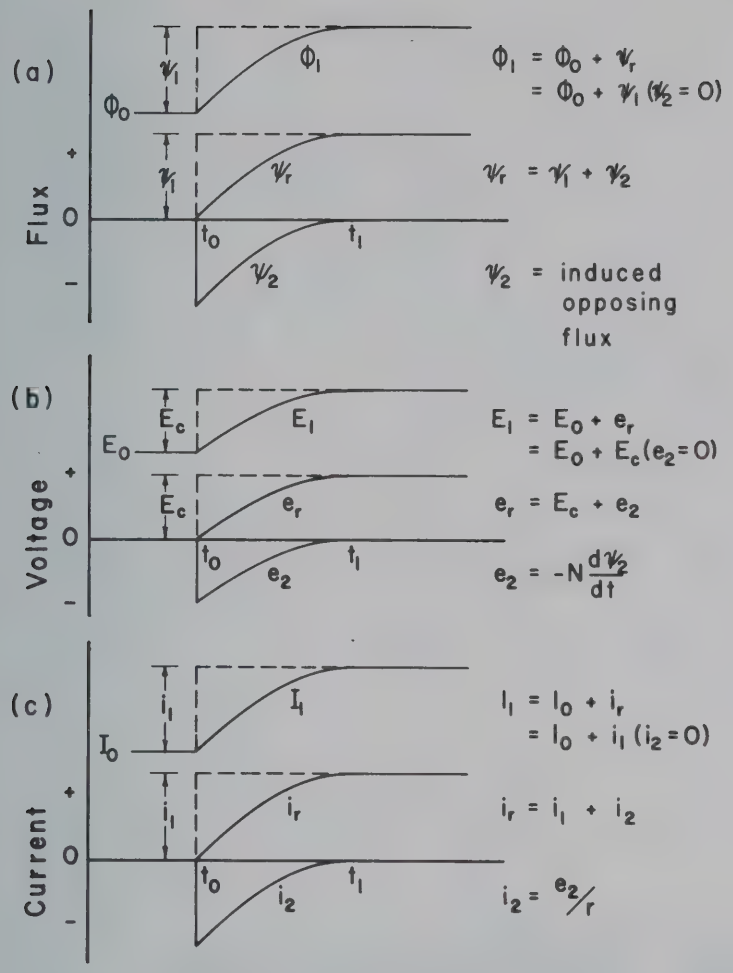

Fig. 1.7 Shapes of time varying quantities when voltage is suddenly increased.

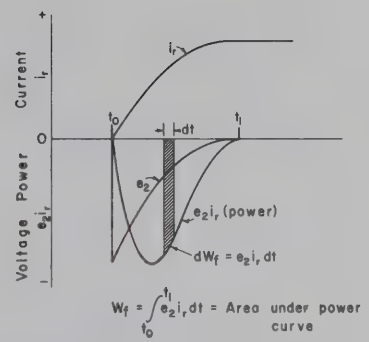

Fig. 1.8 Representation of electric power and energy.

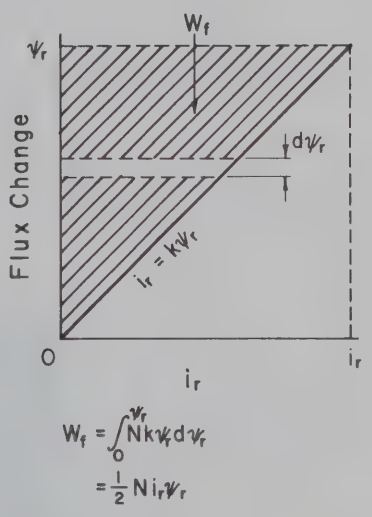

Fig. 1.9 Representation of energy in a magnetic field.

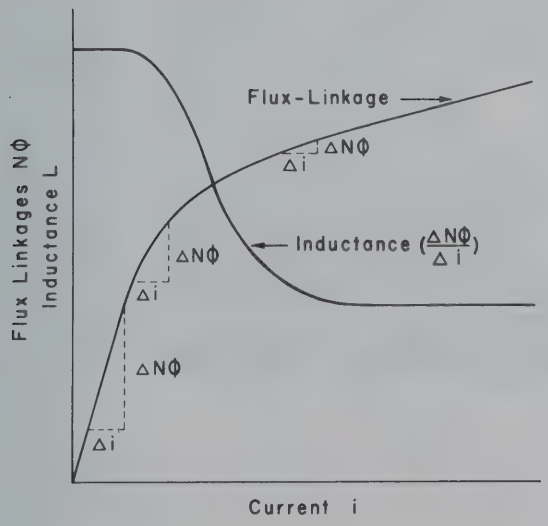

Fig. 1.10 Flux-linkage curve and related inductance.

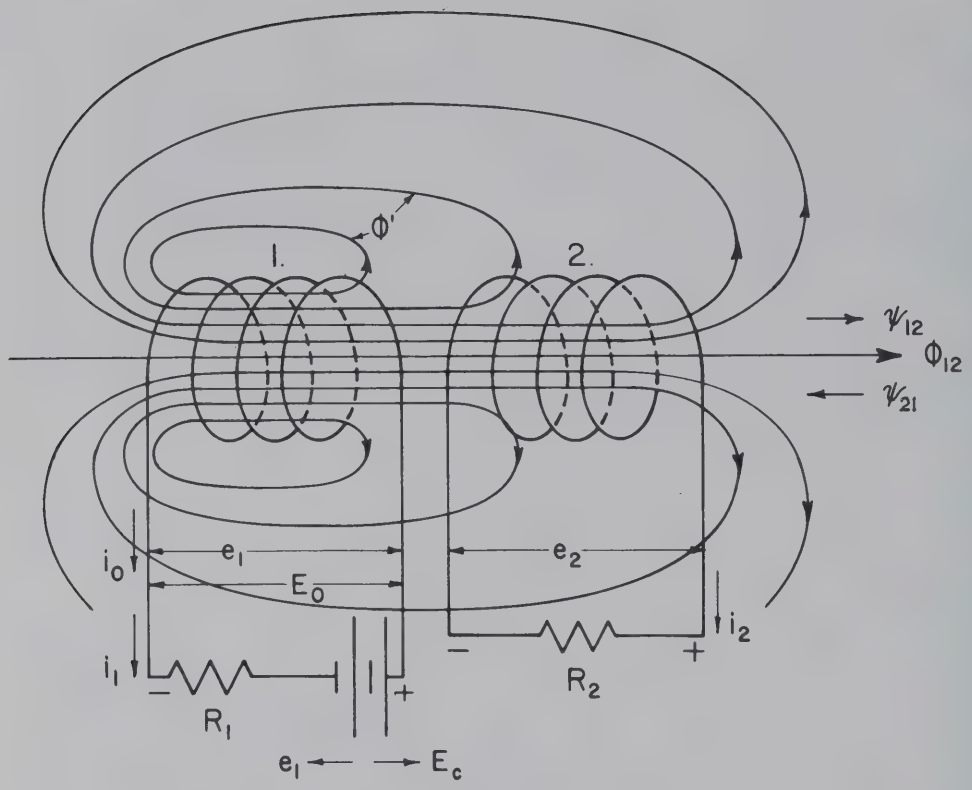

Fig. 1.11 Flux relations in two magnetically coupled coils.

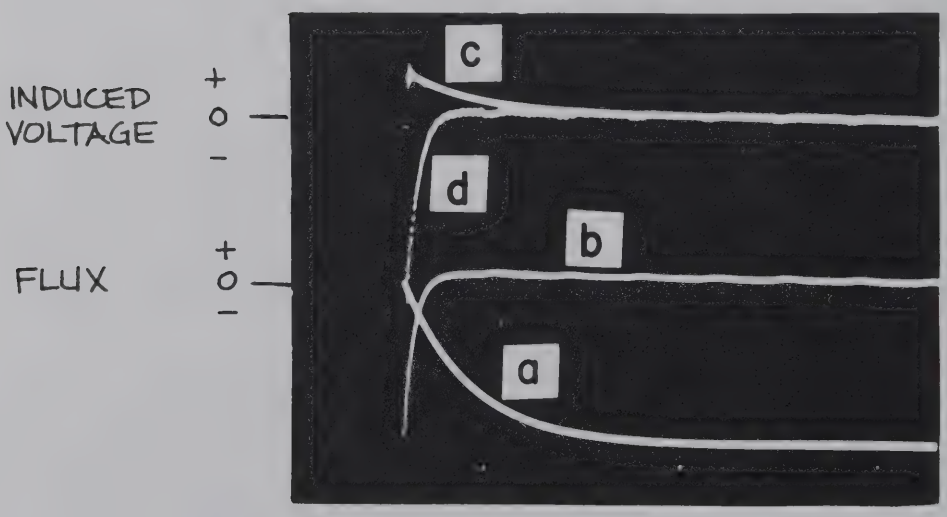

Fig. 1.13 Transients induced by build-up and decay of flux.

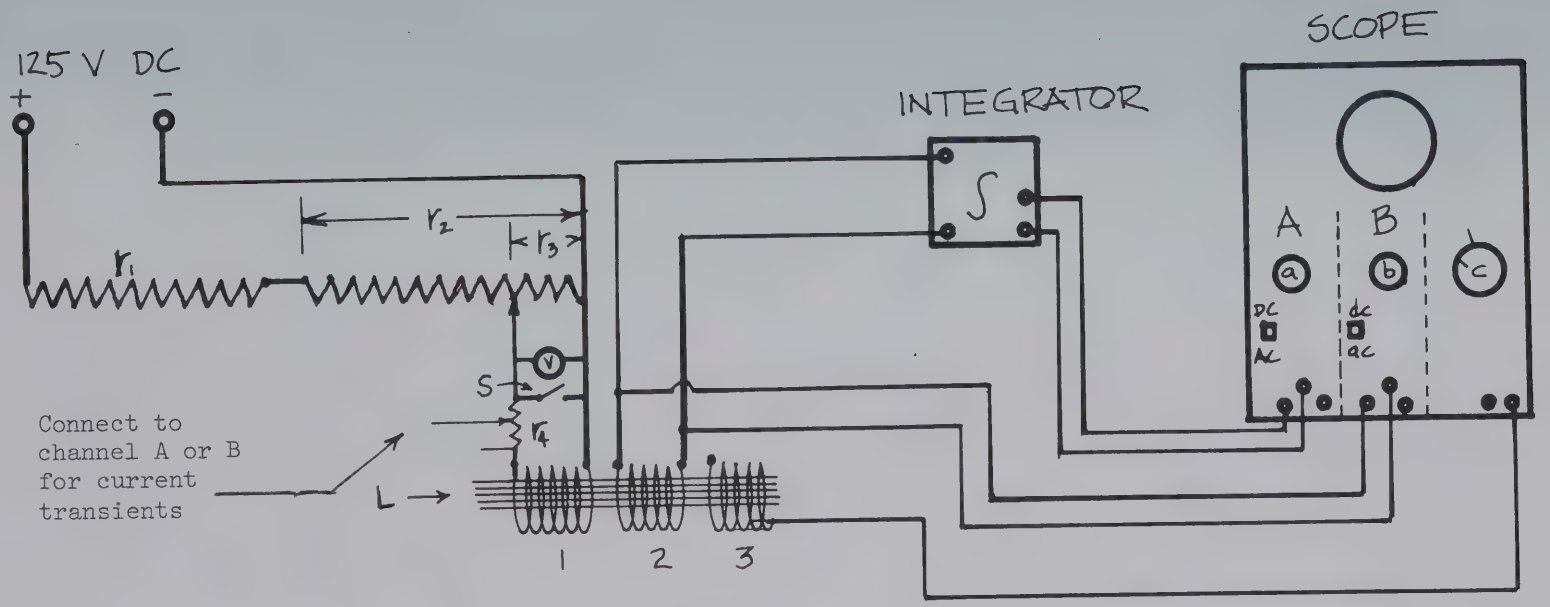

F 1.5

Coils 1,2 - Large wire coils
Coil 3 - Fine wire coil
r_1 - 523 Ohms slidewire
r_2 - 61.7 Ohms slidewire
r_3 - Adjust to give V = 1 volt
r_4 - 1 Ohm for current transient
L_4 - Several laminations (about 10)

Channel A		Channel B	
Attenuator a	1v/div	Attenuator b	1v/div
Input:	DC	Input:	DC

Sweep Control
Sweep Speed X1; 2 or 5 m sec/div
Mode: Normal
Slope: + or -
Coupling: dc
Source: EXT
Trigger Level: Just below continuous sweep

Fig. 1.12 Detailed circuit for observing transients.

N 2.1

NOMENCLATURE FOR CHAPTER TWO

Note: Capital letters are used for RMS values of time varying functions whereas small case letters are used for instantaneous values. (') are used with most quantities associated with leakage flux.

V_1, v_1 - Voltage applied to primary - Line voltage.

V_2, v_2 - Secondary load voltage.

V_o - Secondary no-load voltage - Open circuit voltage.

E_1 - Component of applied voltage opposing induced voltage.

E_2 - Secondary component of load voltage opposing induced voltage also equal to V_o at no-load.

e_r - Voltage drop across line resistor.

e_1 - Induced voltage in primary winding.

e'_1 - Induced voltage in primary due to leakage flux.

e_2 - Secondary induced voltage.

E_3, E_4, e_3, e_4 - Voltages generated in information windings.

V_c - Voltage representing flux.

R_1 - Resistance of primary winding.

R_2 - Resistance of secondary winding.

r_1 - External resistance in series with primary.

r_2 - External resistance in series with load.

r_3 - Resistance across information winding.

r_4 - Load resistor.

X_1 - Primary leakage reactance. (Note: Do not confuse standard transformer terminal markings, X , X , X etc. with reactances).

X_2 - Secondary leakage reactance.

X_m - Magnetizing reactance.

L_1 - Leakage inductance of primary winding.

L_m - Magnetizing inductance.

L_{11} - Self inductance of primary ($L_{11} = L_1 + L_m$)

L_2 - Leakage inductance of secondary winding.

L_{12}, L_{21} - Mutual inductance between primary and secondary windings.

N_1, N_2 - Number of turns on primary and secondary windings.

N_3, N_4 - Number of turns on information windings.

ϕm - Magnetizing flux.

ϕ_1 - Primary flux due to load component of current.

ϕ_{11} - Total primary flux ($\phi_{11} = \phi_1 + \phi_m$).

ϕ_2 - Secondary flux due to load current.

I_m, i_m - Magnetizing current.

I_{h+e}, i_{h+e} - Current to supply hysteresis and eddy current losses.

I_n, i_n - Exciting current.

I_1, i_1 - Load current in primary.

I_{11}, i_{11} - Total primary input current ($I_{11} = I_1 + I_n$).

I_2, i_2 - Load current in secondary.

$\mathcal{R}$ - Reluctance of magnetic path.

ω - Electrical angular velocity ($\omega = 2\pi f$).

f - Frequency.

B - Flux density.

A - Cross sectional area of magnetic path.

θ - Phase angle.

p - Used as subscript - peak value of sinusoidal function.

CHAPTER 2

TRANSFORMERS

When a laminated magnetic core is linked by a single winding such as that in Fig. 1.6, it is called a rector. Its inductance can be designed for any given value, as discussed in Section 1.6, and therefore it is useful to limit the current in an alternating-current circuit. When there are two or more windings, such as those in Fig. 1.11 on a core, it is called a transformer. Power can be supplied to one winding and taken from a second winding, usually at a different voltage since it is the main purpose of a transformer to establish another voltage level. The current that flows when a-c voltage is applied to one winding with the other open is called exciting current and is very small, perhaps only 3% or less of full load current. The a-c current that flows when the second winding is shorted is very high, up to 30 times greater than the full load current. The flux associated with the currents in each winding may be resolved into several components and these are discussed in the next section.

2.1 Leakage Flux, Magnetizing Flux and Total Flux

When the area around an energized transformer core and coil is explored with a small permanent magnet held in the hand, pulsations can be felt. This is due to a-c flux leaking into the air. Since it is principally in air it cannot link with the turns of all the windings on the core. This is illustrated in Fig. 2.1. In the primary on the left, the leakage flux is produced by whatever current is flowing in the winding. This is called primary leakage flux ϕ_2'. The secondary winding has a leakage flux ϕ_2' only when a current is flowing in it. This flux likewise does not link with the turns of each winding. Both the primary and secondary leakage fluxes are considered equivalent fluxes that link with all turns of their own winding but not with the turns of any other winding.

The path of the leakage flux is almost entirely through air, hence there is essentially a linear relation between the flux and the MMF, or current, that produces it. This is an important factor which we will discuss later in more detail. The leakage flux is small compared to the major flux that is contained entirely in the iron core. This is called magnetizing ϕ_m and links with all of the turns of all the windings.

In power transformers, the various types of iron that may be used for the cores may vary considerably in their magnetic characteristics. Each type of core material has a specific saturation curve, similar to Fig. 2.2 in which the flux density is plotted against the MMF per unit length of magnetic path. It is difficult to express this non-linear curve mathematically, hence the MMF, and the magnetizing current required to produce any given flux density is usually taken directly from the saturation curve.

The load current in the secondary winding (MMF of i_2) produces a large component of flux. In power transformers, this flux is cancelled by an equal and opposite flux produced by a component of load current in the primary

(MMF of part of i_{11}). For this reason these load components of flux are seldom considered, although they are mentioned again later in this chapter.

The total flux linking the primary ϕ_{11}, related to the impressed primary voltage by Faraday's law, is the sum of the leakage flux ϕ_1' and the magnetizing flux ϕ_m. Thus

$$\phi_{11} = \phi_1' + \phi_m \qquad 2.1$$

Each of these fluxes induces a component of voltage according to Faraday's Law. Each has associated with it an inductance as discussed in Section 2.2.

2.2 Magnetizing Reactance and Leakage Reactance

The voltages induced by the leakage and magnetizing fluxes, Eq. 2.1, are

$$-N_1 \, d\phi_{11}/dt = -N_1 \, d\phi_1'/dt - N_1 \, d\phi_m/dt$$

$$e = e_1' + e_1 \qquad 2.2$$

If the transformer is operated at no load, with the secondary winding open, and if we assume there are no losses, then the only current in the primary winding is the magnetizing current i_m. The MMF responsible for the leakage flux is $N_1 i_m$, and the reluctance of the leakage path is $G'/A'\mu'$. Thus the leakage flux is

$$\phi_1' = N_1 \, i_m \, A'\mu'/G', \qquad 2.3$$

where A', μ' and G' apply to the leakage flux path.

Substituting in the leakage flux voltage term of Eq. 2.2, we get

$$e_1' = -N_1 \, d(N_1 \, i_m \, A'\mu'/G)/dt$$

$$= (-N_1^2 A'\mu'/G') \, di_m/dt \qquad 2.4$$

The quantity $N_1^2 A'\mu'/G'$ is the leakage inductance L_1 of the primary winding. Eq. 2.4 now becomes

$$e_1' = - L_1 \, di_m/dt \qquad 2.5$$

Assume that the magnetizing current is sinusoidal

$$i_m = I_p \cos \omega t \qquad 2.6$$

where I_p is the peak value of the magnetizing current wave. Substituting Eq. 2.6 in Eq. 2.5, the leakage flux induced voltage becomes

$$e_1' = -L_1 \, d(I_p \cos \omega t)/ dt$$

or

$$e_1' = -L_1 \omega I_p (-\sin \omega t) \qquad 2.7$$

The peak value of leakage voltage from Eq. 2.7 occurs when $\sin \omega t = 1$

$$e_1' \text{ (peak)} = L_1 I_p \omega \qquad 2.8$$

The RMS value of a sinusoidal quantity is peak/$\sqrt{2}$. Thus

$$E_1' = e_1'/\sqrt{2} = L_1 I_p \omega/\sqrt{2} = \omega L_1 I_m \qquad 2.9$$

The quantity ωL_1 is called leakage reactance X_1 and its voltage drop is

$$E_1' = X_1 I_m \qquad 2.10$$

The reluctance of the magnetic core is $G/A\mu$ where all quantities apply to the core path for the magnetizing flux. The induced voltage in the primary due to the magnetizing flux is similar to Eq. 2.4.

$$e_1 = - N_1^2 A\mu/G(di_m/dt) \qquad 2.11$$

or

$$e_1 = - L_m di_m/dt$$

and following a similar process from Eq. 2.6 through 2.9

$$E_1 = \omega L_m I_m \qquad 2.12$$

and

$$E_1 = X_m I_m \qquad 2.13$$

Equations 2.9 and 2.12 are important in the analysis of transformers. The total input voltage neglecting the primary resistance drop is

$$V_1 = \omega L_1 I_m + \omega L_m I_m \qquad 2.14$$

$$V_1 = E_1' + E_1 \qquad 2.15$$

The two induced voltages in Eq. 2.15 are in series. The leakage flux therefore is equivalent to an inductance in series with an "ideal primary winding" which has only the magnetizing flux and no leakage flux. This is illustrated later by the equivalent circuit.

2.3 The Transformer Equation

In the following discussion the English system of units is used, primarily because most data regarding magnetic materials is supplied in this

system. Flux is specified in lines (or Maxwells) and flux density in lines per square inch. If flux is expressed in Webers the 10^{-8} term in the following equations must be omitted.

The second term in Eq. 2.2 is the induced voltage in the primary due to the magnetizing flux.

$$e_1 = -N_1 \, d\phi_m/dt \qquad 2.16$$

Assume now that the magnetizing flux is sinusoidal, and ϕ_p is its peak value

$$\phi_m = \phi_p \cos \omega t \qquad 2.17$$

In power transformers this assumption is quite realistic since the voltage is essentially free of harmonics. If there is a high degree of saturation, the assumption of a sinusoidal magnetizing current, section 2.2, is only an approximation. Substituting Eq. 2.17 in 2.16

$$e_1 = -N_1 \, d(\phi_p \cos \omega t)/dt$$

or

$$e_1 = -N_1 \omega \phi_p (-\sin \omega t) \; 10^{-8}$$

$$= N_1 \omega \phi_p \sin \omega t \; 10^{-8} \text{ volts} \qquad 2.18$$

The peak value of induced voltage occurs when $\sin \omega t = 1$

$$e_{1(p)} = 2\pi f N_1 \phi_p \; 10^{-8} \text{ volts} \qquad 2.19$$

Eq. 2.19 can be converted to RMS values by dividing both sides of the equation by $\sqrt{2}$

$$E_1 = e_{1(p)}/\sqrt{2} = 2\pi f N_1 \phi_p \; 10^{-8}/\sqrt{2}$$

$$E_1 = 4.44 \, N_1 \, f \, \phi_p \, 10^{-8} \text{ volts} \qquad 2.20$$

This is the transformer equation expressing Faraday's Law and useful in designing the transformer windings. Note that the flux is retained as the peak value of the sinusoidal wave since maximum flux density is one of the design parameters. The use of maximum flux density is sometimes more appropriate, hence

$$E_1 = 4.44 \, N_1 \, f \, B \, A \; 10^{-8} \text{ volts} \qquad 2.21$$

where B is expressed in lines per sq. in.; the cross sectional area of the core A, is in sq. inches. The maximum or peak value of B is always used since it represents the magnetic stress of the core material used.

A sinusoidal flux wave was assumed here. Under these conditions the flux induces a sinusoidal voltage wave as indicated in Eq. 2.18. Conversely, on the basis of Faraday's Law, a sine wave of voltage applied to a transformer with negligible resistance and leakage flux will always produce a sinusoidal flux wave. However, because of Faraday's Law anything other than a sinusoidal form of one will create a substantially different shape in the other.

2.4 The Saturation Curve and the Graphical Determination of the Magnetizing Current Wave

The relation between the flux (or flux density) and the MMF (or current since current = MMF ÷ turns) for the magnetic path in iron is represented by the curve in Fig. 2.3(a). This is shown for both the positive and negative half cycles of flux. Assume that the flux wave is established, shown in Fig. 2.3(b) as sinusoidal. The required current wave can be constructed as follows: Begin at a point on the flux wave corresponding to some angular position on the time scale, such as 30°. Transpose to the saturation curve, then project down to an intersection with the 30° line on the time scale of current. This gives one point on the required current wave. Proceed in this manner for several points of time on both the positive and negative half cycle of the flux wave. The result will be the current wave at (c) in Fig. 2.3. This shape is made up of a fundamental and harmonics, including a large 3rd harmonic with the phase position shown in Fig. 2.3(d). The non-linearity in the saturation curve is responsible for the occurrence of these harmonics.

If a sinusoidal current is forced through the primary the flux will contain predominantly the 3rd harmonic. By using a reverse analysis in Fig. 2.3 from (c) to (a) to (b), it is found that the flux has a flat top, indicating that the third harmonics are reversed 180° from those shown at (d) for the current.

The harmonics required for the non-linearity can be supplied by either the current or the flux. For example, in three-phase transformers, one additional winding is often provided in each phase which can be connected with the other phases in series so that the fundamentals cancel but the 3rd harmonics add. This provides a circulating harmonic current in the extra windings, to supply the non-linearity required by the core, hence the magnetizing current in the primary, the flux, and the induced voltage are all sinusoidal.

The distorted magnetizing current in a single phase transformer must flow through any series impedance that may be in the line. The impedance drops are illustrated in Fig. 2.4. The distorted voltage drops when subtracted from a sine wave of line voltage results in a distorted induced voltage. For this reason a transformer that has a high internal winding resistance, or high leakage reactance, can have a distorted output voltage.

Another important fact to notice is that the voltage e_1 in Eq. 2.18 leads the flux in Eq. 2.17 by 90°. We will make use of this significant fact later.

2.5 The Hysteresis Loop and the Graphical Determination of Total Excitation Current

The magnetizing current discussed in the previous section is the major part of the total no-load current, or excitation current i_n. Another component i_{h+e} is the current needed to supply the hysteresis and eddy current losses in the core. The phasor sum of the two components is the total excitation current

$$I_n = I_m + I_{h+e} \qquad 2.22$$

The hysteresis loop is shown in Fig. 2.5(a) corresponding to the flux at (b). When a sinusoidal flux wave is developed in the core, the required excitation current is developed graphically at (c) in a manner similar to that used with Fig. 2.3. The current is now an unsymmetrical wave; that is, the second quarter cycle is no longer a mirror image of the first quarter cycle.

Hysteresis is an energy phenomenon and thus requires a component of current in phase with the voltage of the same frequency. This is a sinusoidal component I_{h+e} leading the magnetizing current by 90°, as shown in Fig. 2.6 (a). The exciting current has the shape shown in Fig. 1(c), but only its fundamental can be represented on the phasor diagram. Figure 2.6(b) shows a more accurate point-by-point addition of the i_m and i_{h+e} waves to produce the total exciting current i_n. This current has the same form as that developed in Fig. 2.5. The dissymmetry is caused by the 90° displaced component for the hysteresis and eddy currents. Some "feel" for the effect of the hysteresis and eddy currents can be had by observing the degree of dissymmetry of the exciting current.

It is interesting to note that the effects of hysteresis and eddy currents tend to oppose any change in flux. When the MMF is increasing in a positive direction (points on the curve marked with o) the flux is less than that of the saturation curve. When the MMF is increasing in a negative direction (points on the curve marked with x) the flux is above the saturation curve. In a way it behaves according to the principle of Constant Flux Linkages.

Let several successive loops be plotted for several successively greater values of voltage and flux. Each loop completely incloses the preceeding one, and the tips of the hysteresis loops follow the saturation curve.

2.6 The Transformer Equivalent Circuit

The transformer can be represented quite accurately by an equivalent circuit and this helps considerably in understanding its behavior. In section 2.2 it was shown that the leakage and magnetizing fluxes can be represented by two inductances in series. There is, in addition, a resistance in the winding that consumes a voltage drop. The sum of all of these voltage drops associated with the primary of the transformer with no load, must equal the voltage applied to its terminals. That is

$$\overline{V}_1 = \overline{I_n R_1} + \overline{I_n \omega L_1} + \overline{I_n \omega L_m}$$

$$= \overline{I_n R_1} + \overline{I_n \omega L_1} + \overline{E_1} \qquad 2.23$$

The core loss can be represented by the current I_{h+e} flowing through a resistor. In the equivalent circuit this resistor can be placed across the induced voltage, that is, in parallel with the magnetizing inductance L_m. The currents I_m and I_{h+e} then combine in parallel to give the exciting current I_n, which flows through winding resistance and leakage inductance in series. Therefore there is a 90° phase displacement between the resistance and leakage reactance drops. Using the reactance equivalent of inductance and complex nomenclature, Eq. 2.23 becomes

$$V_1 = I_n(R_1 + jX_1) + E_1 \qquad 2.24$$

Equations 2.23 and 2.24 are represented by the equivalent circuit in Fig. 2.7(2).

The numerical difference between V_1 and E_1 in high quality transformers is quite small (2 or 3% but in Extra High Voltage transformers up to 12% may be expected). It is the value of E_1 that should be used in the transformer design equation (2.21), although the line voltage V_1 is frequently used because of the small difference.

A similar equivalent circuit represents the secondary, and, of course, it is useful only when the transformer is delivering a load current. The secondary current produces a leakage flux as does the primary current, and likewise there is a secondary leakage inductance L_2 and a secondary leakage reactance X_2. Also the resistance of the secondary winding must be considered.

The secondary induced voltage depends on the number of turns in the secondary winding. (Eq. 1.42)

$$E_2 = N_2/N_1 \ (E_1)$$

The secondary terminal voltage $V_2 = E_2$ at no load, but when current flows in the secondary, the resistance and leakage reactance drops must be subtracted from the induced voltage

$$V_2 = E_2 - I_2 \ (R_2 + jX_2) \qquad 2.25$$

Fig. 2.7(b) is the simplified equivalent circuit for the transformer in which the core loss resistor has been dropped because its effect is usually negligible in voltage relations. There exists other forms, some more complex and others more simple than Fig. 2.7(b). The one shown is the most useful since it is directly related to the phasor diagram discussed next.

2.7 The Transformer Phasor Diagram

The sinusoidal flux wave shown in Fig. 2.8(a) is actually a cosine wave. When this wave is differentiated graphically, the wave identified as $d\phi_m/dt$ is obtained. Faraday's Law has a (-) sign for induced voltage. The (-) of the $d\phi_m/dt$ wave is shown as the induced voltage curve e. The wave e is a sine wave and it is in accordance with Eq. 2.7 and 2.18. The important observation is that the induced voltage wave lags the flux wave by 90°. There must be a component of applied voltage that directly opposes the Faraday Law induced voltage.

The phasor diagram of the transformer with load consists of phasor components of applied voltage and input currents, and also of phasor components of output voltage and current. Strictly speaking the true induced voltage is not shown on the phasor diagrams but the components of applied voltage are used in its place. These components are designed by the symbol E. Thus the magnetizing flux ϕ_m lags the phasor E_1 by 90°, because $E_1 = -e_1$. This is the basis for the transformer phasor diagram.

From Eq. 1.19 the flux and the fundamental of current are in phase. Fig. 2.8(b) shows the waves of all of the parameters, in their proper phase relations, of a transformer on no-load. The no-load phasor diagram showing the same parameters and phase relations is developed in Fig. 2.9(a). The small resistance and reactance drops not shown in Fig. 2.8(b) are exaggerated in the phasor diagram. The resistance drop, of course, is in phase with the current and the reactance drop leads the current by 90°. The phasor equation is:

$$\bar{V} = \bar{E}_1 + \bar{I}_n R_1 + \bar{I}_n X_1 \qquad 2.26$$

The triangle formed by the resistance and reactance drops is called the impedance triangle. In the no-load case the impedance triangle is small and thus V_2 is approximately equal to $V_1 N_2/N_1$. With no load there is no secondary impedance triangle, Therefore $V_o = E_2$.

When a load is added to the secondary there is a current in the secondary winding which produces an impedance drop. In constructing the diagram Fig. 2.9(b) one must start with the load voltage V_2, the load current I_2, and the phase angle δ between them as dictated by the load. The phasor equation for the secondary is:

$$\bar{E}_2 = \bar{V}_2 + \bar{I}_2 R_2 + \bar{I}_2 X_2$$

The components of the impedance triangle can be added to V_2 in their proper phase position to obtain the secondary no-load, (or induced) voltage, E_2. From the position of the latter phasor, the flux ϕ_m can be added.

The primary component of load current is 180° from I_2 and its magnitude is $I_1 = I_2 N_2/N_1$. The primary load current is added to the excitation current to give the total input current and its proper phase position.

The secondary part of the diagram can be rotated 180° and superposed on

the primary, with the proper turns ratio applied to each phasor. The impedance triangles can be combined into one equivalent tirangle. This makes the most simple diagram and from this the equivalent circuit consists of nothing more than an equivalent resistance and reactance in series with the line. This simple diagram is useful for quick calculations but for our purpose of greater understanding we will use diagrams similar to those of Fig. 2.9.

2.8 The No-Load Block Diagram

There is no practical equation for determining the exciting current in a transformer, because the current depends on the requirements of the material through which the flux passes. The saturation curve establishes the magnetizing current I_m for an given flux, flux linkage, or flux density. Manufacturer's curves are available also for all types of core material which s show the total core loss per pound of material for the range of flux densities commonly used. This loss may include both the hysteresis and eddy current losses although each loss is available separately.

The current required to supply these losses (I_{h+e}) can be calculated (I_{h+e} = core loss/line voltage). This current and the value of I_m can be added as phasors as in Fig. 2.9(a), to give the total exciting current I_n. In all cases there must be enough magnetizing current I_m to produce the flux necessary to generate the required induced voltage. Therefore there is a rigorous relation between I_m and E_1. Whenever there is a change in one there is an immediate reaction in the other.

It is helpful to understand all of the relations of all the transformer variables by the circuit approach to the block diagram. The block diagram for the transformer on no load is considered first.

All of the quantities in the transformer equation 2.20 can be considered as constant except ϕ_p. Letting K_1 represent these constants, Eq. 2.20 becomes

$$E_1 = j K_1 \phi_p \qquad 2.27$$

The symbol j is used because the flux and voltage are displaced by 90° in phase. The RMS steady state equation, from Eq. 2.24, can now be written:

$$V_1 = I_n (R_1 + jX_1) + jK_1\phi_p \qquad 2.28$$

Solving for I_n,

$$I_n = \frac{V_1 - jK_1\phi_p}{R_1 + jK_1} = \frac{V_1 - E_1}{R_1 + jX_1} \qquad 2.29$$

The relation between I_m and ϕ_m is established by Equations 1.19 and 1.20

$$\phi_m = N I_m A \mu/G$$

$$\phi_m = H A \mu$$

But the permeability in both equations is not constant. Hence the relation is best depicted by a saturation curve in which ϕ_m is plotted directly against I_m. Such a saturation curve makes it possible to illustrate Eq. 2.29 by a block diagram as in Fig. 2.10. The core loss component of current is included in Eq. 2.28 and shown in the block diagram although its effect generally can be neglected just as in the case of the equivalent circuit.

From Eq. 2.29 as well as the block diagram, the magnitude of I_n depends upon the quantity $(V_1 - jk_1\phi_m)$. A change in V_1 causes a change in current through the saturation curve block. A change in ϕ_m occurs and this in turn changes the value of E_1. The system is stable when the conditions shown in the block diagram are met.

The quantities V_1 and E_1 are phasors and their difference voltage may be caused by a difference in magnitude or phase angle or both. A small change can produce a large difference voltage, resulting in a large change in magnetizing current at no load.

A change in load current can change both the magnitude and phase position and thereby allow a current change to occur in the primary. This is discussed more thoroughly below.

2.9 Flux Reactions Under Load and the Load Block Diagram

Figure 2.11 is a schematic diagram of the transformer used in the laboratory. It includes the several components of flux and the equivalent circuit of the primary and secondary. The leakage fluxes ϕ_1' and ϕ_2' are responsible for the leakage reactances X_1 and X_2. The magnetizing MMF $(N_1 I_m)$ forces the flux ϕ_m through the core.

The secondary current I_2 and the secondary turns N_2 are the source of the MMF that produces the load flux component ϕ_2. For the moment, let us assume that this flux is allowed to link with primary. It would greatly alter the main flux in the core and cause a large change in the voltage in N_1. The latter change would require a large current I_1 to flow in the primary, as dictated by Eq. 2.29. The current I_1 however produces an MMF and flux component ϕ_1 in the primary that directly opposes component ϕ_2. A stable condition is reached when

$$\phi_2 = -\phi_1 \qquad 2.30$$

Both of these flux components flow in the same path and the same reluctance applies. Thus we have another important transformer equation showing a balance of primary and secondary load current MMF's.

$$\phi_2 = N_1 I_2 / \mathcal{R} = -N_1 I_2 / \mathcal{R} = -\phi_1$$

or numerically

$$N_2 I_2 = N_1 I_1$$

or

$$I_1 = (N_2 / N_1) I_1 \qquad 2.31$$

The total current flowing in the primary winding is the phasor sum of the exciting current and the load component as in Fig. 2.9(b)

$$I_{11} = I_1 + I_n \qquad 2.32$$

Since the load flux components cancel, the net flux remaining in the core is ϕ_m, and the only induced voltage is E_1. The total current I_{11} in the primary produces a proportional resistance and reactance drop in the primary. The primary voltage equation now becomes

$$V_1 = I_{11}(R_1 + jX_1) + jK_1\phi_m \qquad 2.33$$

From this

$$I = \frac{V_1 - jK_1\phi_m}{R_1 + jX_1} = \frac{V_1 - E_1}{R_1 + jX_1} \qquad 2.34$$

This equation is amenable to a block diagram representation as in Fig. 2.12. Note that the secondary load current cancels the primary load component I_1, leaving I_n (and thence I_m) as the only current producing flux just as in the no-load condition. The flux density, the magnetizing current, and the induced voltage remain essentially unchanged when load is applied except the small changes required to balance Eq. 2.34. This fact can be demonstrated in one of the experiments described later.

In the application of transformers it is important to identify and maintain proper polarity throughout the system. When current flows into the primary at the + terminal it must flow out of the secondary at the + terminal. In Fig. 2.1 the secondary is shown with its winding linking the flux ϕ_m in the same manner as the primary. If the secondary could be slipped around the core to the primary side it would be identical to the primary. In order to establish the required secondary flux, the current must flow out at the lower or +, secondary terminal. The secondary is wound in the reverse direction in Fig. 2.11, hence the upper terminal is +.

2.10 The High Reactance Transformer

The high reactance transformer is unimportant as a power transformer and it is used for special applications. Its exaggerated leakage flux makes it useful in understanding the physical behavior of flux in some complex transformer phenomena. Some of these are discussed later. The general background in the preceding sections applies equally well to the high reactance transformer, with the consideration of a few additional parameters. Fig. 2.13 is a schematic diagram, similar to Fig. 2.11, except that a shunt path is provided to greatly increase the leakage flux between the primary and secondary. The magnetic flux from the primary divides in two paths; one, ϕ_s, through the secondary and the other ϕ_{sh}, through the shunt path. The path through the secondary is through the same material as that through the primary. The path through the shunt is partially through iron and partially through air. The air path dominates the shunt characteristics and therefore its reluctance is essentially constant.

The MMF across the points o and p in Fig. 2.13 has nearly the same shape

as the magnetizing current i_m and it is shown in Fig. 2.14. The flux ϕ_{sh} through the linear shunt path has the same shape as the MMF. If a sinusoidal voltage is applied to the primary winding, the fluxes ϕ_{sh} and ϕ_s must add to a sine wave of flux ϕ_m in the primary core. Therefore ϕ_s must have a flat top as shown in Fig. 2.14.

The derivative of a flat top flux will induce a peaked secondary voltage wave and this can be experimentally observed in the high reactance transformer used in the laboratory.

The high leakage flux through the leakage shunt path causes a high reactance drop in both the primary and secondary, as shown in the phasor diagram in Fig. 2.15. Due to the high reactance drop in the secondary, the load voltage V_2 lags the induced voltage E_2 by the large angle θ'. The primary reactance drop causes the induced voltage E_1 to lag the applied voltage V_1. The secondary open circuit voltage V_o on the diagram is 180° from V_1. The secondary load voltage therefore lags the open circuit (or no-load voltage by the larger angle θ. This angle may approach 90° in very high reactance transformers. The same result is obtained by rotating the primary part of the diagram 180° whence V_1 superposes on V_o. The rotated primary resistance and reactance drops are shown as dotted phasors. All rotated phasors of voltage and current must be multiplied by the corresponding turns ratio. Voltage phasors rotated into the secondary must be multiplied by N_2/N_1 and current phasors by N_1/N_2.

The load voltage and current waves for a resistance load are shown in Fig. 2.16 in relation to the open circuit voltage, V_o.

The high reactance transformer actually converts a voltage source into a current source. The load current tends to be sinusoidal while the voltage assumes any shape required by the load.

The behavior of the high reactance transformer discussed above is well illustrated by the following example: Let a $\frac{1}{2}$ wave rectifier and resistor in series be connected to the secondary of a high reactance transformer. The currents and voltages are shown in Fig. 2.17 for more than one complete cycle. The current and voltage begin at point a, θ degrees behind the open circuit voltage. During the half cycle from a to b to c, the current and terminal voltage V_2 have the same shape, nearly sinusoidal. At the end of the half cycle the current becomes zero and remains there for the next half cycle. At c the load becomes zero and the voltage at the terminals of the transformer becomes equal to the open circuit voltage at that instant, d. The open circuit voltage follows the curve d, e, f for the next half cycle. At point g, the current flows again and the terminal voltage follows the curve g, h, i for the next half cycle. The terminal voltage that appears on an oscilloscope connected to the secondary terminals is the complex wave a, b, c, d, e, f, g, h, i for one full cycle. The terminal voltage can be very complex, but predictable, when the load is an arc discharge or a fluorescent lamp or neon light.

The secondary flux ϕ_s and terminal voltage V_2 may be complex while the primary voltage and flux are sinusoidal. As previously mentioned, the secondary and shunt fluxes must combine into a sine wave. In order for this to be

possible, the shunt flux must contain harmonics that will cancel those in the secondary flux. This means that the harmonic flux circulates in the secondary core and through the shunt path as shown in fig. 2.13. These facts can be observed experimentally.

2.11 Transformers for Experimental Work

Some special transformers have been designed and manufactured particularly for this laboratory. They are standard transformers in every respect except that special windings have been built-in to provide important information about the internal behavior of the transformer.

Figures 2.13 and 2.11 are simplified representations of the high and low leakage reactance transformer. In the latter both the primary and secondary consists of two windings that can be connected in series for 220 volts or in parallel for 110 volts, or any combinations of windings can be used if the rating of the winding is not exceeded. Six volt windings are provided for the primary and the secondary.

The winding terminals are marked with standard transformer nomenclature, and the actual wiring diagram should be consulted for details.

The simplified diagrams showing only one winding each for the primary and secondary are used in all experimental circuit diagrams. The equivalent resistances and reactances shown, of course, are not physical circuit elements but are internal characteristics of the windings. The induced voltage E_1 therefore is not available for observation or measurement. The voltage E_3 across terminals Y_1 and Y_2 of the information winding N_3 is induced by the same flux ϕ_m that induces E_1. This voltage is at all times proportional to E_1 regardless of the resistance and reactance voltage drops, providing a negligible current is taken from winding N_3. Likewise the voltage E_4 is proportional to the secondary induced voltage E_2. Table I(p.2.14) outlines the quantities that can be observed, measured or calculated from the information windings or from the voltage drop across the resistors r_1, r_2, and r_3 in Fig. 2.11.

2.12 Induced Voltage, Flux and the Integrating Circuit

The two exploring windings in N_3 and N_4 in Fig. 2.11 are useful in experimental work because the generated voltages represent Faraday's Law. The induced voltage in N_3 is directly proportioned to E_1. Thus voltage at terminals of N_3 is

$$E_3 = E_1 N_3/N_1 \qquad 2.35$$

The induced voltage is

$$e_3 = N_3 \, d\phi_m/dt$$

$$d\phi_m = (e_3/N_3)dt \qquad 2.36$$

or

$$\phi_m = \frac{1}{N_3} \int e_3 \, dt \qquad 2.37$$

TABLE I

Quantities Represented by Voltages in Fig. 2.11

VOLTAGE	TERMINALS	QUANTITIES REPRESENTED
V_1	H_1, 1	Line Voltage
V_2	X_1, 2	Load Voltage, or Open Circuit Voltage
E_3, E_4	Y_1, Y_2 or Y_3, Y_4	Voltage induced by ϕ_m
Ir_1	H_4, 1	(a) Excitation Current at no-load I_n (b) Total line current with load ($I_{11} = I_1 + I_n$) (c) Total Flux ($\phi_{11} = \phi_1 + \phi_m$) (d) Total Ampere-turns (or MMF) in primary
Ir_2	X_3, 2	(a) Load Current I_2 (b) Load Component of flux ϕ_2 (c) Ampere-turns (or MMF) in secondary
Ir_3	Y_4, 3	Hysteresis and Eddy Currents I_{h+e}
$I_n r_1 - Ir_3$	H_4, 1 - Y_4, 3	Magnetizing Current I_m with no-load ($I_n - I_{h+e}$)
$I_{11} r_1 - I_2 r_2$	H_4, 1 - X_3, 2	Exciting Current I_n with load
$\int E$	Y_1, Y_2 + Fig. 2.18	Magnetizing Flux ϕ_m

Thus by integrating the induced voltage in N_3 we have a quantity proportional to the flux ϕ_m.

One method of integrating the voltage is with a high resistance in series with a large capacitor connected to the terminals Y_1 Y_2 as in Fig. 2.18. The circuit voltage is

$$e_3 = r_o i_o + \frac{1}{C} \int i_o \, dt \qquad 2.38$$

If r_o is very large compared with the impedance of the capacitor, then

$$i_o \tilde{\sim} ke$$

Thus

$$e_3 = r_o i_o + \frac{k}{C} \int e_3 \, dt \qquad 2.39$$

Hence from 2.37 the voltage across the capacitor is proportional to flux,

$$\phi_m \simeq \frac{k}{C} \int e_3 \, dt = V_c \qquad 2.40$$

2.13 PREDICTING THE BEHAVIOR OF FERRORESONANT SYSTEMS

Ferroresonance is a phenomenon of instability associated with a system consisting of resistance, capacitance and non-linear inductance. A substantial sudden jump in voltage or current may occur across the terminals of one or more elements, and this jump may be initiated by a change in any of the system elements. Occasionally this phenomenon is encountered in various aspects of a power system from a room airconditioner to transmission and distribution system.

Ferroresonance is a mysterious phenomenon with respect to a practical understanding of its physical behavior. A rigorous mathematical analysis is difficult because of the non-linear characteristics, and its complexity does not contribute to a simple physical understanding. The purpose of this section is to present a physical concept and to develop a simplified analysis from which the phenomenon of ferroresonance can be predicted.

A The Ferroresonant Circuit

There are two general forms of a circuit involving resistance, capacitance and a non-linear inductance which will exhibit ferroresonance. One is a parallel circuit shown in Figure 2.24(a) and the other the series circuit, Figure 2.24(b). Both of these circuits may produce ferroresonance if a unique relationship exists between the various elements.

Both circuits are analogous to some conditions on a transmission or distribution system. For example, the parallel circuit is analogous to a transmission line with resistance R and capacitance C connected to a transformer feeding a load r. The series circuit is similar to the distribution circuit where a series capacitor is used with the transformer L.

This paper will analyze only the parallel circuit of Figure 2.24(a), but a similar method of analysis can be applied to the series circuit.

B Simplified Graphical Analysis

The analytical method used nothing more complex than phasor calculations. However, a significant understanding of ferroresonance can be gained by a graphical approach.

There is one important prerequisite for ferroresonance. At some point along the range of operation there must be a conventional resonance between the non-linear inductance and the capacitance. This can be illustrated as follows: Assume the resistance r is very large and its current negligible.

Let the volt-ampere curve for the non-linear inductance be the curve OAQB in Figure 2.25. The values of current and voltage are plotted in RMS values. Let absolute values for the volt-ampere curve OQC for the capacitor be superposed on the curve of the inductance. It must be recognized that these two currents are 180° out of phase. The input current i_o is therefore the horizontal distance between the two curves. The intersection Q is the conventional resonance.

Now let us plot the input current i_o against the voltage V as in Figure 2.26. As V increases i_o will increase, reach a maximum at a_1, go to zero at point O and then increase beyond Q. The value of the capacitor current i_c, Figure 2.25, is greater than i_x to the left of Q but less than i_x beyond Q. Thus there will be a 180° phase reversal in passing through Q. The current in Figure 2.26 however is plotted in absolute values as would be read on an RMS ammeter. Now suppose we force a continuously increasing current through the circuit. The relations between V and i_o will follow the curve o a, to the point a_1. If the current continues to increase, the next higher value will be at a_2 on the curve QC. The voltage will jump from V_1 to V_2. Further increases of current will follow the curve a_2 C.

Now let us begin a gradual reduction of current. The voltage-current relations initially will follow that section of the curve CQ. In a physical circuit, the current at Q will not be zero, because there will always be some real value of r. The current will reach therefore a minimum value of a_3 instead of zero at point Q. When the current is reduced to a_3, the next lower value is at a_4 on the curve section o a, and a sudden jump in voltage from V_3 to V_4 will occur.

The above discussion presents a simplified version of ferroresonance. That section of the curve o a_1, in Figure 2.26 is perfectly stable for all changes in current providing the point a_1 is not exceeded. Once a_1 is passed the curve a_3 C represents another stable condition, providing the current never becomes less than a_3. If i_o does become less than a_3 the stability curve o a_1 is re-established. Thus there are two stable states with a discontinuity between them.

If any one of the quantities indicated in Figure 2.24(a) is varied while the others are held constant, the ferroresonant phenomenon can be observed. Some of these conditions are analyzed from phasor diagrams in the following section.

C Phasor Analysis

The phasor diagram for Figure 2.24(a) is shown in Figure 2.27. The linear capacitor current can be represented by the equation,

$$i_c = k\ V \qquad 2.41$$

where k is a constant.

Let a simple equation representing the general shape of the saturation curve for the iron core inductance be

$$i_x = M\ V^4 \qquad 2.42$$

where M is a constant.

From the phasor diagram the following relations apply:

$$i_o = i_c - i_x \qquad 2.43$$

substituting 2.41 and 2.42 in 2.43,

$$i_o = k\,V - M\,V^4 \qquad 2.44$$

The line current is,

$$I = [i_o^{\,2} + i_r^{\,2}]^{1/2} \qquad 2.45$$

but

$$I_r = \frac{V}{r}$$

Therefore,

$$I = [(k\,V - M\,V^4)^2 + (\frac{V}{r})^2\,]^{1/2} \qquad 2.46$$

also,

$$V_R = I\,R$$

$$= R\,[\,(k\,V - M\,V^4)^2 + (\frac{V}{r})^2\,]^{1/2} \qquad 2.47$$

Again from the phasor diagram

$$E^2 = V^2 + V_R^{\,2} + 2\,V_R\,V\cos\theta \qquad 2.48$$

where,

$$\cos\theta = \frac{i_r}{I}$$

Therefore,

$$E^2 = V^2 + [\,(k\,V - M\,V^4)^2 + (\frac{V}{r})^2\,]\,R^2 + \frac{2IRVi_r}{I} \qquad 2.49$$

$$= V^2 + R^2\,k^2\,V^2 - 2\,k\,M\,R^2\,V^5 + M^2\,R^2\,V^8 + \frac{V^2\,R^2}{r^2} + \frac{2\,V^2\,R}{r} \qquad 2.50$$

$$= V^2\,[\,M^2\,R^2\,V^6 - 2\,k\,M\,R^2\,V^3 + (\frac{R^2}{r^2} + \frac{2\,R}{r} + R^2\,k^2 + 1\,)\,] \qquad 2.51$$

or finally,

$$M^2\,R^2\,V^6 - 2\,k\,M\,R^2\,V^3 + \frac{R^2}{r^2} + \frac{2\,R}{r} + R^2\,k^2 + \frac{V^2 - E^2}{V^2} = 0 \qquad 2.52$$

Equation 2.52 permits the values of V to be calculated for a range of any one parameter when all other values are held constant. Thus the value of E for incremental values of V is:

$$E = [\, M^2 R^2 V^8 - 2 k M R^2 V^5 + Y V^2 \,]^{1/2} \qquad 2.53$$

where

$$Y = \left(\frac{R^2}{r^2} + \frac{2R}{r} + R^2 k^2 + 1 \right)$$

Throughout the analysis a reference circuit is used with circuit values as in Table I.

TABLE I

$M = 19.5 \times 10^{-8}$

$R = 50$ ohms

$r = 80$ ohms

$k = 0.1$

$E = 125$ volts

Any one of these parameters may be considered as a variable (as E in equation 2.53, and the relation of this variable to V can be obtained.)

D Ferroresonance as a Function of Line Voltage

If E (equation 2.53) is calculated for a range of values of V while all other parameters are held constant, the curve in Figure 2.28 is obtained. As the line voltage is increased from zero to 208 volts the value of V follows the stable path o a_4 a_1. This is stable state I. If E is increased beyond 208 volts the voltage V jumps from 50 volts to 88 at a_2 and thereafter follows curve a_2 c. The circuit is now in a stable state II and will remain in this condition until the line voltage is reduced to 129 volts or to point a_3. A further reduction causes the circuit to suddenly return to stable state I. Figure 2.29 shows a family of curves each similar to Figure 2.28 except for different values of line resistance R. Note that if R is less than 17 ohms the curve has no maximum and minumum values and therefore no ferroresonance will occur.

The criteria for ferroresonance is the minimum and maximum values in the E vs V curve. These points can be calculated by taking the derivative of equation 2.52 and setting it equal to zero. When this is done we obtain the value of V at which ferroresonance occurs. Thus,

$$V_1 = \frac{\frac{+1.25\,k}{M} - \left[\left(\frac{1.25k^2}{M}\right) - 4 \left(\frac{Y}{4M^2R^2}\right) \right]^{1/2}}{2} \qquad 2.54$$

and

$$V_2 = \frac{+1.25k}{M} + \frac{\left[\left(\frac{1.25k}{M}\right)^2 - 4 \left(\frac{Y}{4M^2R^2}\right) \right]^{1/2}}{2} \qquad 2.55$$

E Ferroresonance as a Function of Line Resistance

From equation 2.52 a quadratic equation for the line resistance R in terms of all other parameters can be obtained. This equation is,

$$R = \frac{-2}{rP} \pm \frac{\left[\left(\frac{2}{rP}\right)^2 - 4 \left(\frac{V^2 - E^2}{V^2 P}\right) \right]^{1/2}}{2} \qquad 2.56$$

where,

$$P = (M^2 V^6 - 2 k M V^3 + \frac{1}{r^2} + k^2)$$

The 1620 computer was programmed to solve this equation and the family of curves in Figure 2.30 was obtained. It is possible, but quite difficult to take the derivative dR/dW of this equation and determine the maximum and minimum values of R at which the jumping phenomenon will occur. Figure 2.30 shows however, that ferroresonance will not occur for any value of R if the load resistance is 20 ohms or less as shown by curve 3. A change in M shifts the value of V at which ferroresonance occurs.

F Ferroresonance as a Function of Load Resistance

Equation 2.52 may be re-arranged as a quadratic equation for the load resistance r, in terms of other circuit parameters. Thus,

$$r = \frac{-2R}{T} \pm \frac{\left[\left(\frac{2R}{T}\right) - 4 \frac{R}{T} \right]^{1/2}}{2} \qquad 2.57$$

where,

$$T = \frac{V^2 - E^2}{V^2} + R^2 k^2 - 2 k M R^2 V^3 + M^2 R^2 V^6$$

Figure 2.31 is a family of curves of r plotted against V for several circuit parameters for a range of load resistance. The same criteria for ferroresonance applies as before, that is a maximum and minimum value in the curve. Curve 3 has no maximum or minimum value and hence ferroresonance cannot occur. This condition exists for a line voltage of 200 volts and a series resistance of 30 ohms. Other values are the same as in the reference circuit. This circuit is therefore stable for all values of load resistance.

G Ferroresonance as a Function of Capacitor Size

The value of k in equation 2.41 is a measure of the size of the capacitor. Re-arranging equation 2.52 to solve for k we have

$$k = \frac{2 M V^3 + [(2 M V^3)^2 - 4(Z)]^{1/2}}{2} \qquad 2.58$$

where,

$$Z = M^2 V^6 + \frac{1}{r^2} + \frac{2}{Rr} + \frac{V^2 - E^2}{V^2 R^2}$$

Figure 2.32 shows the relationship of k and V, for two sets of circuit parameters. The curves are somewhat different from those in Figures 2.29, 2.30 and 2.31. The curves shown have no maximum value because the quantity under the square root becomes negative at point c, b_1, d_1 and a_2 for curves in Figure 2.31. The ferroresonant behavior for the solid line curve is as follows:

As the value k decreases (decreasing size of capacitor) the voltage follows the curve o a a_1 to point a_1. If k is further reduced ferroresonance occurs and the voltage jumps to stable state II at point a_2 on curve b a_2 b_1. This curve is obtained by using the - sign in equation 2.58 while the curve o a a_1 c is for the + sign. When k is further reduced the voltage V follows the curve a_2 b. If k is now increased the voltage follows b a_2 b_1 to b_1 at which the voltage jumps to stable state I at point b_2 on the original curve.

H General Considerations

Ferroresonance can be created by changing the shape or magnitude of the saturation curve of the inductance, but calculations have not been completed for this condition. The analysis above has been made on an assumed circuit. All of the phenomena described have been observed experimentally, and the behavior is identical to that predicted above. However an actual comparison of experimental and predicted behavior on a physical circuit has not been made.

It is reasonable to predict that ferroresonance will be encountered by the Electric Utilities more frequently in the future. Higher transmission and distribution voltages will present a different relationship between the transformer saturation curve and line capacitance. This change is in the direction of a greater probability for ferroresonance.

An electromagnetic relay with a non-linear saturation curve may, in conjunction with some circuit capacitance, experience ferroresonance. This in turn could cause an unexplained malfunction because there may be no retained evidence that ferroresonance occured.

2.14 Experiments

A great many experiments and observations can be made with these special transformers in the laboratory. The oscilloscope is the ideal instrument for observing the behavior of various quantities. It has one input terminal grounded, and may need to be connected to any of several places in the circuit. Furthermore some of the experiments require the interconnection of windings and circuit elements. For these reasons it is important for the source of supply voltage to be insulated and isolated from ground. One of the standard test transformers can be used for this isolating purpose by inserting it in the line ahead of everything else. In all of the circuits for experiments this transformer will not be shown but it is assumed that it is permanently connected in the line.

Excellent flexibility is gained by using a variable voltage source, hence the Volt-Pac is shown in all the circuit diagrams.

TRANSFORMER EXCITATION

Experiment No. 2.1

1) Adjust V_1 in Fig. 2.19 to zero voltage. Connect the vertical plates of a scope to points 2 and 3. Observe the variation in distortion of the magnetizing current as V_1 is increased from zero to maximum. Adjust the sweep so that about two full cycles can be observed. Photograph or trace this wave shape for several values of voltage. It represents the exciting current I_n. Note the change in distortion and particularly the dissymmetry, as V_1 is varied.
2) Connect the scope to Y_1Y_2 and observe and record the shape of induced voltage over a range of input voltage.
3) Insert 25 to 50 ohms in the H_1 line. Now repeat 1 and 2.
4) Make enough variations in experiments to allow you to explain all of the observed results.
5) Re-connect the same as for (1) without the resistor in the H_1 line. Set the sweep of the scope at its lowest speed. Set V_1 in the neighborhood of 100 volts. Open and close switch several times and observe the transient in exciting current.
6) Connect a potentiometer r_3 in Fig. 2.20 of at least 1000 ohms across terminals Y_3 and Y_4. Connect a portion of this voltage in series opposition to the voltage across r_1. Set V_1 at about 100 volts and close the line switch. Now adjust r_3 until the resultant wave appears to be completely symmetrical. The wave now represents the magnetizing component I_m. Explain.
7) Explain all of the observations made.
8) Proceed with other experiments that may occur to you.

OBSERVING THE BEHAVIOR OF MAGNETIZING FLUX

Experiment No. 2.2

The connections for the experiment are shown in Fig. 2.21. The integrator

is connected across terminals Y_1 and Y_2 with its output connected to the vertical deflection plates of the scope. Set the sweep speed to about 30 cycles so that two complete cycles of flux may be observed.

1) Vary V_1 from zero to its maximum value. Observe the shape of the wave representing the magnetizing flux.
2) Set V_1 at about 100 volts and open and close the line switch and observe the transient behavior of flux. Set the sweep at its lowest speed.
3) Insert 50 to 100 ohms in series with the H line. Place the scope across the terminals Y and Y . Adjust the resistance and the voltage V_1 until the voltage across $Y_1 Y_2$ is distorted. Note its shape. Now connect the scope again to the integrator. Note its shape compared to that of the induced voltage.
4) Explain all of the observations.
5) Proceed with other experiments that may occur to you.

Experiment No. 2.3

OBSERVING THE HYSTERESIS LOOP AND AC SATURATION CURVE OF A TRANSFORMER WITH VARIOUS INPUT VOLTAGES AND LOAD CURRENT.

In Section 2.5, is included a discussion of the effect of the hysteresis loop on the wave shape of the magnetizing current. In this discussion and from Fig. 2.5 and 2.6 it is evident that the hysteresis loop is made up of the saturation curve plus a sinusoidal component. This means that if we could subtract from the hysteresis loop a sinusoidal current equivalent to i_{h+e} in Fig. 2.6a we should get the saturation curve. This can be done according to the diagram, Fig. 2.22.

When a load is placed on the secondary of a transformer, the load component of current in the primary completely obscures the exciting current. Figure 2.22 includes a circuit for subtracting the load component from the line current so that the magnetizing phenomenon can be studied even though the transformer is under load.

This experiment is divided into two parts: Part 1 without load and Part 2 with load.

Part 1: Observing the hysteresis loop and ac saturation curve of the transformer without load.

The load is not connected in this experiment and potentiometers r_4 and r_5 are set at the zero position. Voltage V_3 therefore does not exist. The voltage V_4 represents the transformer induced voltage and when integrated, represents the magnetizing flux. This is connected to channel A of the scope and is the vertical axis of the displayed pattern.

From the potentiometer r_1 the voltage V_1 is obtained which represents the total exciting current, or MMF. With potentiometer r_2 and r_3 set at zero, the only signal supplied to the B channel, the horizontal deflection is the voltage V proportional to the MMF. Set the scope to display A vs B. The conventional hysteresis loop now is observed. Varying the input voltage

will display the loop over a wide range of saturation. As the voltage is varied notice that the tips of the loop describes a path along the center line of the hysteresis loop. This center line is the ac saturation curve.

The voltage from information winding Y_3Y_4 is the induced voltage. Hence the adjustable voltage V_2, is in phase with the induced voltage and when it has the proper magnitude it represents the I_{h+e} component of exciting current. If V_2 is connected in opposition to V_1 and with its magnitude properly adjusted by r_2 and r_3, the hysteresis loop collapses to a single trace ac saturation curve. Theoretically this balance is valid for only one flux density because the eddy currents are proportional to ϕ_m^2 while the hysteresis component is proportional to $\phi^{1.6}$. If the hysteresis portion of losses is small compared to the eddy current losses, the cancellation will be nearly correct for all values of input voltage. (Note: The actual components of I_{h+e} contain some harmonics which may not be canceled exactly by the voltage taken from the information winding Y_3 and Y_4, hence the curve may not be a single trace throughout its length). Observe the behavior of the saturation curve over a wide range of input voltage.

A new type of core loss loop can be obtained as follows: when V_2 is adjusted to cancel the I_{h+e}, this voltage, represents the MMF component due to the core loss. Remove the leads connecting Channel B and connect another pair of leads from channel B directly to the voltage V_2. The image is now an oval with an area equal to that of the hysteresis loop, as shown in the figure 2.23.

Part 2: Observation of the hysteresis loop of the transformer supplying a load.

Connect a medium load to the transformer with r_4 set at zero and V_2 adjusted to cancel I_{h+e}. The image on the scope completely destroys the saturation curve. When the polarities are correct, potentiometer r_4 and r_5 for fine control, can be adjusted to cancel the load component of line current and the image will return to a single trace (approx) saturation curve.

Observe the behavior of the saturation curve, and hysteresis loop by reducing V_2 to zero, over a wide range of loads and input voltages. This provides an experimental varification of the balancing of primary and secondary ampere-turns.

Observe the transient behavior of the hysteresis loop and saturation curve, with and without load, at several values of line voltage, by opening and closing the line switch.

ADDITIONAL SUGGESTIONS FOR EXPERIMENTAL STUDIES-CONVENTIONAL TRANSFORMER

Some suggestions for experimental studies that can be made with the transformer in Fig. 2.19 are:

a. Faraday's Law, constancy of excitation flux and induced voltage.
b. Integral-differential relations between excitation flux and induced voltage, graphical integration and differentiation.
c. Wave shapes of flux, induced voltage, applied voltage, excitation current.
d. Balance of ampere turns, current fluxes, separation of excitation flux in the primary.
e. Study of the physical phenomenon which permits additional current to flow in the primary when a change of load current occurs in the secondary.
f. The behavior of transformer fluxes, induced voltage, and currents when supplying a load controlled by an SCR.
g. Dynamic behavior of flux, induced voltage, excitation current, and load voltage, when suddenly applied to the line, when the line voltage is suddenly changed, when a load current is suddenly applied, when the load current is suddenly changed, and when load is continuously varying or pulsating.
h. Variation of secondary voltage wave shape with series resistance, potentiometer and variac, in the primary.
i. The autotransformer.

EXPERIMENTAL STUDIES WITH HIGH REACTANCE TRANSFORMER

a. Distortion of secondary flux ϕ_s due to excessive leakage flux ϕ_{sh}. Effect of load currents on leakage flux and wave shapes. Consider resistance load, incandescent lamp load, fluorescent lamp load.
b. Analysis of system consisting of high reactance transformer and gas discharge tube (fluorescent lamp). Voltampere curve for lamp load. Flux distribution and wave shapes. Harmonic flux paths.
c. Operation of fluorescent light with different sources of series impedances, (resistance, reactance, capacitance). High reactance for arc stabilization.
d. Conversion from voltage source to current source with high reactance transformer (in the voltage source, voltage tends to remain sinusoidal in the current source, currents tend to remain sinusoidal).
e. Effect of capacitor load on load and induced voltage. Effect on load and induced voltage of sudden change of load with series and parallel capacitors. This phenomenon is related to light flicker in homes when the neighbor's air conditioner starts, and the minimizing of the flicker with capacitors.

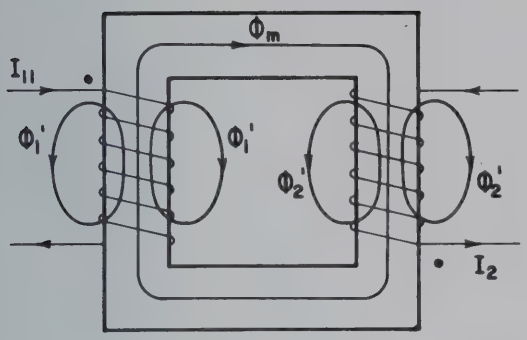

Fig. 2.1 Magnetizing flux ϕ_m, leakage fluxes ϕ_1' and ϕ_2' in a transformer.

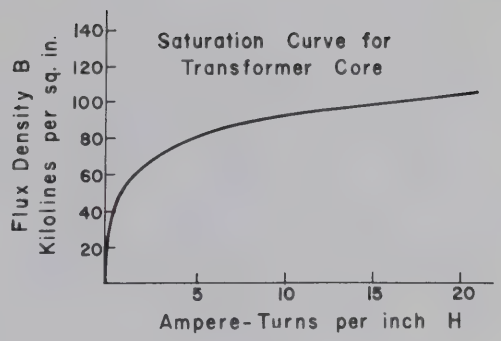

Fig. 2.2 Typical shape of saturation curve for magnetic material.

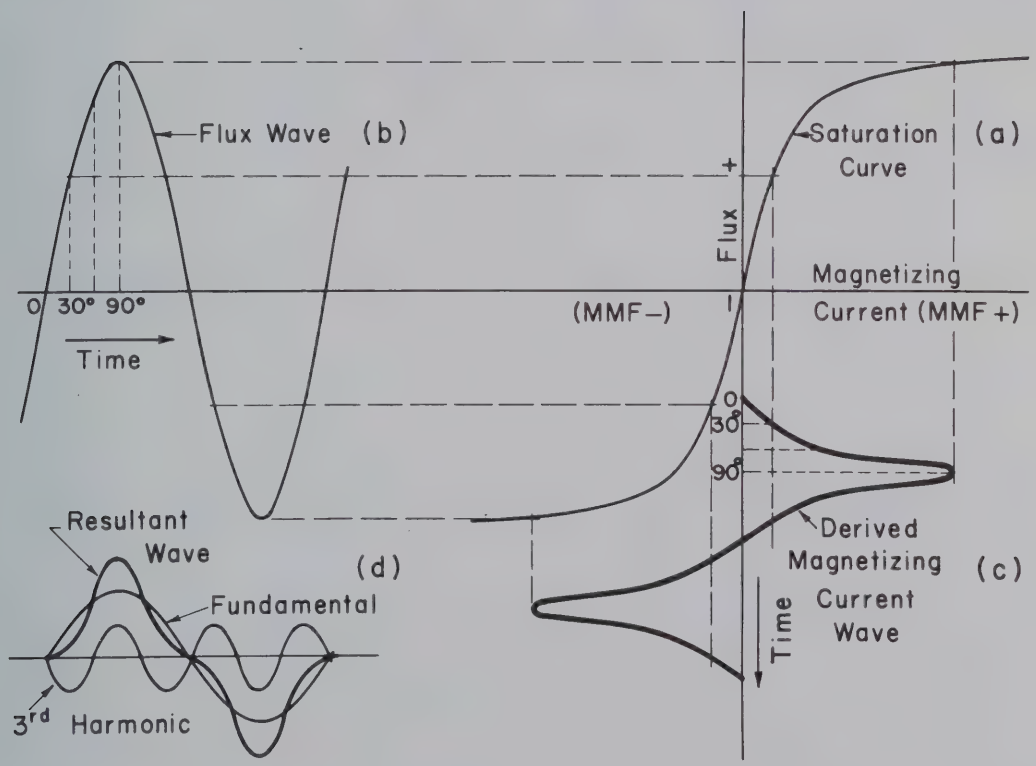

Fig. 2.3 Derivation of the magnetizing current wave from the saturation curve.

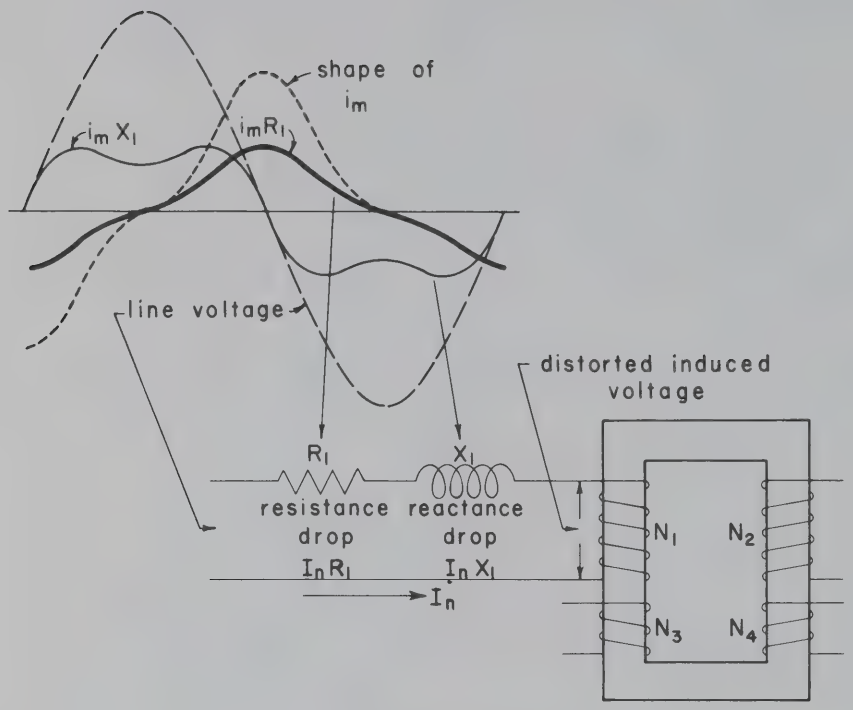

Fig. 2.4 Illustration of the reason for distortion of the induced voltage.

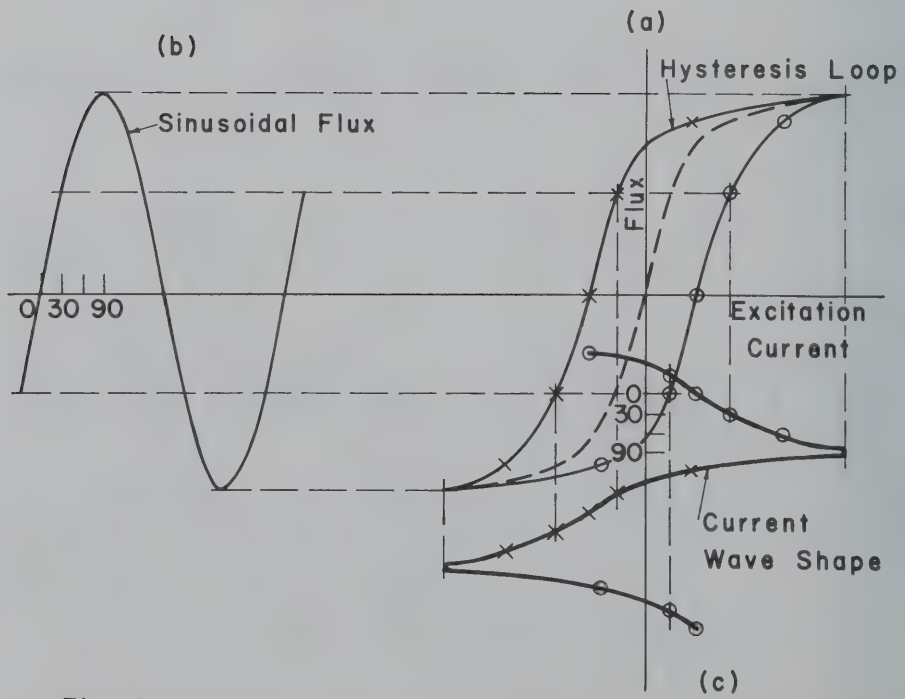

Fig. 2.5 Derivation of the exciting current wave from the hysteresis loop.

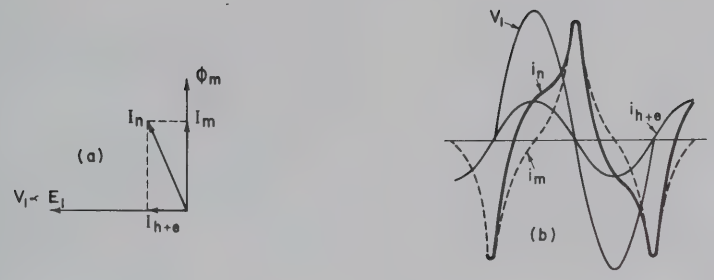

Fig. 2.6 Addition of components of exciting current.
(a) Phasor addition (fundamental of each component.)
(b) Instantaneous addition of component waves.

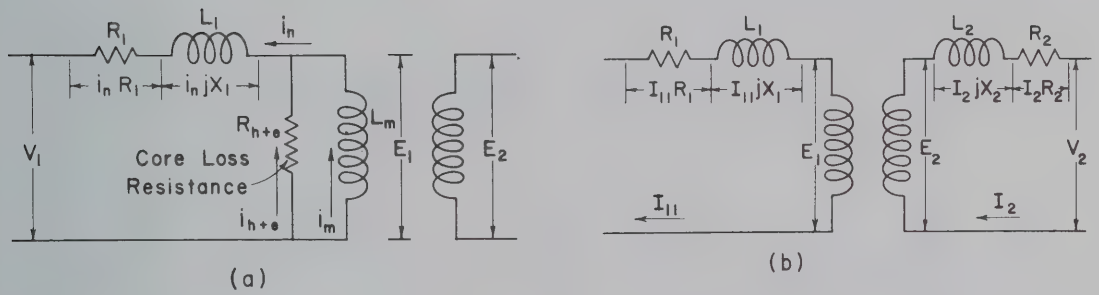

Fig. 2.7 Transformer equivalent circuits.
(a) No Load (b) With load

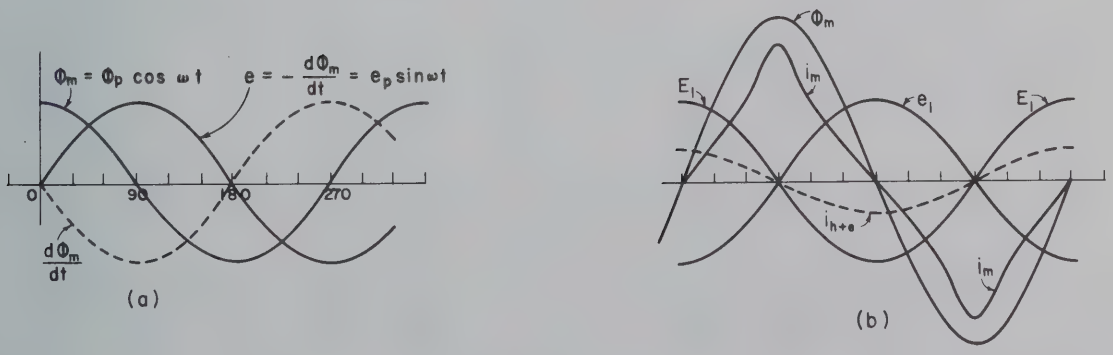

Fig. 2.8 Phase relations and wave shapes of primary quantities at no load.
(a) Flux and induced voltage. (b) All quantities.

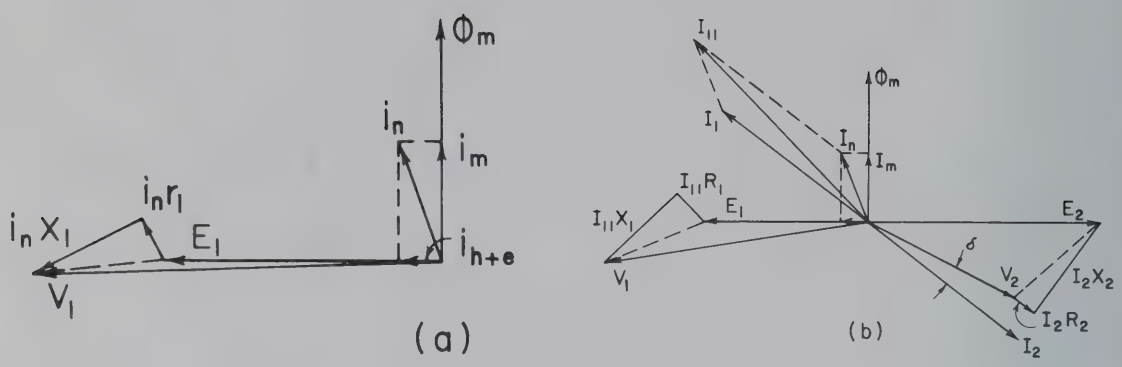

Fig. 2.9 Phasor diagram for a transformer.
(a) No load (b) With load

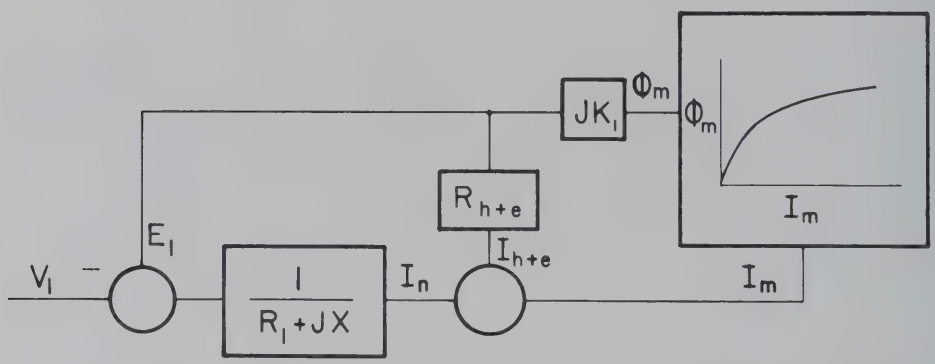

Fig. 2.10 Block diagram for a transformer with no load.

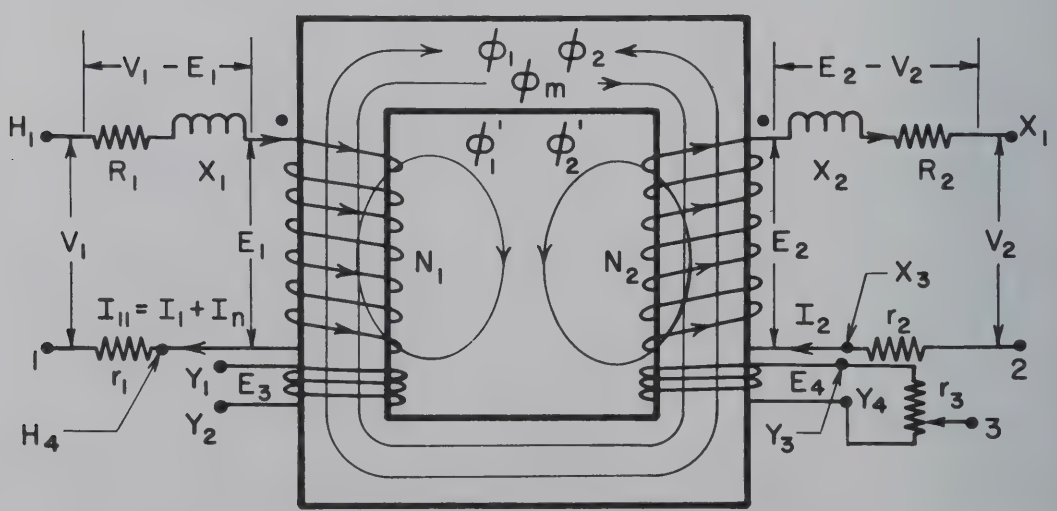

Fig. 2.11 Flux components in a loaded transformer.

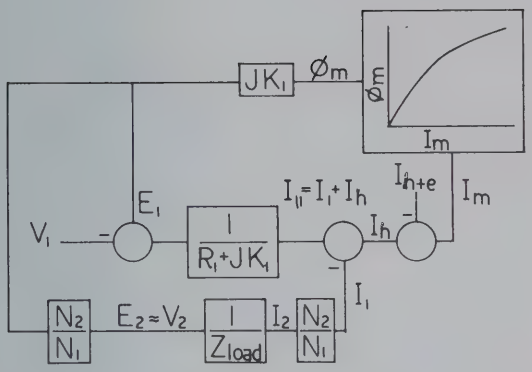

Fig. 2.12 Block diagram for a transformer with load.

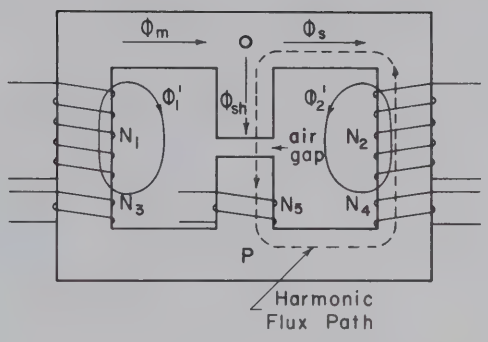

Fig. 2.13 Schematic diagram of high reactance transformer showing flux paths and location of information windings N_3, N_4, and N_5.

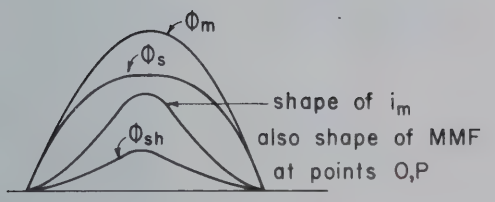

Fig. 2.14 Wave shapes of flux in primary, secondary, and shunt paths.

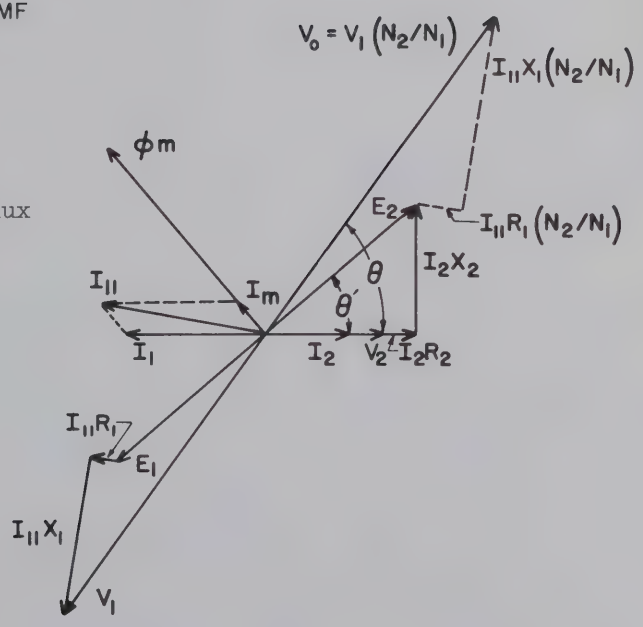

Fig. 2.15 Phasor diagram for a high reactance transformer supplying a resistance load.

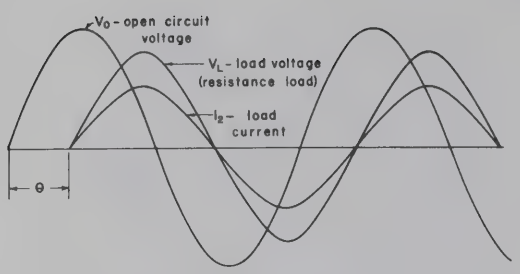

Fig. 2.16 Phase relations between open circuit voltage V_o and load voltage V_2 with resistance load current I_2.

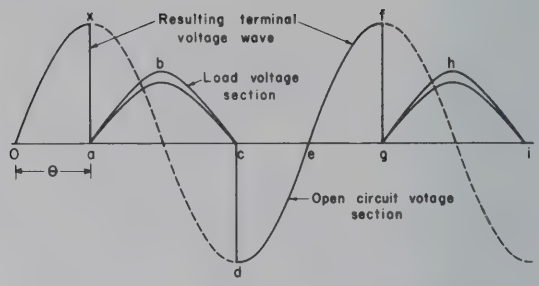

Fig. 2.17 Derived wave shape of terminal voltage of high reactance transformer supplying a resistance load through a one half wave rectifier.

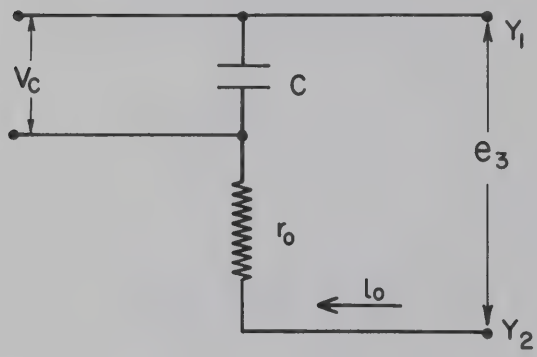

Fig. 2.18 The integrating circuit suitable for 60 Hz.

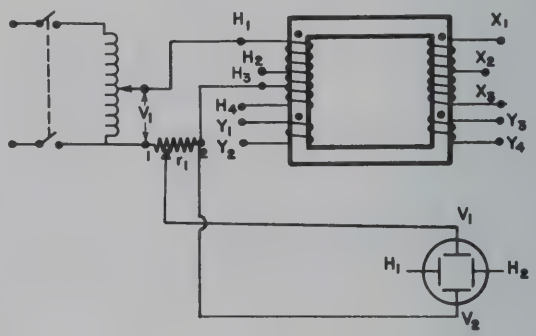

Fig. 2.19 Circuit diagrams for excitation experiments.

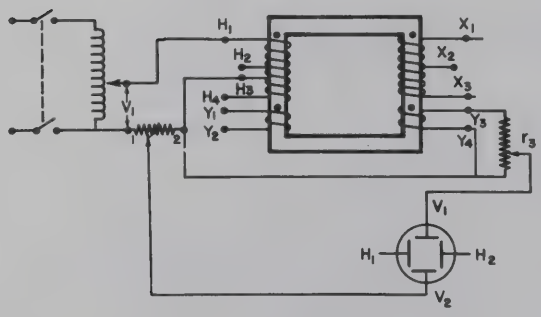

Fig. 2.20 Circuit diagram for displaying the magnetizing component.

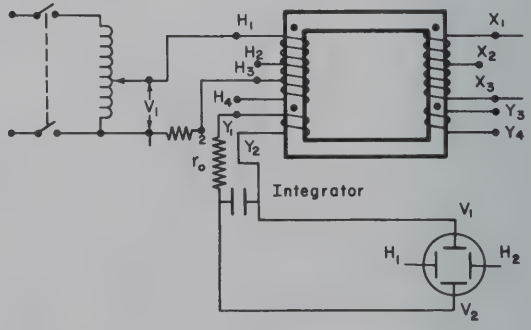

Fig. 2.21 Circuit diagram for displaying magnetizing flux.

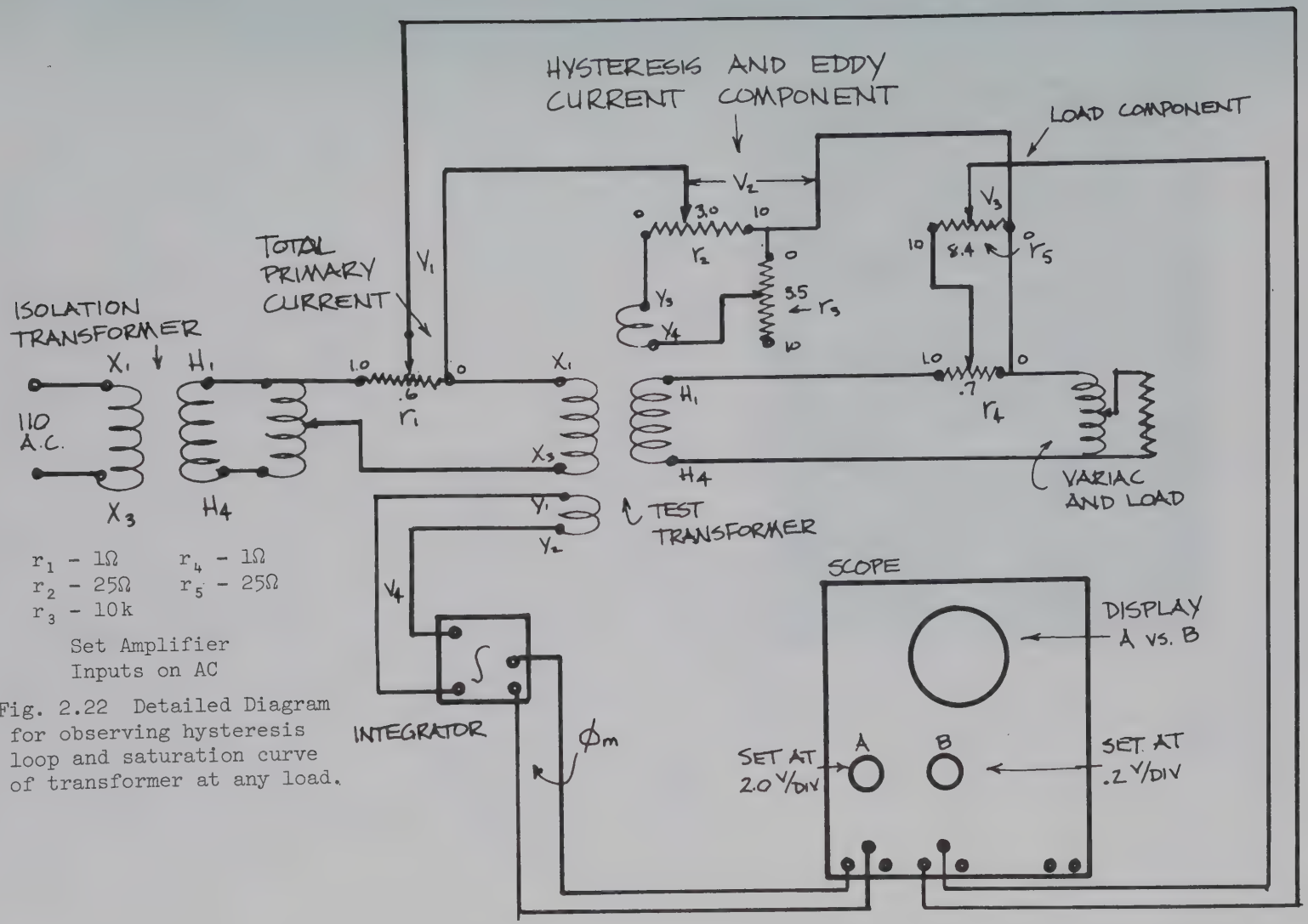

r_1 - 1Ω r_4 - 1Ω
r_2 - 25Ω r_5 - 25Ω
r_3 - 10k

Set Amplifier Inputs on AC

Fig. 2.22 Detailed Diagram for observing hysteresis loop and saturation curve of transformer at any load.

F 2.7

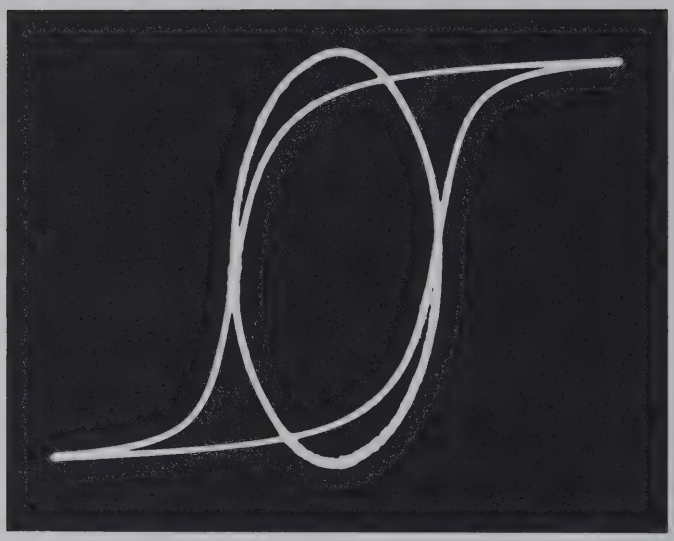

Fig. 2.23 Conventional Hysteresis loop, and loss loop formed by cancellation of magnetizing current.

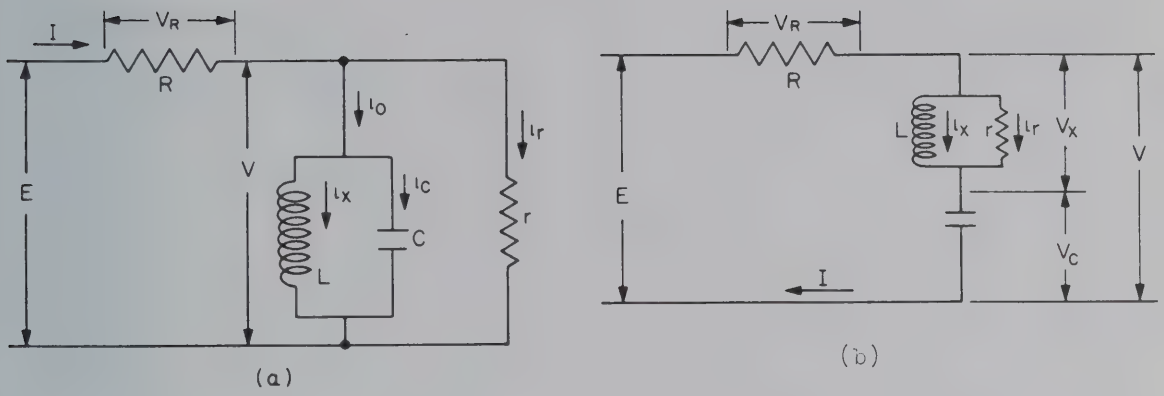

Fig. 2.24 General forms of ferroresonant circuit involving non-linear reactor.
a) parallel circuit. b) series circuit.

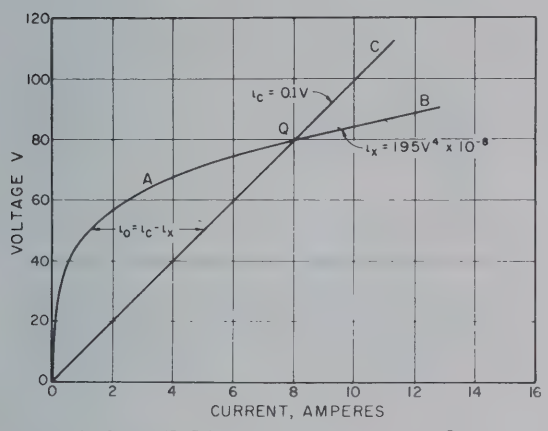

Fig. 2.25 Volt-ampere curves for non-linear reactor and capacitor plotted in RMS values.

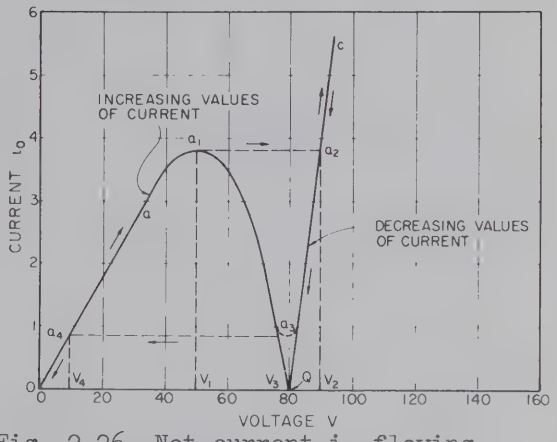

Fig. 2.26 Net current i_o flowing through parallel branch of non-linear reactor and capacitor.

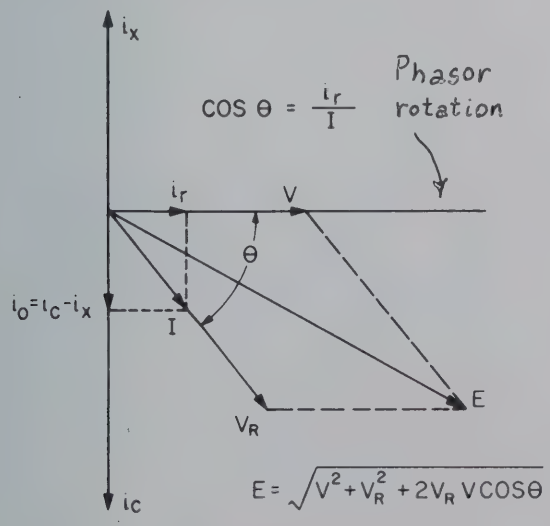

Fig. 2.27 Phasor diagram for parallel ferroresonant circuit.

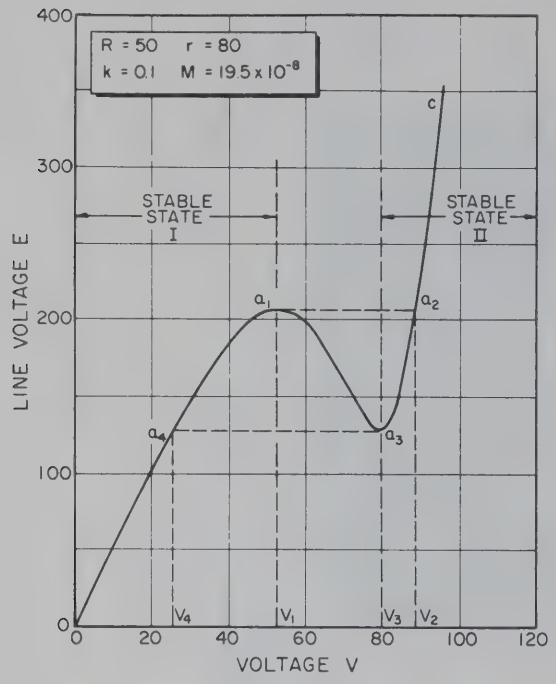

Fig. 2.28 Instability curve calculated for a given circuit applied to a variable line voltage.

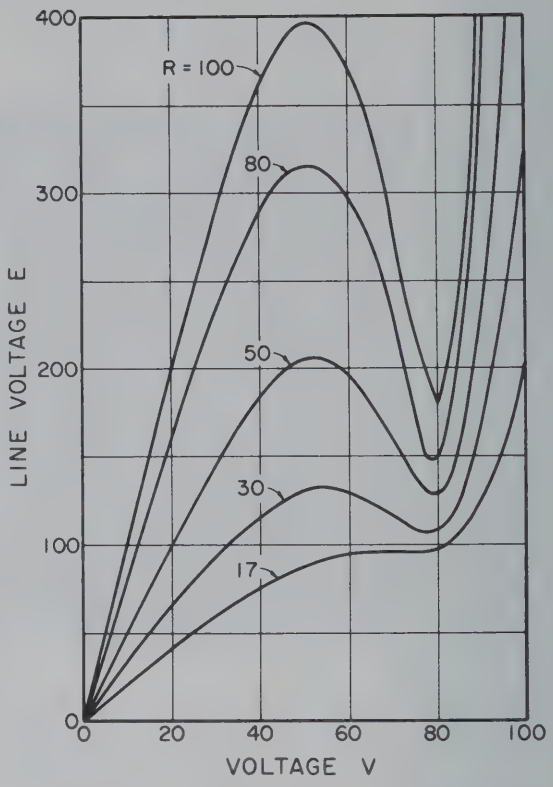

Fig. 2.29 Family of curves for a variable line voltage for different values of series resistance R.

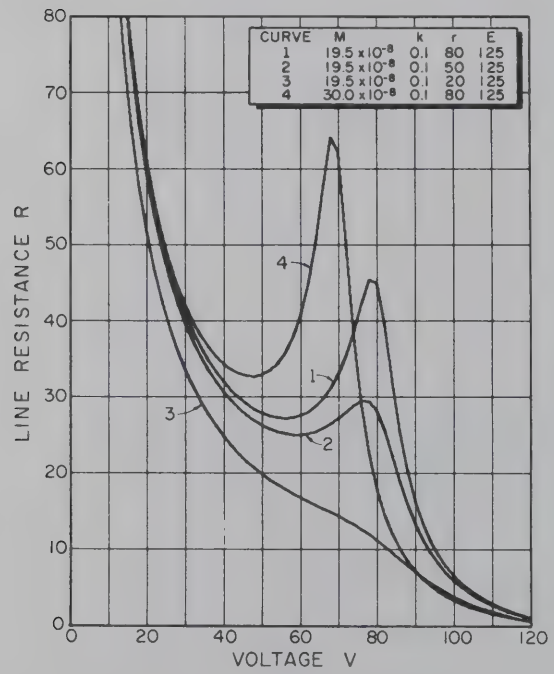

Fig. 2.30 Family of curves calculated and plotted by a computer when the series resistance R is varied. Different curves are obtained with different circuit parameters.

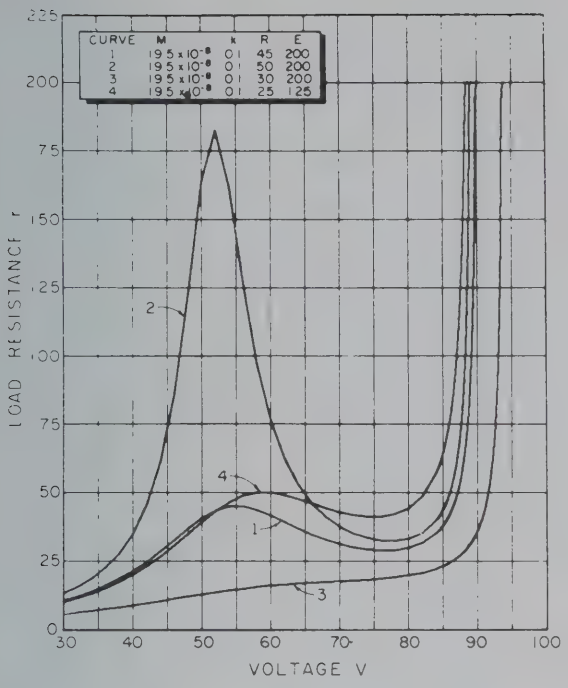

Fig. 2.31 Ferroresonant curves as a function of load resistance r. Calculated and plotted by computer.

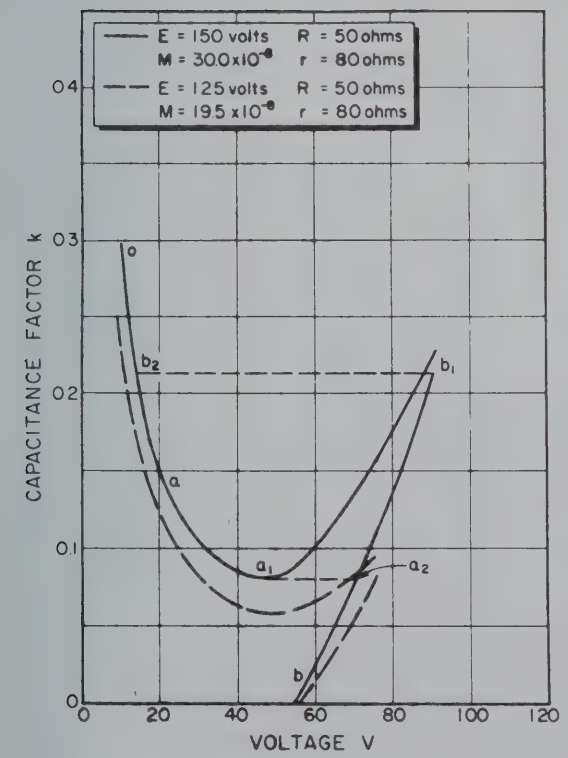

Fig. 2.32 Ferroresonant curves as a function of the capacitance factor k.

NOMENCLATURE FOR CHAPTER 3

V_1 - Voltage applied to phase A.

V_{dc} - DC voltage applied to phase B.

V_o - Open circuit secondary voltage at rotor terminals.

E_1 - Induced voltage in phase A.

E_3 - Generated voltage in information winding N .

E_4 - Generated voltage in information winding N .

I_n - Excitation current in phase A.

i_B - DC current in phase B.

I - Total input current.

N_A - Turns in phase A winding.

N_B - Turns in phase B winding.

N_2 - Turns in rotor winding (secondary).

N_3 - Turns in information winding N .

N_4 - Turns in the information winding N .

R_A - Resistance of phase A.

R_B - Resistance of phase B.

X_A - Leakage reactance of phase A.

r_1 - Resistance in series with phase A.

$\mathcal{R}_A$ - Reluctance of magnetic path of phase A.

$\mathcal{R}_B$ - Reluctance of magnetic path of phase B.

$\mathcal{R}_d$ - Minimum reluctance of phase A.

$\mathcal{R}_q$ - Maximum reluctance of phase A.

T_δ - Instantaneous torque.

T_α - Average torque.

ϕ_m - Magnetizing flux in phase A.

ϕ_B - DC flux in phase B.

continued

δ - Angular position of rotor with respect to phase A.

α - Torque angle produced by load.

$\approx$ - "is proportional to"

CHAPTER 3

THE TRANSFORMER WITH A ROTATING SECONDARY AND THE RELUCTANCE MOTOR

3.1 Description of Equipment for Experimental Work

The transformer with a secondary winding that can be rotated out of and into the primary flux field has a useful purpose in electric power, as an induction regulator. There is a great similarity in the flux behavior of a motor and a transformer, and the induction regulator is a good device to relate the two. The device used in the laboratory is actually a reluctance synchronous motor. The primary of the transformer is one phase of the stator, and the secondary is the rotor winding with its terminals connected to collector rings. The diagram in Fig. 3.1 is drawn to look like a transformer although the machine mechanically is like a motor.

The stator has two identical windings N_A and N_B spaced 90° apart, that represent phase A and phase B of the motor. The magnetic paths of the flux for the two phases are symmetrical but not shown as such in the figure.

Information windings N_3 and N_4 in each phase are so wound, that each links the magnetizing flux of its phase. Because of the 90° displacement there is no coupling between the two information windings as long as the axis of the rotor is in line with the axis of one phase of the stator. No information winding is placed on the secondary core because of the complexity of adding additional collector rings and brushes.

Unlike other motors, the reluctance motor must have salient poles instead of a cylindrical rotor. The commercial induction regulator is constructed with a cylindrical rotor with uniform air-gap. However the laboratory equipment described and shown in Fig. 3.1 adequately demonstrates the similarity between the transformer and the motor, and the salient pole construction accentuates other important principles.

When the salient poles are in line with the path of flux ϕ_m of phase A, the air-gap is short and the reluctance in the flux path is low. When the rotor turns 90°, and is in line with phase B, the air-gap and reluctance in the phase A flux path are large. The secondary winding N_2 has a varying flux with ϕ_m of phase A as the rotor is turned, so that the voltage induced in N_2 will depend on the rotor position.

3.2 Output Voltage as a Function of Rotor Position - The Induction Regulator

When the primary is energized, it creates the magnetizing flux field ϕ_m. The maximum value of flux that links with the secondary occurs when the angle δ in Fig. 3.1 is zero. The induced voltage at this rotor position is maximum. This induced, or open circuit, voltage can be observed on an oscilloscope connected to terminals 3, 4. The voltage varies from maximum to zero as the secondary is turned through 90°. Beyond 90° the voltage again increases to a maximum at 180°, but its polarity is reversed. The output voltage is in effect a modulated voltage when the secondary is continuously turned, as shown in Fig. 3.2(a).

The airgap between the primary and secondary at some given value of δ

causes a large leakage reactance. A load added to the secondary causes a large reactance voltage drop, and consequently a drop in the load voltage. This can be counteracted by reducing the angle δ to increase the flux linking the secondary. The voltage can thus be regulated to its original value. This is the basis for the induction regulator. It can be used as compensation for the impedance drop in distribution lines and in the associated transformers. Automatic control is used for regulating the voltage at some predetermined point in the system.

A preferable arrangement for an induction regulator is shown in Fig. 3.1(b). Here the secondary is connected in series with the line and thus does not supply the major part of the load. It supplies only enough voltage to take care of the voltage regulation by bucking or boosting the supply line voltage.

3.3 Magnetizing Flux and Excitation Current

With no load on the secondary the primary resistance and reactance drops will be relatively small. The primary induced voltage then is essentially constant because the supply is from a constant line voltage. Even though the secondary core is nearly removed from the flux path when δ is 90°, the flux ϕ_m must remain the same when the supply voltage remains the same. (In this kind of transformer, there will be some reactance drop due to the high exciting current when δ is 90°; therefore the induced voltage is not strictly constant, hence the flux through the airgaps may be somewhat less at this position). Assuming constant flux, the Ohms Law equation for the magnetic circuit is true.

$$\phi_m = \text{MMF}/\mathcal{R} = N_1 I_n/\mathcal{R} \qquad 3.1$$

The exciting current is

$$I_n = \phi_m \mathcal{R}/N_1 \qquad 3.2$$

With constant flux, the exciting current varies directly as the reluctance of the flux path. Fig. 3.2(b) shows the variation in exciting current as the rotor is turned through 180°. It too is a modulated wave when the rotor is continuously turned. It never reaches a zero value, as does the voltage, because a small excitation current is required when δ is zero.

The behavior of the flux can be observed experimentally by integrating the voltage of the information winding N_3, and applying the result to a scope. The exciting current can be observed as the voltage drop across resistor r_1, and the secondary voltage by connecting the scope to terminals 3, 4. These observations should be made without load on the secondary, although similar observations can be made with load.

3.4 Torque as a Function of the Rotor Position

Instead of considering the device represented by Fig. 3.1 as a transformer, let us now consider it as a motor. Let phase A be energized without load connected to the rotor winding (referred to as the secondary in the previous discussion). Let no force be applied to the shaft so that the rotor is

free to turn. It will assume a position where the rotor poles are in line with the poles of phase A, or when $\delta = 0$. Now apply a force to the shaft, by hand, and turn the rotor slowly through an angle of 90°. Initially the force required to turn the rotor is zero but it rapidly increases to a maximum value and then decreases again to zero as the 90° position is reached.

The force required to turn the rotor through a distance of 90° represents the mechanical energy which is transferred to the magnetic field. If we assume constant flux and constant flux density, the discussion in section 1.8 beginning on page 1.12 and Eq. 1.50 apply. Energy is transferred continuously as the rotor turns until the maximum is accumulated at 90°, but at this point the torque is zero. "Magnetic lines of force"act like rubber bands; energy is required to stretch them and they are capable of giving up energy when they return to their normal position.

Assume that the rotor is turned initially in the clockwise (CW) direction. The magnetic lines of flux are stretched and skewed to the right at the top poles and to the left at the bottom. The distorted flux lines will try to turn the rotor in a counter-clockwise (CCW) direction. At the 90° position the rotor is geometrically symmetrical with respect to the stator poles of phase A. The flux lines are skewed as much to the right as to the left at both poles, and thus there is no tendency for torque to be exerted on the rotor.

The rotor torque will overcome a restraining force of slightly less magnitude than that required to turn the rotor in the CW direction. It will deliver this torque until $\delta = 0$ where the air-gap and flux lines are shortest, where the reluctance is lowest and where the flux lines are symmetrically distorted. The energy originally transferred to the magnetic field has now been re-transferred to mechanical energy.

When the voltage of phase A is increased, the flux is increased and therefore there is an increase in the torque and energy transferred. From these observations we can formulate some important facts about reluctance torque:

1. The rotor torque is always in the direction which reduces the air-gap or reluctance of the magnetic path.
2. The reluctance must vary as the rotor turns. This is the reason for the salient pole construction. A cylindrical rotor will not produce reluctance torque.
3. The energy in the field is converted into mechanical energy as the reluctance varies from a maximum to a minimum.
4. The magnitude of the torque depends on both the magnitude of flux and the rate of change in reluctance.

3.5 Analysis of Instantaneous and Average Torque and Torque at Synchronous Speed

Many electrical machinery texts present a mathematical analysis of the reluctance motor. The differential equation for the torque at any angular position T_δ is

$$T_\delta = -\frac{1}{2}\ \phi_m^2\ d\mathcal{R}/d\delta \qquad 3.3$$

A graphical analysis of this equation is helpful in understanding the behavior of the reluctance motor.

Figure 3.3(a) shows the rotor positions with respect to the field poles of phase A at each 90° for one full revolution. The reluctance is at its minimum $\mathcal{R}_d$, at positions a, c, and e and at its maximum $\mathcal{R}_q$ at b and d. Let us assume that the reluctance varies sinusoidally between these points. This variation is shown in Fig. 3.3(b) as curve $\mathcal{R}$ corresponding with the rotor positions in (a). Note that the reluctance curve has two complete cycles per one revolution of the rotor.

The rate of change of reluctance with respect to angle δ is shown as curve $d\mathcal{R}/d\delta$; it is, of course, the space derivative of the reluctance curve.

Let us take the realistic situation where the maximum flux occurs at position a in Fig. 3.3(a). Now let the rotor move 90 mechanical degrees while the flux is changing 90 electrical degrees from its maximum to zero. This occurs at position b. While the rotor is turning another 90° to position c the flux reverses and reaches its maximum negative value. This process is repeated during the next 180 degrees to position e when all conditions are identical with those at position a. The rotor is turning one complete revolution per cycle of flux or at 3600 revolutions per minute. This is synchronous speed and the rotor will remain locked in step with the flux. If this synchronism is broken by adding a sudden heavy load to the shaft, or by interrupting the line voltage and then reclosing it a moment later, the rotor will come to a stop at position a or c. In other words the rotor cannot deliver torque at any speed other than synchronous speed. Let us look at the torque graphically.

Equation 3.3 specifies a ϕ_m^2 term. The flux wave in Fig. 3.3(b) squared and the $d\mathcal{R}/d\delta$ wave are shown in Fig. 3.4. These two waves are multiplied graphically to obtain the shape of the torque curve T_δ. Notice that the areas under the positive torque periods are exactly equal to those under the negative torque periods. Therefore the average torque is zero, but there are four torque pulsations per revolution of the rotor. The difference in area between the positive and negative torque period represents the average torque.

If the $d\mathcal{R}/d\delta$ curve crosses the zero axis in Fig. 3.5 a few degrees later than that shown in Fig. 3.4, the negative torque will be greater than the positive torque, and an average torque in the CCW direction exists. This condition can exist only if the rotor reaches position "a", a few degrees after the flux has reached its maximum. The rotor position then lags the flux wave. With no load the angle of lag α, the torque angle, is only a few degrees- just enough for the average power delivered by the rotor to overcome the friction losses. If a load is added to the shaft the angle α increases until the average torque is balanced by that required by the load. It can be proven graphically as well as mathematically that the maximum torque occurs when α is 45°. The equation for the average torque is:

$$T_\alpha = \tfrac{1}{8}\,\phi_m^2\,(\mathcal{R}_q - \mathcal{R}_d)\,\sin 2\alpha \qquad 3.4$$

where $\mathcal{R}_q$ and $\mathcal{R}_d$ are maximum and minumum reluctances from Fig. 3.3(b). Note that the torque angle α does not change when the load is constant while the angle δ is constantly changing as the rotor turns.

When the motor is delivering a torque to a load, it is converting magnetic field energy into mechanical energy. This energy comes form electrical energy supplied from the line. When the motor is delivering no load, the torque angle α is nearly zero. The induced voltage in the stator is nearly equal to the line voltage, thus the input current is low and the electrical energy input is low. When load is added to the shaft, the angle α increases. This causes a reduction in the induced voltage and allows more current to flow into the stator. The equation for the stator current is similar to that in a transformer, Eq. 2.34.

$$I = (V_1 - E_1)/(R_A + jX_A) \qquad 3.5$$

The torque is non-linearly related to the current, as shown by the curve in the block diagram in Fig. 3.6. The torque is related to the angle α by another non-linear curve, and finally the angle α is related to the induced voltage. The motor operates in a stable condition when the conditions of the block diagram are met.

3.6 Starting and Synchronizing the Reluctance Synchronous Motor

The single-phase reluctance synchronous motor has a salient two-pole wound rotor. It will run at a synchronous speed of 3600 rpm, and it it not self starting. The rotor must be brought up to nearly synchronous speed by some other drive motor capable of attaining nearly 3600 rpm. The single phase two pole induction motor will run at no load at around 3500 rpm which is adequate for the reluctance motor to pull into synchronism.

The reluctance motor should be belted to a 3450 rpm single phase induction motor. The induction motor should be connected to the 120 volt source before the stator of the reluctance motor is energized, otherwise the salient poles will tend to lock in a position where the rotor poles are aligned with the stator field. When the machines are up to speed, the power can be connected to the stator of the reluctance motor, and it should pull into synchronism with a speed of 3600 rpm. It is advisable to connect the volt-pac or variac in the line supplying the reluctance motor stator and gradually increase the voltage until synchronism occurs. Synchronism can occur with either of the salient poles aligned with the stator at the time of maximum stator flux.

If dc is applied to the reluctance motor rotor, synchronism may be a little more difficult to achieve. Synchronism can be obtained with only one position of the salient poles, because now the polarity of the dc rotating field must be the same as that of the flux in the stator. When the stator is energized, the rotor may be 180° from its required position and the rotor must slip $\frac{1}{2}$ of a revolution.

The torque produced by the single phase synchronous motor is a pulsating torque, and the motor is likely to produce a rather loud noise. There is

also a strong radial force on the rotor when its poles are in line with the stator field. This produces a radial vibration of the rotor which contributes additional noise.

3.7 Suggested Experimental Studies

a. Steady state rotor torque vs rotor position with dc excitation applied to phase A.

b. (1) Variation in reluctance and flux as rotor turns at synchronous speed.

(2) Measurement and recording of $d\mathcal{R}/d\delta$ and simultaneous recording of flux.

(3) Manual multiplication (or squaring and multiplying elements) to get ϕ_m^2 and $\phi_m^2 \, d\mathcal{R}/d\delta$. This will give the shape of the instantaneous torque wave.

(4) Observations and recording of change in $d\mathcal{R}/d\delta$, ϕ_m^2, and $\phi_m^2 \, d\mathcal{R}/d\delta$ as α varies.

c. Study the "control mechanism" that permits current and power to flow into the motor by observing and/or recording the influence of α on E.

d. Observe and/or record the maximum torque angle α, and look for possible rotor oscillations as the load is suddenly changed.

e. Observe the influence on the motor behavior by introducing into the rotor circuit:

(a) dc

(b) sine wave of line frequency

(c) half wave and full wave dc

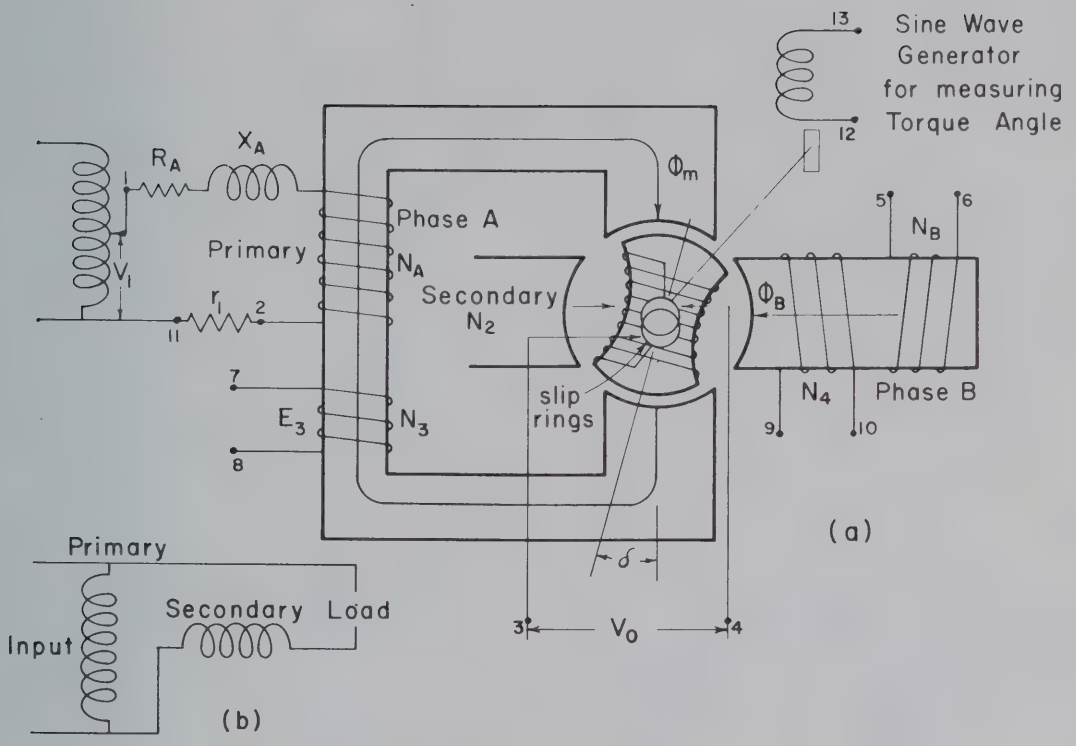

Fig. 3.1 Schematic diagram of reluctance synchronous motor (a), and induction regulator (b).

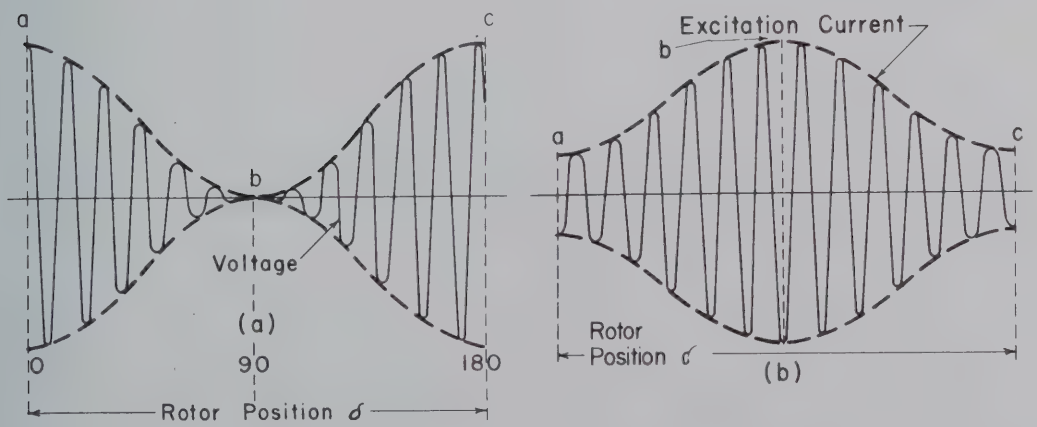

Fig. 3.2 Variation in voltage (a) and excitation current (b) with rotor position.

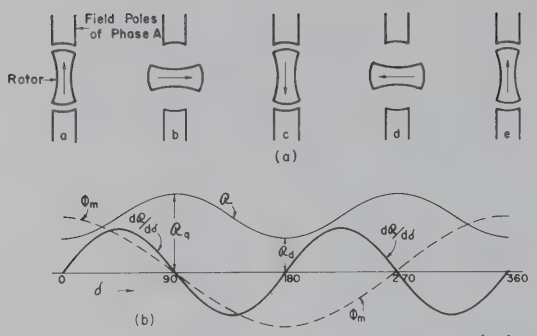

Fig. 3.3 Reluctance variation (b) of phase A with rotor position.(a)

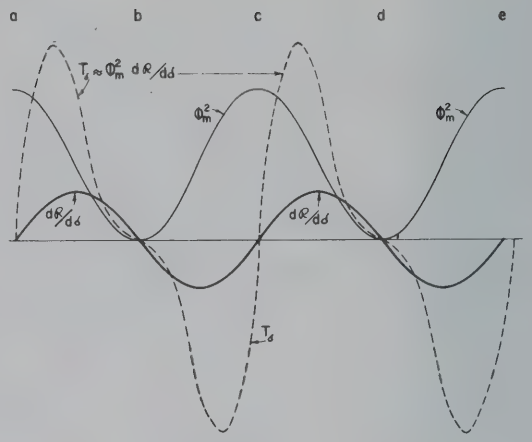

Fig. 3.4 Shape of instantaneous torque during one revolution at no load.

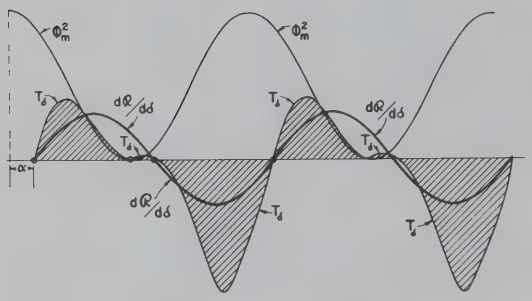

Fig. 3.5 Shape of instantaneous torque curve during one revolution with load.

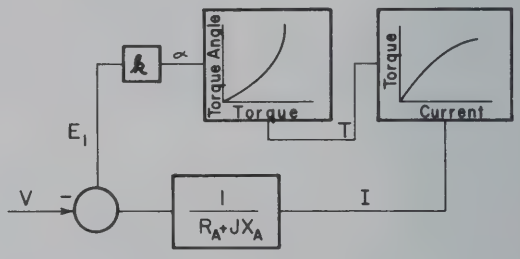

Fig. 3.6 Block diagram for reluctance synchronous motor.

NOMENCLATURE FOR CHAPTER 4

V_A - Voltage applied to phase A.

V_B - Voltage applied to phase B.

e - Voltage induced in rotor bars at standstill.

e_r - Voltage induced in rotor bars at some slip frequency.

e_t - DC tachometer generator voltage.

ϕ_A - Flux in phase A.

ϕ_B - Flux in phase B.

ϕ_s - Rotating stator flux.

ϕ_{sr} - Stator flux linking

ϕ_r - Rotor flux produced by induced current in rotor bars.

ϕ_p - Peak value of sinusoidal flux.

I_A - Exciting current in phase A.

I_B - Exciting current in phase B.

i - Current induced in rotor bars at standstill.

i_r - Current induced in rotor bars at some slip frequency.

θ - Phase angle.

σ - Angular position of rotor.

δ - Angular position of rotating field.

γ - Angular position in distributed flux field.

α - Angle between two flux fields.

t_1, t_2 etc. - Instants of time.

Δt , Δt_2 etc. - Time intervals.

T_o - Standstill torque.

T - Torque.

TM - Motor speed-torque characteristic.

TL - Load speed-torque characteristic.

K - Conversion factor.

continued

s - Slip.

S - Speed of rotation.

r - Resistance of rotor bars.

x_r - Reactance of rotor bars.

z_r - Impedance of rotor bars.

$\mathfrak{R}$ - Reluctance of rotor flux path.

J - Moment of inertia.

CHAPTER 4

SINGLE PHASE INDUCTION MOTORS

4.1 The Rotating Magnetic Field

All induction motors depend on the rotating magnetic field for the torque they develop. In fact the rotating field is present in almost all ac rotating machines. There are two principle requirements for producing the rotating field.

1. There must be at least two separate windings on the stator which are mechanically displaced on the circumference of the stator, preferably by 90 electrical degrees.
2. There must be currents in each winding and out of phase in time.

Rotating fields can be produced by three phase, two phase, or from a single phase source from which two out-of-phase currents are established. The latter is known as the split phase arrangement. The two phase rotating field is the most simple to understand, although it is rarely used in practical power applications. It is, however, quite similar to the more important split phase rotating field.

4.2 Balanced Two Phase Rotating Field

The motor for studying rotating fields in the laboratory is represented diagramatically by Fig. 4.1(b). It is designed with a high degree of flexibility and can be used as a two phase or as a split phase motor. Two identical stator windings A and B are mechanically spaced 90° apart. The magnetic paths for the fluxes ϕ_A and ϕ_B are equal and the magnetic circuit for one is symmetrical with that of the other. An information winding is wound in each phase so that it links only with the flux of that phase. These information windings N_3 and N_4, measure the induced voltage in their phase and, with an integrator, indicate the flux in that phase. The motor has a squirrel cage rotor.

A two phase system is one in which two identical voltages V_A and V_B are out of phase by an angle of 90 electrical degrees, with V_B lagging V_A. The voltage V_A is applied to winding A and V_B to winding B. The fluxes ϕ_A and ϕ_B are equal and in phase with the exciting currents in the respective windings. The fluxes are also displaced by 90 electrical degrees with ϕ_B lagging ϕ_A and are assumed to be sinusoidal as in Fig 4.1(a). Also the exciting currents are equal $I_A = I_B$.

At the time t_1 in Fig. 4.1(a) ϕ_A has a maximum value a_1 while ϕ_B at this instant is zero. Let us assume that the flux produced by $N_A i_A$ at this instant is upward through coil A, as shown in Fig. 4.2. The total flux in the stator at any instant is the phasor sum of the two fluxes $(\phi_A^2 + \phi_B^2)^{1/2}$. At t_1 the phasor sum is ϕ_1 and coincides with a_1.

At time t_2 the two fluxes in Fig. 4.1(a) are a_2 and b_2. Let us assume that the flux produced by current i_B at this instant passes through coil b, horizontally to the right. The fluxes produced by a_2 and b_2 combine as the phasor ϕ_2 at t_2. Thus during the increment of time $\Delta t_1 = t_2 - t_1$, the

resultant flux phasor has rotated clockwise through the angle $\Delta\delta_1$. At time t_3 the fluxes are a_3 and b_3 and produce a resultant phasor flux ϕ_3. During this next equal interval of time $\Delta t_2 = t_3 - t_2$ the flux has rotated another angle $\Delta\delta_2 = \Delta\delta_1$. If this process is repeated throughout the cycle in Fig. 4.1(a), a complete revolution of the resultant flux is achieved as in Fig. 4.2. This rotating flux field has the following unique characteristics:

a.) It is produced by two oscillating fields. The field from coil A oscillates in a vertical line from its maximum positive position at a_1 to its maximum negative position at a_7 and back to a_1. Flux from coil B oscillates along a horizontal line from its maximum positive position at b_4 to its maximum negative position at b_{10}, and back to b_4 but 90° later than the flux in A.

b.) The magnitude of the resultant flux field is constant if $a_1 = b_4$.

c.) The angular velocity $\Delta\delta/\Delta t$ is constant.

d.) The result is essentially the same as that which would be produced by a permanent magnet rotating at the same constant angular velocity. Thus the rotating flux field is physically real.

If an integrator is connected to terminals 5,6 and another connected to terminals 7,8 of the information windings in Fig. 4.1(b) the rotating flux field can be shown in Fig. 4.3(a). The electron beam at every instant assumes a position representing the maximum value of resultant flux of the currents in both windings. Thus it will describe the circle indicated in Fig. 4.2. If the frequency could be reduced to about 5 cycles per second the electron beam could be seen to rotate. The direction of rotation can be reversed by reversing the current in either coil A or B, but not in both at the same time.

4.3 Unbalanced Two Phase Rotating Field

Let us pass a lower value of current through coil B and let the flux ϕ_B be represented by curves c_1, c_2, c_3 etc. in Fig. 4.1(a). The resultant rotating flux field is shown in Fig. 4.4. The time intervals are all equal, but the resultant flux rotates 17° between t_1 and t_2 and 49° between t_3 and t_4. Its angular motion therefore is no longer uniform. A plot of the angular motion during one revolution is shown in Fig. 4.5.

4.4 Split Phase Rotating Field With Two Equal Fluxes

In a split phase system a single phase source supplies current for the two windings in Fig. 4.1(b) and 4.3(b). Some impedance must be used in series with one winding to obtain currents and fluxes in the two windings which are displaced in time by some angle α. The phasor diagram with different impedances in both phases is shown in Fig. 4.8. In order to obtain fluxes in the two windings which are equal in magnitude, the number of turns, reactance, resistance of each winding and the series impedance in each need to be carefully proportioned. A 90° phase displacement in currents could be realized but would not economically be practical.

Let curves a and b in Fig. 4.6 represent equal MMF's and fluxes in each

winding. These are shown displaced in time by $\alpha = 60°$. The resulting rotating flux is an ellipse along a 45° line shown in 4.7. The angular velocity $\Delta\delta/\Delta t$ is not constant and the angle $\Delta\delta$ is plotted for a complete revolution as curve 1 in Fig. 4.11.

4.5 Split Phase Rotating Field With Unequal Fluxes

Let the MMF and flux ϕ_B due to the current in coil B, be cut in half. The flux waves are shown in Fig. 4.9 and the rotating field as in Fig. 4.10. The $\Delta\delta$ in degrees is shown for each equal interval of time Δt and the result plotted as curve 2 in Fig. 4.11.

Experimentally, all these rotating fields can be displayed on the scope by using circuit diagram Fig. 4.3(a). By adjusting the impedance in each of the field coils the resulting rotating field can be observed, and experimentally the field can be made to rotate at a uniform velocity. A non-uniform rotating field can cause torque pulsations in any induction motor because the rotor attempts to follow the motion of the field.

4.6 Sinusoidal Distribution of a Rotating Magnetic Field

A rotating magnetic field established by a 3-phase, 2-phase, or split-phase arrangement is essentially the same (except for some differences in instantaneous velocity) regardless of the source. We can study the torque produced without considering the source if we assume a uniform velocity of rotation.

In the previous discussion the field is represented by a single rotating vector. In reality, the stator windings producing the component fields are distributed around the interior circumference of the stator. This causes a band of flux to be created which approximates a sinusoidal circumferential distribution.

Fig. 4.12(a) shows a stator with windings omitted, a rotor, and exaggerated air-gap, and a representation of the sinusoidally distributed field. The flux is much more dense in the center and diminishes to zero 90° each side of center. This type of field represents a 2-pole field where the electrical and mechanical angles are equal. This field rotates at synchronous a speed of 3600 rpm when produced by a 2-pole stator winding supplied from a 60 cycles source.

Two pairs diametrically opposite bars 1, 2 and 3, 4 of a squirrel cage rotor are shown. These are an integral part of the rotor, which has many bars, a few degrees apart completely surrounding the rotor iron. End rings short all bars together.

The axial length of the air-gap is the same as the stator thickness W.

The flux in the air-gap or stator flux ϕ_s can be represented by Fig. 4.12(b) and by the following equation:

$$\phi_s = \phi_p \sin \gamma \qquad 4.1$$

where γ is the angular position of the sinusoidally distributed field.

4.7 Torque Exerted on Two Diametrically Opposite Stationary Rotor Bars.

Now let the sinusoidally distributed field rotate while the rotor is held in the stationary position shown in Fig. 4.12(a). Let the angle of rotation δ of the field be measured in a clockwise direction from the reference axis, (or from the rotor bar loop 1,2) to the center of the field. The field is shown in the figure rotated 90° from the reference position. At this position the flux ϕ_{sr} passing through the loop is the entire flux ϕ_s of the rotating field. When the angle δ was zero, 90° previously, the center of the field was parallel to the plane of the loop and thus the flux ϕ_{sr} linking the rotor loop, was zero. The flux through the loop is again zero when the field rotates another 90° from the position in Fig. 4.12(a), that is, when $\delta = 180°$. Fig. 4.13 shows the curve of flux ϕ_{sr} linking rotor bars 1,2 during one revolution of the field.

The equation of the flux linking the loop 1,2 is

$$\phi_{sr} = \phi_p \sin \delta \qquad 4.2$$

The voltage generated in the rotor bars can be visualized by referring again to Figures 4.12 and 4.13. At the position shown when $\delta = 90°$ there is no change in flux linking the bars 1 and 2 for a small angular rotation, hence the voltage generated is zero. However 90° later or when $\delta = 180°$ the change in flux and generated voltage is greatest. This is verified by differentiating Eq. 4.2. Thus

$$e = - d\phi_{sr}/dt = \phi_p \cos \delta \qquad 4.3$$

The voltage curve is shown as curve e in Fig. 4.13.

Let us now assume that the impedance of the loop formed by the rotor bars 1,2 is a pure resistance. Then the current in the loop is

$$i = e/r = (\phi_p \cos \delta)/r \qquad 4.4$$

The flux produced by this rotor current is in phase with it and equal to

$$\phi_r = Ni/\mathfrak{R} = N \phi_p \cos \delta / (r\mathfrak{R}) \qquad 4.5$$

where $\mathfrak{R}$ is the reluctance of the magnetic path to the flux ϕ_r.

The waves of e, i, and ϕ_r, shown in Fig. 4.13, are all in phase and sinusoidal in shape. All of them are associated with the rotor. The rotor flux ϕ_r reacts with the revolving field flux ϕ_s to produce a torque which can be specified as

$$T = K\phi_s\phi_r \sin \alpha \qquad 4.6$$

Where K is a conversion constant and α is the angle between the two

fields as illustrated in Fig. 4.8. When α is 90°, the torque is maximum.

$$T = K\phi_s\phi_r \sin 90° = K\phi_s\phi_r \qquad 4.7$$

The two fields tend to align themselves along the same physical position. The flux ϕ_r produced by the current in the stationary rotor bars 1,2 is an oscillating flux along the vertical axis of the 1 turn loop. As the stator field rotates, the rotor field oscillates from + ϕ_r to - ϕ_r and back to + ϕ_r for each 360° of rotation. Thus the frequency of the current in the bars is the same as the rotational frequency ϕ_s. Flux passing vertically through the loop 1,2 is arbitrarily assigned as positive (+).

The rotating stator flux ϕ_s tends to pull the rotor flux ϕ_r, and the rotor bars 1, 2 along with it. The torque pulsates however at double the rotational frequency. The torque can be visualized as the product of the horizontal projection of ϕ_s and the vertical magnitude of the rotor flux ϕ_r.

The torque can be obtained from Fig. 4.13 by multiplying the ϕ_s curve by the ϕ_r curve or by applying Eq. 4.7.

4.8 Multiple Stationary Rotor Bars Having No Inductance

Instead of considering a pair of diametrically spaced rotor bars 1,2 imagine a number of pairs of bars spaced around the squirrel cage rotor. As the stator flux rotates while the rotor is held stationary, the flux will oscillate along the axis of each pair of bars, but the maximum flux produced in any pair of bars is always 90° behind the rotating stator flux. Thus there is a sinusoidally distributed rotating magnetic field produced by the current in the rotor 90° behind that of stator.

During each revolution of the rotating field the torque will be the sum of the instantaneous torque in each pair of rotor bars and this sum is constant throughout the revolution.

4.9 Squirrel Cage Rotor Free to Rotate

When the rotor bars 1,2 in Fig. 4.12 are held stationary, the frequency of the voltage generated in them is the same as the rotational speed of the stator field. If the rotor bars are rotated at the same speed as the rotating field, $d\delta/dt = d\sigma/dt$, there is no change of flux linking the bars because there is no relative motion. Therefore, the voltage, current, rotor flux and torque are all zero. If the rotor bars are turning at a speed slightly less than the revolving field, there will be a slow change of flux linking the rotor which will generate a low voltage at a slip frequency equal to the difference between the actual rotor speed and the revolving stator field. Slip is defined as a percentage of synchronous speed

$$s = \text{Slip} = \frac{\text{sync speed - rotor speed}}{\text{sync speed}} \times 100 \text{ percent} \qquad 4.8$$

From this equation:

rotor voltage = voltage in rotor at standstill time % slip
rotor frequency = rotor frequency at standstill times % slip
rotor speed = sync speed - (sync speed times% slip)

The following tabulation gives the relationship of several rotor quantities as the rotor varies from standstill to synchronous speed (the speed of the stator revolving field).

sync speed	rotor speed	rotor voltage	rotor voltage frequency	% slip
3600	0	100%	60 ~	100%
3600	900	75%	45 ~	75%
3600	1800	50%	30 ~	50%
3600	2700	25%	15 ~	25%
3600	3600	0	0	0

4.10 Rotor Reactance

The squirrel cage rotor can never have pure resistance characteristics. Any physical arrangement will have some inductance, and its inductive reactance varies with frequency. Hence the inductive reactance of the rotor will be greatest at standstill, and lowest at near synchronous speed. The resistance of the bars remains essentially constant. The power factor of the rotor therefore varies from a very low value at standstill to near unity at low slip.

Fig. 4.14 shows the torque curve for one revolution of the stator field in stationary bars 1,2 when the inductive reactance is such that the current lags the rotor voltage by the angle $\theta = 30°$. An opposing torque is developed during the interval of time while the stator field is rotating from 90° to 120° and again from 270° to 300°.

When a complete squirrel cage rotor is used the torque is constant and equal to

$$T = \phi_r \phi_{sr} \sin (90° + 30°) = .866 \phi_r \phi_{sr} \qquad 4.9$$

Thus, when reactance is present in the rotor the standstill torque is less than when resistance alone is present.

The changing generated voltage and reactance both affect the rotor current and flux, and therefore the torque changes as the rotor speed changes.

The constant torque produced by two fields of constant magnitude rotating

at any given speed is given by Eq. 4.6.

$$T = K \phi_s \phi_r \sin \alpha$$

The optimum torque is obtained when $\alpha = 90°$ and when the rotor power factor is unity. At a power factor of angle of θ, the torque is

$$T = K \phi_s \phi_r \sin (\alpha + \theta) \qquad 4.10$$

When $\alpha = 90°$

$$T = K \phi_s \phi_r \sin (90° + \theta) = K \phi_s \phi_r \cos \theta \qquad 4.11$$

Since ϕ_s is constant and ϕ_r is proportional to the current i, we can write

$$T \tilde{} \; i \cos \theta \qquad 4.12$$

The following analysis shows the basic characteristics of an induction motor even though the numbers are purely arbitrary. The rotor quantities at any slip are:

$x_r = sx$ $\qquad\qquad$ $\cos \theta = r/z_r$

$e_r = se$ $\qquad\qquad$ $i_r = se/(r^2 + sx^2)^{\frac{1}{2}}$

$z_r = (r^2 + (sx)^2)^{\frac{1}{2}}$ $\qquad\qquad$ $T \tilde{} \; i_r \cos \theta$

We can now calculate a table of relative numbers showing the relationship of all quantities as slip varies from 100% (standstill) to 0% (synchronous speed). For this table, let e = 10, r = 1, x = 2, sync speed = 1800

RPM	s	se	r	x_r	z_r	i_r	Cos θ	Torque
0	100	10	1.0	2	2.25	4.45	.45	2.0
360	80	8	1.0	1.6	1.88	4.22	.53	2.25
720	60	6	1.0	1.2	1.56	3.85	.64	2.46
900	50	5	1.0	1.0	1.40	3.55	.707	2.5
1080	40	4	1.0	0.8	1.28	3.12	.78	2.42
1440	20	2	1.0	0.4	1.08	1.85	.93	1.72
1800	0	0	1.0	0.0	1.00	0.0	1.0	0

The tabulated data is plotted in Fig. 4.15.

In order to demonstrate the effect of rotor resistance let us make another tabulation with r = 2

RPM	s	se	r	x_r	z_r	i_r	Cos θ	Torque
0	100	10	2.0	2.0	2.82	3.53	.707	2.5
360	80	8	2.0	1.6	2.55	3.13	.785	2.45
720	60	6	2.0	1.2	2.34	2.56	.86	2.2
900	50	5	2.0	1.0	2.23	2.23	.90	2.01
1080	40	4	2.0	0.8	2.15	1.86	.93	1.73
1440	20	2	2.0	0.4	2.04	.98	1.0	.96
1800	0	0	2.0	0	2.00	0		0

The speed torque for these data are also plotted in Fig. 4.15. Notice that the maximum torque is the same for the two rotor resistances. The lower resistance causes the maximum torque to occur at a slip of 50% while the higher resistance produces a maximum torque at standstill. Thus by proper variation of the rotor resistance, a variety of speed-torque characteristics can be obtained. Notice also that the speed change for a given torque change is less for the lower resistance. The lower resistance produces the higher full load torque but the higher resistance will start a heavier load.

The induction motor cannot deliver torque at synchronous speed, because there is no voltage generated in the rotor, and no currents in the rotor, hence no flux. It can only deliver torque by slowing down to a speed where the induced voltage in the rotor can create enough flux to supply the torque needed. This is unlike the synchronous reluctance motor discussed in Chapter 3 which can deliver torque only at synchronous speed.

4.11 Inertia Torque

When a motor is started with no external load, all of the motor torque is expended in accelerating the rotor. It is called inertia torque and is defined as

$$T = J\, d^2\sigma/dt^2 = J\, dS/dt \qquad 4.13$$

where the conventional nomenclature is

J = the inertia of the rotor shaft plus any connected inertia of the load.
σ = the angular displacement of the rotor.
S = rotational speed, or velocity = $d\sigma/dt$; and $d^2\sigma/dt$ is acceleration.

4.12 Speed Build-Up At No Load

The inertia torque as given in equation 4.13

$$T = J\, dS/dt$$

In terms of small increments of speed and time

$$T = J\, \Delta S/\Delta t \qquad 4.14$$

or

$$\Delta S/\Delta t = T/J$$

Assume the speed-torque for a motor is that of Fig. 4.16. The initial slope of the speed-time curve, Fig. 4.17, is

$$\Delta S_1/\Delta t_1 = T_o/J \qquad 4.15$$

where T_o is the standstill torque from Fig. 4.16 and the subscript 1, 2, 3 etc. refer to successive increments of time.

The slopes at the next successive intervals of time are

$$\Delta S_2/\Delta t_2 = T_1/J$$

$$\Delta S_3/\Delta t_3 = T_2/J \quad \text{etc.}$$

From Eq. 4.15

$$\Delta S_1 = (\Delta t_1/J)\, T_o$$

We will select numbers for the value of $\Delta t_1/J$ such that at the end of the first unit of time, ΔS_1 will also be equal to 1 unit of speed. Let each equal interval of time be one unit. Thus, with $T_o = 1.5$ from Fig. 4.16

$$\Delta S_1 = (\Delta t_1/J)\, T_o = (\Delta t_1/J)\, 1.5 = 1$$

Therefore $\Delta t_1/J$ must equal 1/1.5 and it remains constant.

Thus at the end of one unit of time Δt_1 the speed S_1, is $0 + \Delta S = 1$ At this new speed the new torque $T_1 = 1.55$, from Fig. 4.16

$$\Delta S_2 = (1/1.5)\, 1.55 = 1.03$$

The accumulated speed is

$$S_2 = S_1 + \Delta S_2 = 1 + 1.03 = 2.03$$

At a speed of 2.03 the new torque is $T_2 = 1.61$ and

$$\Delta S_3 = (1/1.5)\, 1.61 = 1.07$$

also

$$S_3 = S_2 + \Delta S_3 = 2.03 + 1.07 = 3.10$$

This process is continued until a final steady state speed is attained. The resulting inertia speed-time curve is shown in Fig. 4.17. This curve is plotted in terms of relative numbers to show the general shape of the curve and to indicate the internal phenomena which creates the curve. The speed time curve can be plotted in real time and speed if torque is in Newton Meters, J is in MKS units, and time in seconds. The speed, as well as ΔS, is then in

radians per second.

4.13 Speed Build-Up With Load

Let the motor having a speed-torque curve TM in Fig. 4.18 be connected to load which requires a speed-torque characteristic TL. At standstill the motor has 1.5 torque units of which 0.1 unit is required to start the load. Thus the torque available for acceleration is

$$T = TM - TL \quad \text{or } 1.4 \text{ units}$$

as in the previous analysis, Eq. 4.14

$$T = J\, \Delta S/\Delta t$$

where J is now the combined inertia of the motor and load rotating components. Again let us select a value for $\Delta t/J$ such that ΔS_1 is one unit of speed. Thus

$$\Delta S_1 = (\Delta t_1/J)\,(TM_o - TL_o) = (\Delta t_1/J)\,(1.5 - 0.1) = 1$$

or $(\Delta t_1/J)$ must be 1/1.4 and remain constant.

By a step by step process similar to Sect. 4.13, the speed-time curve in Fig. 4.19 is obtained.

4.14 Measurement of Torque by the Inertia Method - Experiment 4.1

From Eq. 4.13 the torque is the product of the constant inertia, J, and the derivative of the rotor speed. The speed is easily measured by measuring the no-load voltage of a dc tachometer generator coupled to the shaft. Thus, the tachometer voltage is

$$e_t = K\, S \;\tilde{}\; \text{velocity}$$

$$de_t/dt = K\, dS/dt \;\tilde{}\; \text{acceleration}$$

Hence the torque is

$$T = K\, dS/dt = K\, de_t/dt \qquad 4.17$$

The speed-torque curve can be plotted while the motor is accelerating from standstill to full no-load speed by a circuit shown in Fig. 4.20. The curve can be displayed on a CRO and observed, photographed or recorded on an X-Y plotter. Torque pulsations or torque changes will be displayed but no response to steady state torque is obtained.

When the motor is running at no-load speed and a load is added, a torque change is noted because the motor must reduce its speed. The indicated torque represents that supplied to the load by the decelerating inertia of the rotor. When the supply voltage to the motor, running at full speed at no load, is

removed the rotor begins to decelerate. The rate of change of speed represents the friction and windage torque. The ciruict in Fig. 4.20 can also be used for indicating the behavior of these losses.

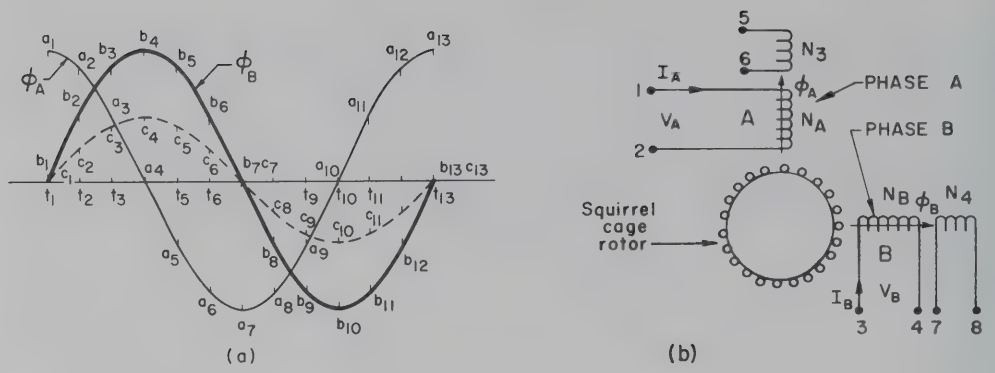

Fig. 4.1 Internal behavior of a two-phase motor.
a) Flux relations in phase A and phase B.
b) Phase A and phase B winding relations with respective information windings N_3 and N_4.

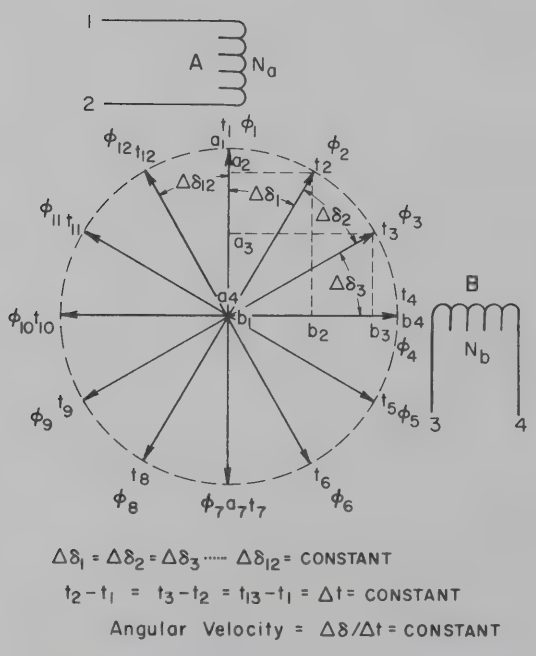

Fig. 4.2 Development of a symmetrical rotating magnetic field from a balanced two-phase supply.

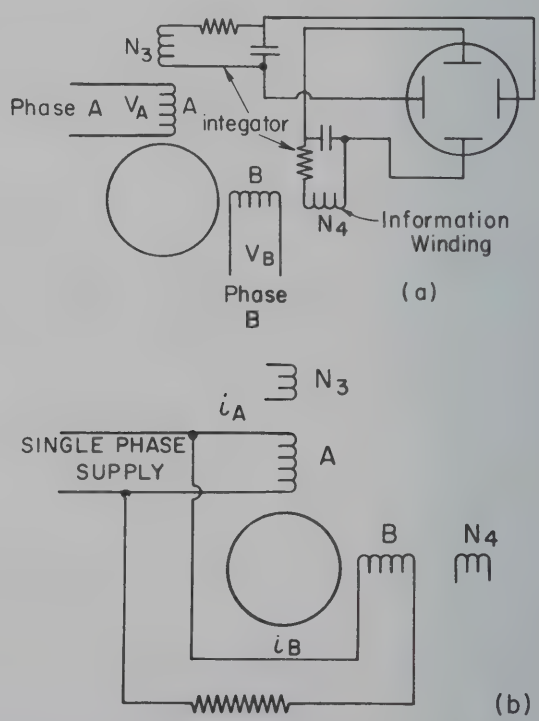

Fig. 4.3 The rotating magnetic field. a) Circuit diagram for displaying the rotating magnetic field. b) Method of producing a rotating field from a single-phase supply.

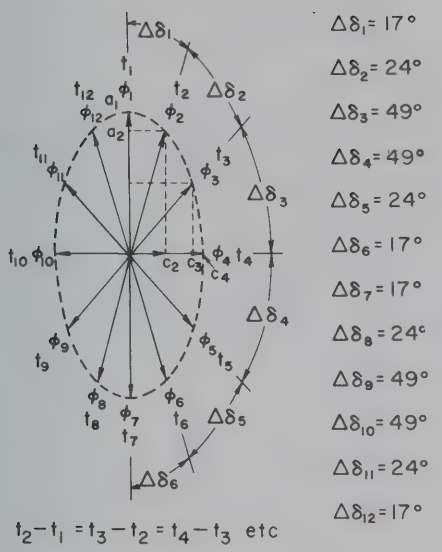

Fig. 4.4 The non-uniform rotating magnetic field produced by unequal two-phase source.

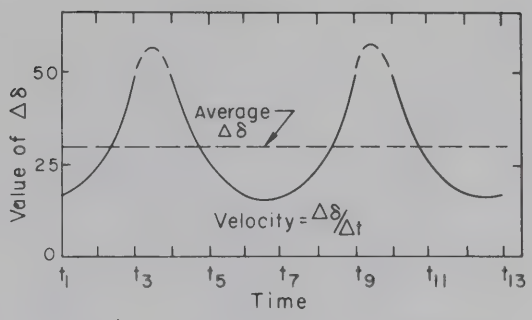

Fig. 4.5 Variation in angular rotation of the field produced by an unequal two-phase source.

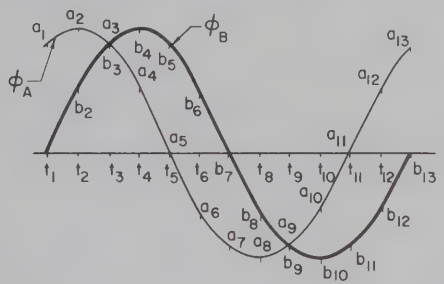

Fig. 4.6 Flux relations in a split-phase motor with 60° displacement between fluxes.

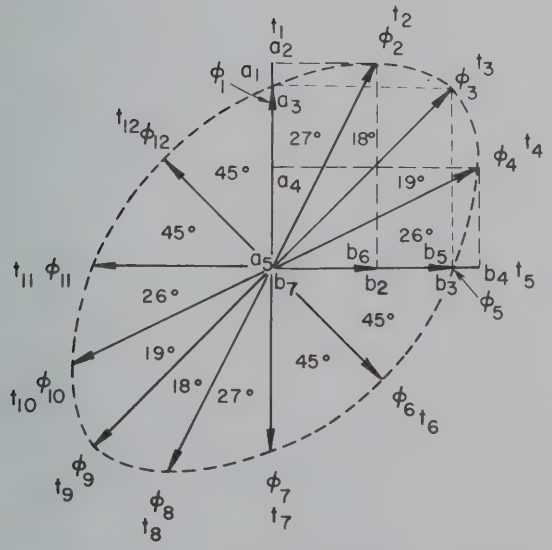

Fig. 4.7 Non-uniform rotating field produced by fluxes shown in Fig. 4.6.

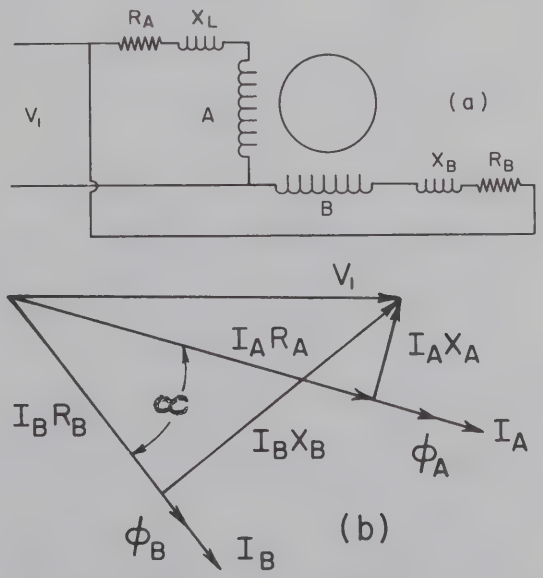

Fig. 4.8 The split-phase motor. a) Equivalent impedance in each winding to produce a flux displacement of ∝°. b) Phasor diagram.

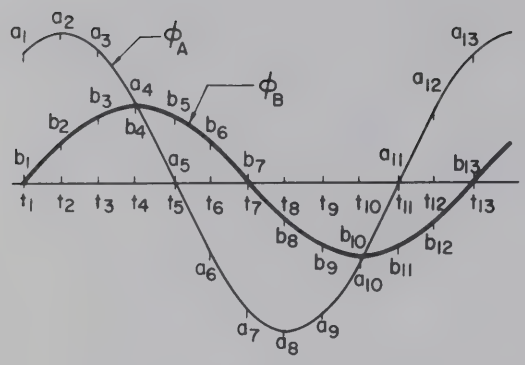

Fig. 4.9 Split-phase motor with unequal fluxes displaced by 60°.

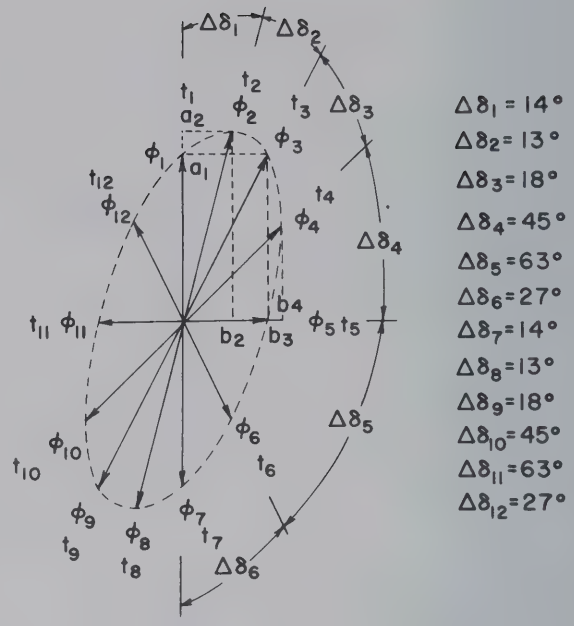

Fig. 4.10 Non-uniform rotating field produced by fluxes in Fig. 4.9.

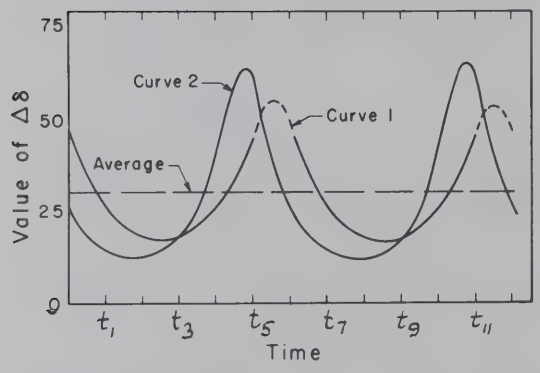

Fig. 4.11 Variation in angular rotation of magnetic field. a) Equal split-phase fluxes 60° apart. b)Unequal split-phase fluxes 60° apart with $\phi_B = \frac{1}{2}\phi_A$.

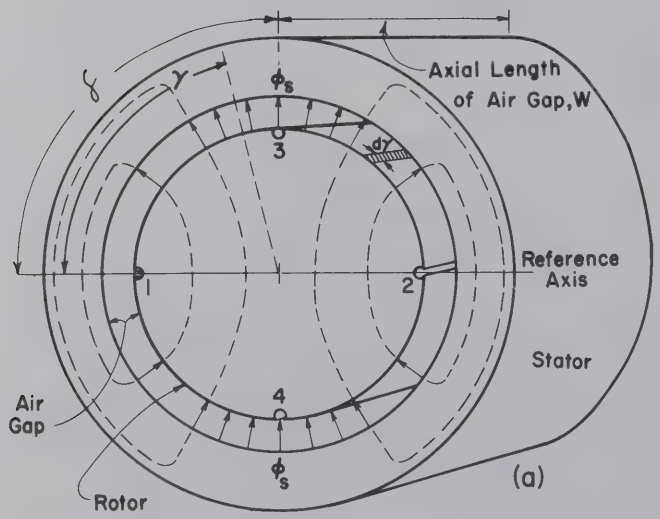

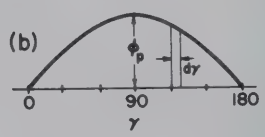

Fig. 4.12 The single-phase induction motor. a) Induction motor with squirrel cage rotor (stator winding not shown). b) Sinusoidal space distribution of stator flux.

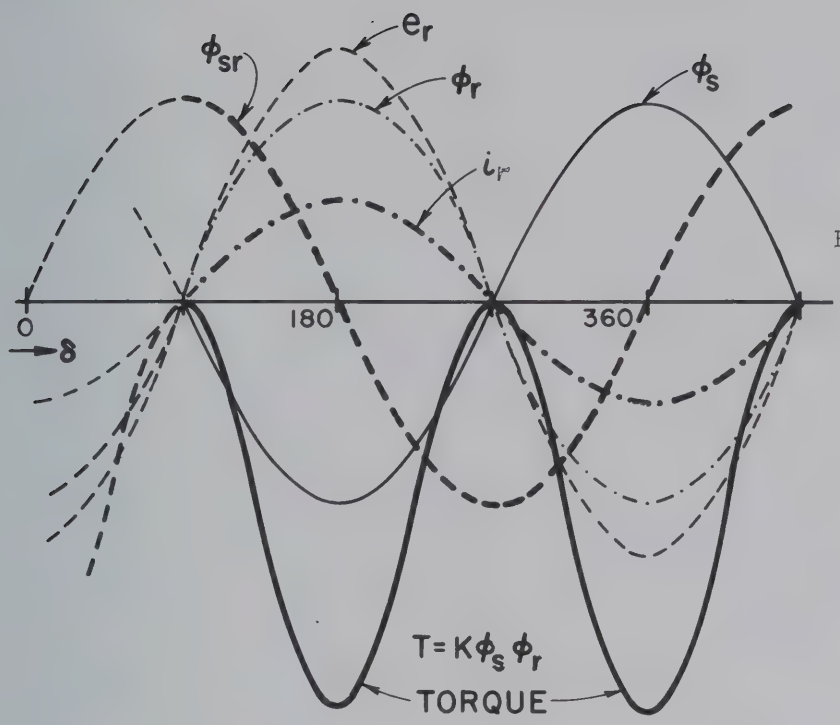

Fig. 4.13 Flux and torque behavior in two diametrically opposite stationary rotor bars, with unity power factor in rotor.

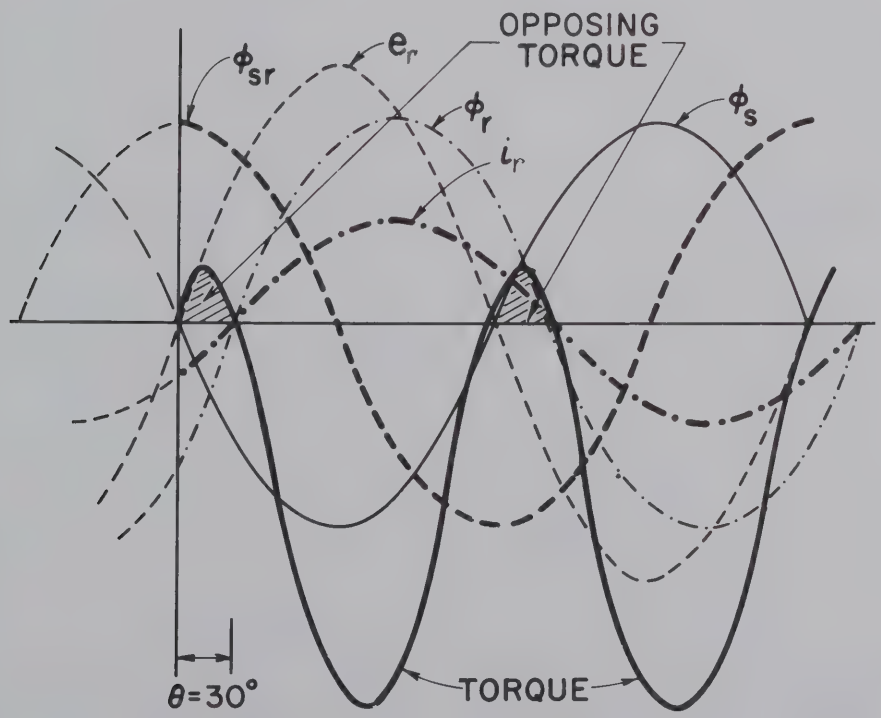

Fig. 4.14 Instantaneous torque similar to Fig. 4.13 except with power factor angle of 30° in the rotor.

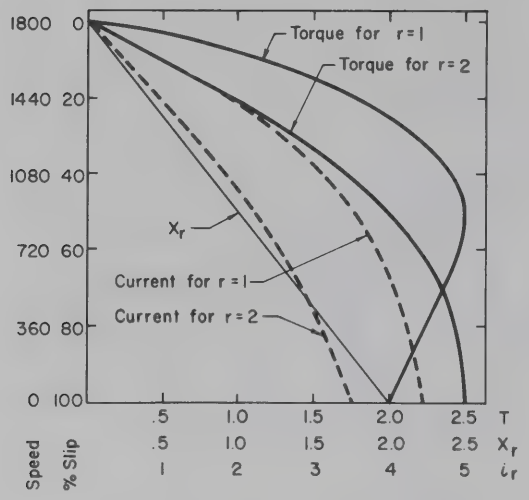

Fig. 4.15 General shape of characteristic curves of induction motor calculated from assumed data.

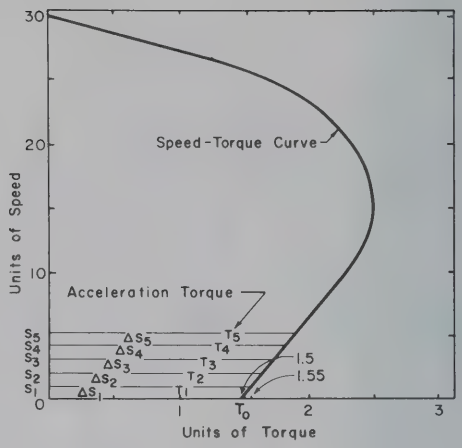

Fig. 4.16 Speed-torque characteristic of induction motor from which the build-up of speed can be predicted.

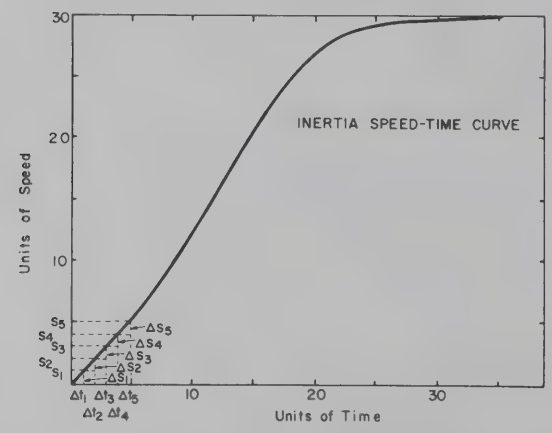

Fig. 4.17 Predicted speed-time curve produced by acceleration torque.

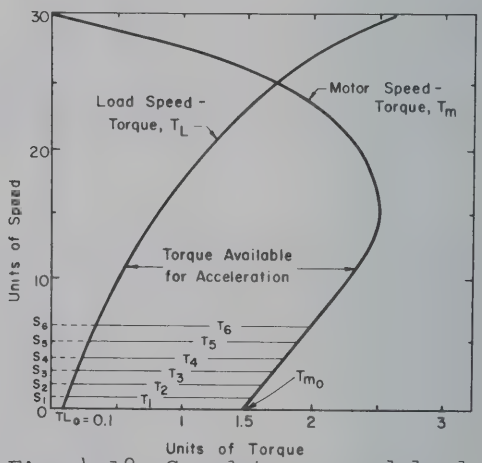

Fig. 4.18 Speed-torque and load curves from which build-up of speed can be predicted.

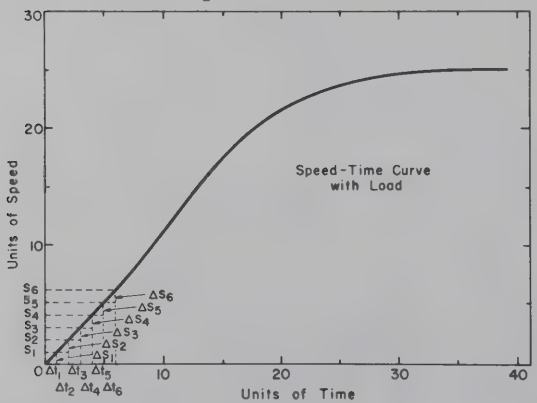

Fig. 4.19 Predicted speed-time curve from Fig. 4.18.

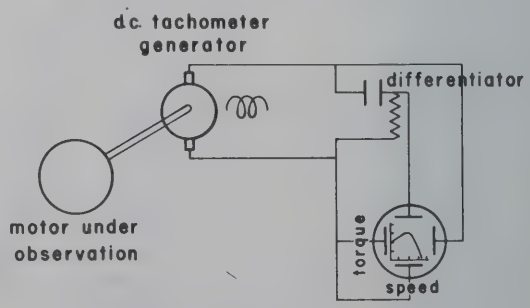

Fig. 4.20 Method for displaying the inertia speed-torque curve.

NOMENCLATURE FOR CHAPTER FIVE

E_{xa}, E_{yb}, E_{zc} - Phase voltages in stator windings A, B and C.

E_{ab}, E_{bc}, E_{ca} - Line-to-line voltages.

E_s - Voltage drop due to stator flux (Armature reactance drop).

E_g - Voltage generated by air-gap flux.

V_{xa} - Terminal voltage of phase A.

ϕ_r - Rotor, or field flux.

ϕ_{sr} - Field flux that links with stator winding A.

ϕ_s - Stator flux produced by current in winding A.

ϕ_g - Air-gap flux, a combination of ϕ_r and ϕ_s.

i_f - Current in the field winding on the rotor.

i_{xa} - Excitation current in phase A.

I_{xa} - Load current in phase A.

R - Stator resistance.

X - Stator leakage reactance.

X_f - Fictitious reactance due to armature reaction.

X_s - Synchronous reactance X_f + X.

δ - Torque angle.

θ - Power factor of load current.

CHAPTER 5

SYNCHRONOUS MACHINES

5.1 The Generation of Three-Phase Voltage

Three phase voltages are gnerated by a rotating magnetic field linking with three separate stator windings. The windings are spaced 120 electrical degrees apart and are shown in the most simple arrangement in such a manner that the rotating field will generate practically a fundamental frequency sine wave of voltage in each winding. Refer to Figure 5.1(a) and (b).

The rotating field in this case is produced by a winding on the rotor. Direct current is supplied to the rotor through slip-rings. The flux produced rotates with the rotor; the magnitude of the flux can be controlled by the dc in the rotor winding.

When the field is rotating in a counter-clockwise direction, the voltage wave E_{xa} in Fig. 5.1(b) is generated in winding A. A similar voltage E_{yb} is generated in winding B but it is displaced 120 degrees later in time than the voltage E_{xa}. Likewise the voltage E_{zc} in winding C occurs 120 degrees later than the voltage E_{yb}.

The windings A, B and C are similarly wound. Corresponding terminals of the windings can be connected together as in Fig. 5.2(a). In three phase analysis a double subscript notation is most often used to keep polarities straight. The phasor diagram representing the three voltages E_{xa}, E_{yb} and E_{zc} is shown in Fig. 5.2(b). The voltages between the terminals a, b and c are the line-to-line voltages. determined from the phasor diagram as:

$$E_{ab} = E_{ax} + E_{yb} = - E_{xa} + E_{yb}$$

The phasor E_{ax} must be reversed to obtain E_{xa}. The sum of the two phase voltages now can be added as in Fig. 5.2(b). Likewise

$$E_{bc} = E_{by} + E_{zc}$$

where phasor E_{bc} lags E_{ab} by 120°. Located another 120° later in time is the voltage E_{ca}.

The line-to-line voltages are greater than the phase voltages by the $\sqrt{3}$. Thus

$$E_{ab} = \sqrt{3}\, E_{ax}$$

$$E_{bc} = \sqrt{3}\, E_{by} \qquad \text{and lags } E_{ab} \text{ by } 120°$$

$$E_{ca} = \sqrt{3}\, E_{cz} \qquad \text{and lags } E_{bc} \text{ by } 120°$$

5.2 Armature Reaction: Generator With Unity Power Factor

When the generator is connected to a load, current flows in the stator windings A, B and C. This current produces a flux which reacts with the rotating field. The phenomenon is called Armature Reaction and it imparts some important characteristics to the generator. The same effect is produced when current flows in the stator windings of a synchronous motor.

The effect of armature reaction varies somewhat with the construction of the rotor. The general schematic construction of a salient pole machine is shown in Fig. 5.1(a). Here the reluctance of the magnetic circuit in line with the axis of the rotor poles is low because of the small air-gap, while the reluctance along aline perpendicular to the axis of the poles is high since there is a large air-space between the rotor and stator iron.

It was shown in Chapter 4 and in Fig. 4.12 and 4.13 that the voltage generated in a winding is zero when the flux linking it is at its maximum. In Fig. 5.3 the flux ϕ_{sr} is that portion of the constant rotor flux ϕ_r that links with the winding A at any instant. When the rotor is in the position of 0° as shown, ϕ_{sr} is maximum and the generated voltage is zero. After the rotor turns 90° the flux ϕ_{sr} linking the winding is zero but its rate of change is greatest. Therefore the generated voltage E_{xa} is maximum.

The effect of armature reaction depends very greatly on the phase angle of the current flowing in the stator. The stator reactance is generally quite high and complicates the simple explanation of armature reaction. For the purpose of this discussion the stator reactance and resistance can be neglected by referring the current to the induced voltage. Three conditions are considered. One in which the current is in phase with the induced voltage E_{xa} (unity power factor); another where the current lags the induced voltage by 90°; and the third, in which the current leads by 90°.

Let us now consider the unity power factor case. Let the winding A be connected to a load such that the stator current I_{xa} and likewise the stator ϕ_s are in phase with the voltage E_{xa}. The conditions when the rotor is in the position of 0° are shown in Fig. 5.3.

The stator flux ϕ_s is produced by the current flowing in the stator due to the connected load. It is a pulsating flux acting along the axis of the winding A. In the actual three-phase machine three of these out-of-phase pulsating fluxes create a revolving magnetic field of constant magnitude, but for simplicity, only the single phase relations are considered. This flux reacts with the constant flux rotating with the rotor and produces a net air-gap flux ϕ_g. Thus

$$\phi_g = \phi_s + \phi_r \qquad 5.1$$

In our single-phase example the pulsating stator flux combines with constant rotor flux. The relations of these two fluxes for the rotor at 0° and 90° are shown in Fig. 5.4(a) and (b). The addition of the fluxes as indicated by Eq. 5.1 at the 90° position is shown in Fig. 5.4(c). The net air-gap flux is somewhat greater than the rotor flux and is greatly influenced by the high reluctance of the stator path for this rotor position. The net flux is skewed

toward the trailing pole tip, as in Fig. 5.5(b), and as a result the air-gap flux is no longer sinusoidally distributed. The generated phase voltage E_{xa} will not be sine wave and its peak is shifted toward the trailing end of the wave. However, this distortion is not present in the line-to-line three phase voltage.

During the second 90° of rotation of the rotor, see Fig. 5.3, the stator flux decreases and becomes zero at 180°. During each half revolution of the rotor the air-gap flux ϕ_g varies from ϕ_r to $(\phi_s^2 + \phi_r^2)^{1/2}$ and back to ϕ_r at twice the rotational frequency as shown in Fig. 5.5(a). This air-gap flux links with the rotor field winding and generates in it voltage harmonic of double frequency.

It is important to note that, under these particular conditions, armature reaction produces a somewhat higher air-gap flux than that at no-load.

It should be understood that the addition of fluxes presupposes that the result of the addition does not alter the reluctance of the magnetic path. Thus for each phasor addition we assume linearity. Actually the magnetic path may be saturated and at each value of flux density the quantities may be added only under the above assumption. Under this condition the result of the addition of component flux waves is accurate. For situations requiring a more rigorous machine analysis it is advisable to add MMF's instead of fluxes.

5.3 Armature Reaction: Generator With 90° Lagging Power Factor

The single phase voltage E_{xa} and the rotor position at 0° is shown again in Fig. 5.6. Let the stator winding A be connected to an inductive load so that the current lags the voltage E_{xa} by 90°. It is now obvious that the stator flux ϕ_s is maximum when the rotor is in the 0° position. Furthermore, the stator flux is directly opposing the rotor flux. In this case the air-gap flux is the arithmetic difference between the two. Thus

$$\phi_g = \phi_r - \phi_s \qquad 5.2$$

The air-gap reluctance is low due to the short air-gap for the stator flux, therefore, the stator flux is much larger than for a unity power-factor load. The flux is more nearly sinusoidally distributed. Again, there is a voltage of double frequency generated in the field winding; its magnitude is greater than that for unity power factor because of the direct opposition of the stator flux which produces a greater variation in air-gap flux linking the rotor (Fig. 5.7). The net air-gap flux is not displaced from the normal position of ϕ_r and the wave shape of the generated voltage E_{xa} is more nearly sinusoidal. These conditions are more clearly illustrated in Fig. 5.4(d) and (e), and in Fig. 5.7. The air-gap flux is now much less than that at no-load. That is $\phi_g << \phi_r$.

5.4 Armature Reaction: Generator With 90° Leading Power Factor

The single phase voltage E_{xa}, the stator current, and flux for a 90° leading power factor and the rotor position at 0° are shown in Fig. 5.8. Now the stator flux is maximum and aiding the field flux ϕ_r. The flux variation

through the field winding again produces a double frequency voltage in the winding. Other physical conditions are generally the same as for a lagging current, except that saturation is more likely to exist. These conditions are more clearly represented in Fig. 5.5(f) and (g) and in Fig. 5.9, and $\phi_g >> \phi_r$.

5.5 Voltage Regulation and Phasor Diagram

Synchronous generators are usually three phase machines. This means that the stator flux, and air-gap flux are rotating fields of constant magnitude similar to that of the rotor. However, for simplicity, we will continue to use one phase in considering the phasor diagrams.

Fig. 5.10(a) shows the stator phase winding A, the rotor in the position of maximum flux linkages ϕ_{sr}, and the no-load generated phase voltage E_{xa}. This voltage lags the flux linkages by 90°. The rotor flux, which also indicates the axis of the field poles, and the generated voltage can be represented by phasors. This phasor relation is shown in Fig. 5.10(b). It is exactly analogous to the transformer phasor diagram of excitation flux and induced voltage. At no-load the air-gap flux ϕ_g is identical to the rotor flux ϕ_r, and they occupy the same position in time and space. This is because there is no stator flux hence no armature reaction.

Assume that the load current flows in a resistance load, in phase with the terminal voltage V_{xa}. Let us not neglect the stator reactance and resistance. For the moment let us establish the current I at some angle greater than 90° lagging the rotor position ϕ_r, as shown in Fig. 5.11.

The load current establishes a stator flux in phase with the current. This flux ϕ_s adds vectorily to the rotor flux ϕ_r to produce the resultant air-gap flux ϕ_g. Associated with each component of flux is a corresponding voltage lagging by 90°. Thus the no-load, open circuit voltage E_{xa} lags the rotor flux ϕ_r by 90° and the new air-gap flux ϕ_g generates E_g 90° behind ϕ_g. Even though the armature reaction is caused by a load current, the voltage E_g is internally generated by the air-gap flux, and it is not considered as a load voltage. The terminal or load voltage V_{xa} is obtained by subtracting vectorily from E_g, the winding resistance and leakage reactance drops. Thus

$$V_{xa} = E_g - (IR + IX) \qquad 5.3$$

If the current is now in phase with the load voltage, V_{xa}, we have confirmed our assumptions. If not we must try again with I in a different phase position. This method is not adequate for establishing a working phasor diagram, and special techniques have been established to do so. (See "Alternating Current Machines" by Puchstein, Lloyd, and Conrad, pages 204-206, 3rd Edition, John Wiley & Sons, Inc., 1954.

If an inductive load is applied, the phasor diagram is represented by Fig. 5.12(a). Note how drastically the armature reaction reduces the air-gap flux and the corresponding generated voltage E_g. The terminal voltage becomes still lower when the resistance and leakage reactances are considered.

A capacitive load placed across the terminals of the generator causes the current to lead the voltage as in Fig. 5.12(b). Now the air-gap flux and generated voltage are increased beyond the no-load conditions of ϕ_r and E_{xa}.

In all of the phasor diagrams the voltage E_s is due to the stator flux ϕ_s and lags it by 90°. It is directly in phase with the leakage reactance drop. Some simplification is useful by combining these voltages. The voltage E_s can be replaced by a reactance drop IX_f, where X_f is a fictitious reactance to account for armature reaction. Thus,

$$E_s + IX = IX_f + IX \qquad 5.4$$

The reactances X_f and X can be further combined into a term called Synchronous Reactance X_s.

$$X_s = X_f + X$$

and

$$IX_s = IX_f + IX \qquad 5.5$$

The drastic influence of the armature reaction is caused by the magnetizing or demagnetizing effect of the stator flux, and this is equivalent to the voltage drop IX_f. The terminal voltage V_{xa} is further affected by the stator resistance and leakage reactance drops. The phase angle of the load current has an important effect on the magnetizing or demagnetizing component of stator flux. Therefore, changing the magnitude of the load current and the power factor of the load causes the terminal voltage to vary greatly. This can not be tolerated in power systems, and some means of voltage regulation is necessary. The regulation is effectively accomplished by varying the field current. In Figs. 5.11 and 5.12(a) an increase in field current increases ϕ_r, E_{xa} and E_g. Thus the terminal voltage increases, and it can be adjusted to any desired value. This is done automatically in power systems. On the other hand, decreasing the field excitation in Fig. 5.12(b) will reduce the terminal voltage, and the generator can be made to maintain a constant output regardless of load or power factor.

A few facts about armature reaction in a synchronous generator are important:

1. The axis of the rotor is always in advance of the air-gap flus by some angle δ.

2. The generated voltage E_g is produced by the resultant air-gap flux, and lags it by 90°.

3. The resultant air-gap flux may be greatly different from its no-load value, depending on the magnitude and phase angle of the load current.

4. The angle δ in Figs. 5.11 and 5.12 is a power angle proportional to the power output and is useful in synchronous machine analysis.

5. Armature reaction produces a drastic effect on the terminal voltage and some means of regulation is necessary.

6. The magnetizing or demagnetizing components of stator flux is the cause of terminal voltage variation.

5.6 Synchronous Motor With No-Load and With Normal, Under and Over Excitation

Synchronous motors behave in a manner similar to synchronous generators, except that the effect current is reversed. That is, a lagging current supplied to the motor produces a stator flux which aids the rotor field, and a leading current opposes the field.

Consider a motor running a synchronous speed, without load, and with some excitation current i_f in the rotor field winding. A voltage E_{xa} is generated in the stator winding, phase A, as shown in Fig. 5.13. The rotor and the voltage E_{xa} are shown in the same position with respect to the stator winding as that in Fig. 5.3.

When an external voltage is applied to the stator winding an induced voltage is produced just as in a transformer. Let the voltage V_{xa} be applied to the stator winding of the motor under consideration, in the phase position shown in Fig. 5.13. The induced voltage will then be in phase with E_{xa}, but may not have the magnitude required to balance the applied voltage. An additional flux is then supplied by the stator in the following manner:

An excitation current i_{xa} flows in the stator winding and produces a stator flux ϕ_s which adds directly to the rotor flux. The magnitude of excitation current automatically adjusts to produce a stator flux which when combined with ϕ_r creates the exact amount of air-gap flux to generate the required value of E_{xa}. This is illustrated in the phasor diagram in Fig. 5.14 (a). The value of ϕ_g must remain constant as long as the value of E_{xa} is required. Now if the current i_f is increased in the field winding, a greater rotor flux ϕ_r will be produced by this current. The stator excitation will have to supply only enough flux ϕ_s to maintain the air-gap flux ϕ_g constant, $\phi_g = \phi_r + \phi_s$. Therefore the excitation current in the stator will decrease as shown in Fig. 5.14(b). The field current can be increased to the exact amount to establish the entire value of ϕ_g. Under these conditions, the stator excitation current becomes zero, as in Fig. 5.14(c).

Now let the field current i_f be increased still further. This will produce a rotor flux ϕ_r greater than required so the stator excitation must supply a subtractive flux ϕ_s to re-establish ϕ_r. That is $\phi_g = \phi_r - \phi_s$. This can be accomplished only by the stator drawing a leading current from the line as shown in Fig. 5.14(d).

The synchronous motor running without load can draw either a lagging or leading current of variable magnitude from the line. It thus may act as an inductance or as a capacitor. It is frequently used in substations as a synchronous condenser to current the power factor of the system.

Normal excitation is defined as that value of field current which requires no excitation current in the stator. Under excitation is a value of field current less than normal which causes the stator to draw a lagging current from the line. Over excitation is a value of field current greater than normal which causes the stator to draw a leading current from the line.

5.7 Behavior of Synchronous Motor with Load - Instability

Consider first the synchronous motor with normal excitation but without load as represented by phasor diagram Fig. 5.14(c). The voltage equation is similar to that for a transformer

$$V_{xa} = E_{xa} + i_{xa} (R + jX_s)$$

from which

$$i_{xa} = (V_{xa} - E_{xa}) / (R + jX_s) \qquad 5.6$$

When $V_{xa} - E_{xa} = 0$, no current flows in the stator as in the above situation.

When a load is applied to the motor shaft, a situation developes which permits current to flow into the stator. Since there is no electrical power input to the motor at the instant the load is applied, all of the energy during the first instant must be supplied by the mechanical energy stored in the rotating inertia of the rotor. It begins to slow down. As soon as the rotor drops behind its no-load position by a few degrees, the generated voltage E_{xa} also drops back. It is no longer in direct phasor opposition to the applied voltage but appears as in Fig. 5.15. A stator current flows from Eq. 5.6 and a stator flux ϕ_g is produced which is nearly 90° leading the rotor flux. The reaction between these two fluxes produces the required torque.

The rotor must always rotate at synchronous speed. The rotor decelerates while the torque angle δ is being established, but it must then immediately accelerate back to synchronous speed. There is a permanent displacement between the actual position of the rotor and its no-load position. This angle is the torque angle δ and the size of the angle depends on the load. If the angle exceeds a limiting value, the motor falls out of synchronism and comes to rest because it can deliver no torque.

In establishing the required torque angle, the rotor cannot stop accelerating or decelerating instantly because of its inertia. As a load is applied the rotor decelerates to the required torque angle and beyond. An excess of torque is then developed which accelerates the rotor back to the required value of δ and again goes past it. This time there is a deficiency of torque and again the rotor slows down. This process may be repeated several times with a diminishing amount of overswing. After a few cycles the stable torque angle is established. For a full study of instability the student is referred to any good text on electrical machines.

Fig. 5.16 shows the phasor relationship between the fluxes involved.

The stator flux, ϕ_s and the angle δ are the variables. The torque angle must be just right for the flux ϕ_s to supply the torque required by the load. Also the following equation must be satisfied; $\phi_g = \phi_s + \phi_r$. It must be remenbered that the air-gap flux resulting from this equation must remain constant. Also the rotor flux is fixed by the dc excitation in the field winding. The phase angle of the stator flux and therefore the phase angle of the stator current are fixed by the magnitudes of ϕ_g, ϕ_r and the angle δ. The phase angle of the stator current θ can be controlled by adjusting the value of ϕ_r by varying the field current.

The voltage that would be generated by the rotor flux alone is lagging its no-load position by the angle δ. The voltage generated at the no-load position is now generated by the resultant air-gap flux. It is now indicated as E_g.

5.8 Synchronous Motor with Load and with Normal, Under and Over Excitation

If the motor discussed in Sect. 5.7 above has its field excitation reduced but retains the same power angle δ, the armature reaction automatically takes care of the situation. The component of generated voltage E_{xa} due to the rotor flux, is reduced, permitting more current to flow in the stator. The magnitude and phase angle of this current is governed by the stator flux ϕ_s required to close the triangle between ϕ_r and ϕ_g. This is shown in Fig. 5.17. The stator flux has a large magnetizing component d, a direct axis component. The component of current m in phase with the segment d is responsible for the reactive power taken by the motor. The horizontal component of stator flux q is a cross axis flux. The component of current n in phase with q is the power input. The two components of stator flux give rise to the following equations:

$$m = I \sin \theta \tilde{} \text{ reactive power} \qquad 5.7$$

$$n = I \cos \theta \tilde{} \text{ real power} \qquad 5.8$$

If the rotor current is increased a high rotor flux is produced and a leading current is drawn from the line Fig. 5.18. This causes a demagnetizing action component d and a constant air-gap flux is again retained. Thus the synchronous motor can be used to correct a system power factor while it is at the same time doing useful work.

5.9 Transient Behavior of Synchronous Machines

The small machines used in the Laboratory are well suited for displaying the underlying fundamentals of transient and instability phenomena found in large machines. The small machines have characteristics which are not representative of scaled-down models of the large units. In fact, the small motors and generators have many characteristics which are deliberately designed out of the large power machines to promote better stability in the latter. Fortunately, for our purpose, the instability features are exaggerated, and therefore it is relatively easy to demonstrate and record some complex instability phenomena of synchronous machines.

The three-phase wound rotor induction motor can be operated very well as a synchronous motor. The salient pole machine can be used also as a synchronous motor but it is not self starting and must be brought up to nearly synchronous speed by some external drive. The wound rotor, on the other hand, can be started and brought up to speed as a conventional induction motor and then converted to a synchronous machine. In addition, the wound rotor has other advantages in that the affects of different degrees of rotor damping can be observed.

Fig. 5.22 is a schematic diagram of the rotor and stator of the three-phase wound rotor induction motor used as a synchronous motor. The stator is connected to a three-phase, 120 volt supply. The motor can be started by shorting together the three terminals of the rotor phase windings a, b, and c. The rotor will come up to a speed near enough to pull into synchronism by opening the rotor circuit and applying dc to two of the phase windings such as a and b, as shown in the figure. Phase winding c can be left open or it can be connected in parallel with winding b as shown by the dotted line. The two connections will produce different degrees of damping resulting in different transient behavior of the rotor as will be seen later.

A single-phase induction motor belted to the synchronous motor can be used as a load. This is also shown in Fig. 5.22. A dc placed on one of its stator windings will induce heavy currents in the squirrel cage rotor as it revolves in the dc field, and a strong force opposing the rotation will be established. The magnitude of the load can be controlled by the amount of dc excitation, and any load can be switched on and off in rapid succession.

Instantaneous rotor speed changes can be observed and recorded by the simple circuit shown in Fig. 5.23. The dc tachometer generator is driven by the belt from the synchronous motor and represents actual synchronous rotor speed. At synchronous speed the tachometer voltage is nullified by an opposing constant voltage referred to as the synchronous speed voltage. The difference voltage, represents the instantaneous change of speed and can be applied directly to the x-y recorder with a time base.

When a load is suddenly applied to a synchronous motor, all of the energy required by the load, during the first instant of time, is supplied by the rotating mass of the rotor. There is a brief period of deceleration when the instantaneous speed of the rotor drops, but the position of the rotor never drops behind its no-load position by as much as $\frac{1}{2}$ or $\frac{1}{4}$ revolution. Due to the mass of the rotor, it cannot instantly stop decelerating when the rotor displacement reaches the value just sufficient for the electrical power input to supply the load, explained in Sect. 5.7. The rotor overshoots this position and as a result more torque is produced than the load requires. The rotor then begins to accelerate and the instantaneous speed may increase above synchronous speed. Now the torque angle is too small to supply the load and the rotor again slows down. After a few oscillations the rotor establishes a stable position where the torque angle is just enough for the electrical energy to supply the load requirements. Fig. 5.24 is a record of the instantaneous speed when the load is repeatedly applied and removed.

5.10 Transient Power in a Synchronous Motor

Transient power can be represented by the product of the current and voltage in one phase of the stator winding of the synchronous machine. If the induced voltage from the information winding is multiplied by the phase current, as in Fig. 5.25 the product represents the power in the rotor and does not include the stator losses. Fig. 5.26 is a recording made by the x-y plotter with a time base, when connected directly to the output of the multiplier. It shows the instantaneous power developed as the dc is repeatedly applied and removed from the stator winding of the single-phase squirrel cage motor.

The curve A in Fig. 5.26 was taken with the synchronous motor field excitation applied to phases a and b with phase c open in Fig. 5.22, and thus the rotor had its lowest damping property. The record shows however that there is a much greater damping when the load is applied than when the load is removed. This is because the rotor of the single-phase motor, acting as a load, adds additional damping when the load is applied but this effect is not present when the load is removed.

Curve B of Fig. 5.26 was taken with phase c of the synchronous motor rotor winding connected in parallel with phase b. The rotor is now highly damped and no oscillations appear in the record for either the load applications or removal, and the transient power is much more stable.

5.11 Effect of Rotor Excitation

The salient pole synchronous machine can be driven by a dc, induction, or another synchronous motor and it can be used to supply power to the stator in Fig. 5.22. Greater instability may be encountered with this system. As an example, Fig. 5.27(a) shows the effect of rotor excitation on the synchronous motor stability. Curve A was obtained with 1.3 amperes of excitation in the synchronous motor field when winding c was connected in parallel with winding b. There is no instability of transient power when load is applied or removed.

With only 0.4 amperes of dc excitation applied to the same rotor connection, significant oscillations appear in the instantaneous power as shown in Fig. 5.27(b)

5.12 Experiments

DIRECT AND QUADRATURE AXIS RELUCTANCES AND REACTANCES

Experiment 5.1

A voltage of about 50 volts can be applied to one phase of the three-phase synchronous machine, with no excitation in the field, that is, $i_f = 0$. The stator flux remains essentially constant because of the required induced voltage. The excitation current depends on the reluctance of the magnetic

circuit. Thus

$$i_{xa} = \phi_s \mathcal{R} / N \qquad 5.1a$$

The excitation is also the input current from the line. It can be observed by connecting a scope across a series resistance in the line as in Fig. 5.19. The resistor should be low enough to produce no more than one volt drop.

Rotate the rotor slowly and observe the variation in excitation current which is directly proportional to the reluctance of the flux path.

The reactance of the stator is high when the axis of the rotor is in line with the stator winding. This is called Direct Axis Reactance X_d. It is low when the axis of the rotor is 90° from the stator winding. It is called Quadrature Axis Reactance X_q. These reactances can be measured approximately by the following

$$X_d = V_{xa}/i_{xa} \quad \text{(Minimum value)} \qquad 5.1b$$

$$X_q = V_{xa}/i_{xa} \quad \text{(Maximum value)} \qquad 5.1c$$

The constancy of the stator flux can be checked by connecting the information windings s_1, s_2, to an integrator and then to a scope as in Fig. 5.19.

SYNCHRONOUS MACHINES

Experiment 5.2
Self Excitation

A leading power factor load on a synchronous generator creates a stator flux which directly aids the field flux. See Fig. 5.4f.

A machine driven by a motor at a speed which will generate 60 Hz is shown in Fig. 5.20. A capacitor of 10 mfd is shown connected to phase A. If there is enough residual flux in the rotor, a small voltage should be generated which will cause a leading current in the stator. This in turn will create a stator flux which will aid the rotor flux and build up a higher voltage.

Try a larger capacitor, say 100 mfd.

If there is not enough residual flux, apply a low value of dc current i_f to the field without the capacitor. Then connect the capacitor to determine if the voltage builds up. If it does remove the dc excitation and observe the behavior of the machine for self excitation.

Self excitation can be observed in a single phase, capacitor start motor also by an experiment represented by Fig. 5.21. A residual flux can be created in the rotor by energizing phase A with dc and opening the dc switch while the machine is running with a capacitor connected to phase B.

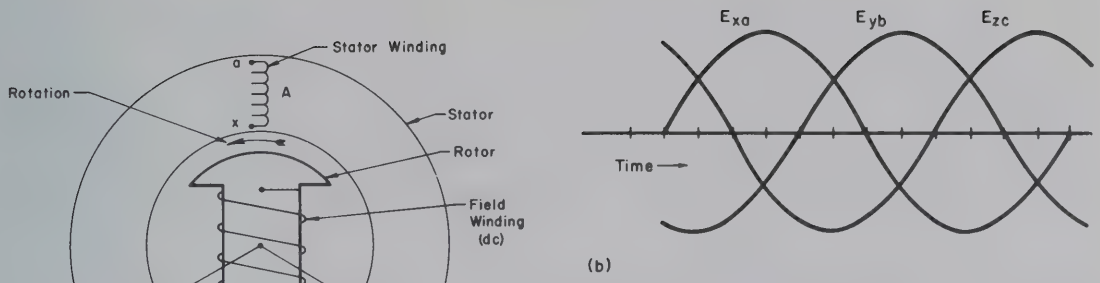

Fig. 5.1 The generation of three-phase voltages. a) Stator winding relationship. b) Phase relation between the three voltages generated windings A, B and C.

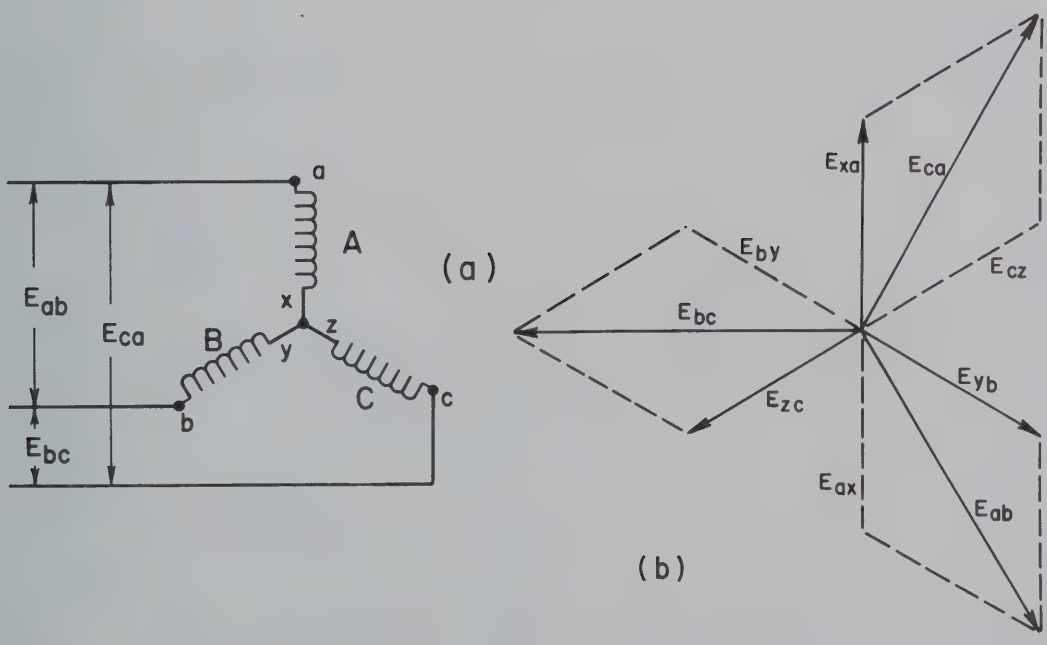

Fig. 5.2 Phase and line voltages. a) Three-phase Y connection. b) Phasor diagram of phase and line voltages.

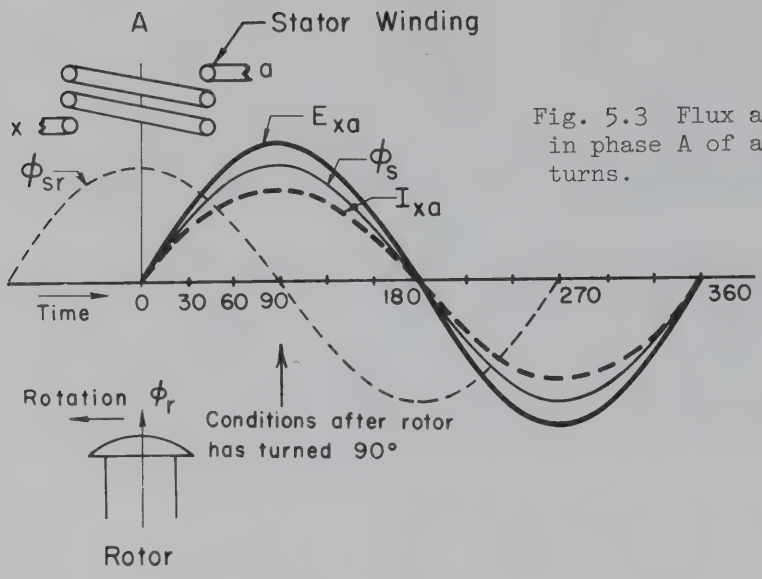

Fig. 5.3 Flux and voltage relations in phase A of a generator as the rotor turns.

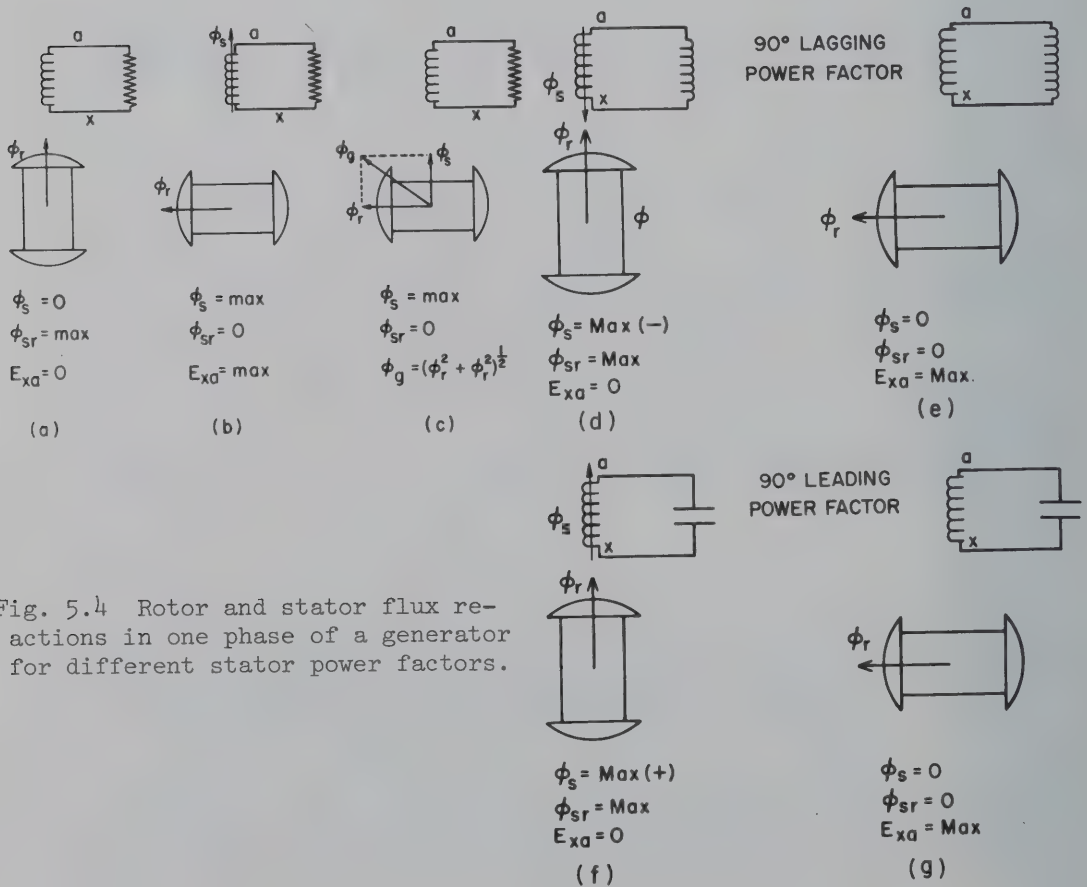

Fig. 5.4 Rotor and stator flux reactions in one phase of a generator for different stator power factors.

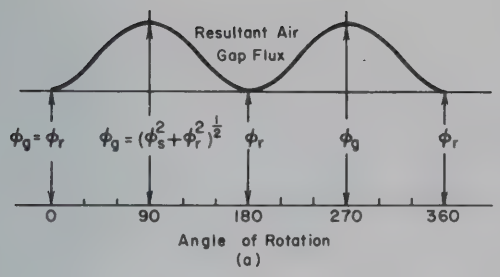

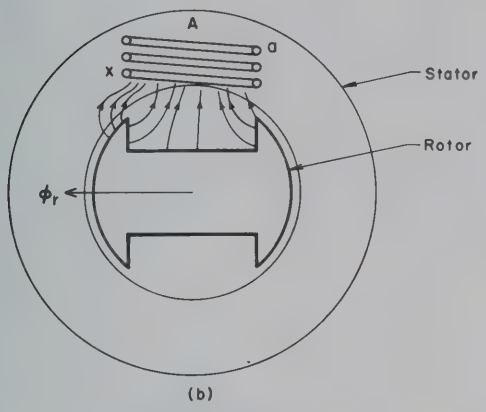

Fig. 5.5 Air-gap flux. a) Net air-gap flux in one phase of a generator with unity power factor. b) Skewed air-gap flux due to stator MMF and salient pole rotor.

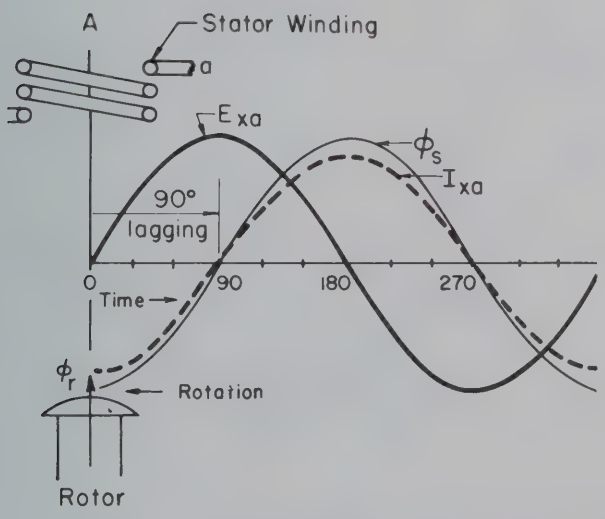

Fig. 5.6 Flux and voltage relations in phase A of a generator with 90° lagging phase angle in stator winding.

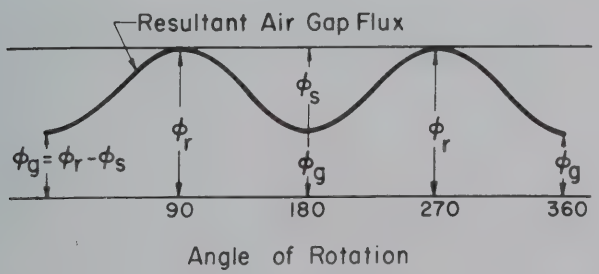

Fig. 5.7 Net air-gap flux variation resulting from rotor and stator fluxes when stator phase angle is 90° lagging.

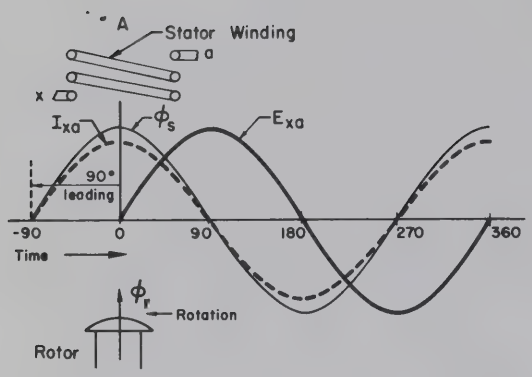

Fig. 5.8 Flux and voltage relations in phase A of a generator with 90° leading phase angle in stator winding.

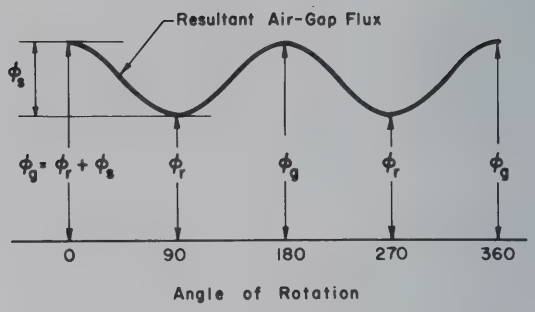

Fig. 5.9 Net air-gap flux variation resulting from rotor and stator fluxes when stator phase angle is 90° leading.

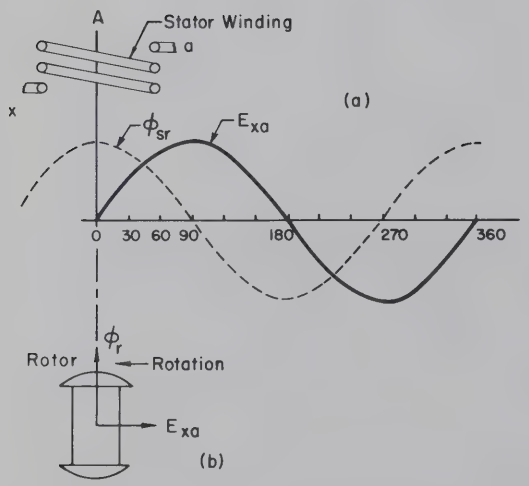

Fig. 5.10 No-load generated voltage with rotor shown in position for maximum flux linkage with stator. a) Phase and time relations of flux linkages ϕ_{sr} and no-load voltage E_{xa}. b) Phasor diagram for ϕ_{sr} and E_{xa}.

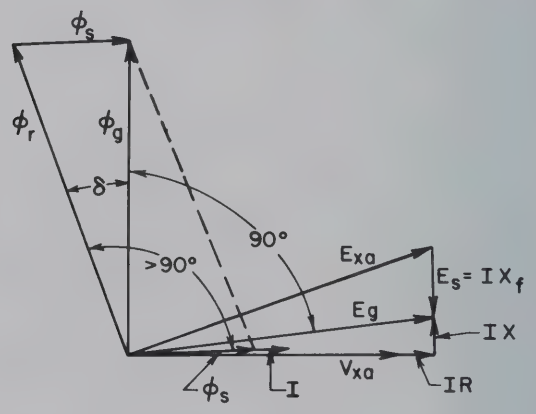

Fig. 5.11 Phasor diagram for one phase of a synchronous generator with unity power factor in the stator winding.

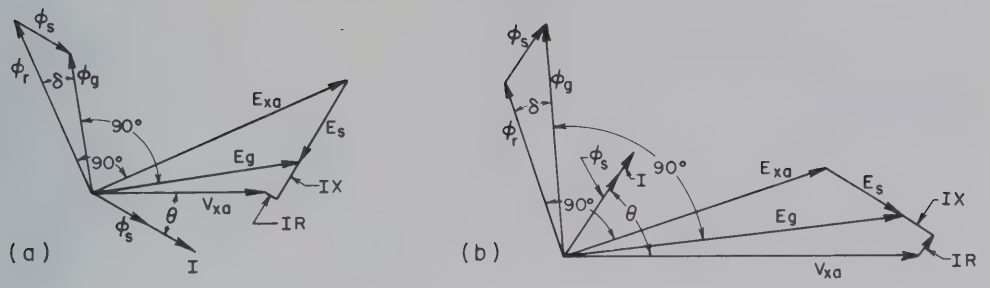

Fig. 5.12 Phasor diagram for one phase of a synchronous generator. a) lagging phase angle in stator. b) leading phase angle in stator.

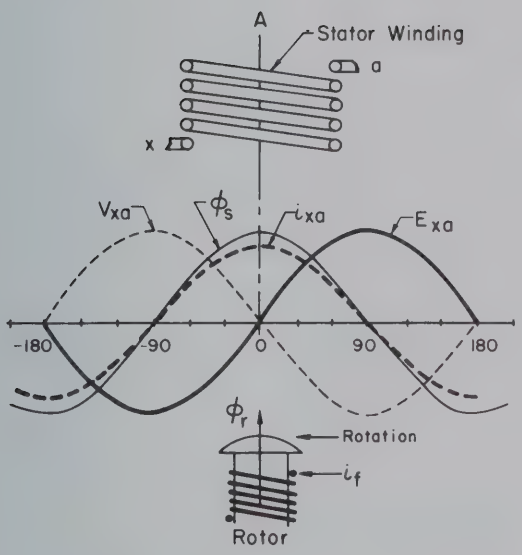

Fig. 5.13 Flux and voltage relations in a synchronous motor with no-load and with under excitation.

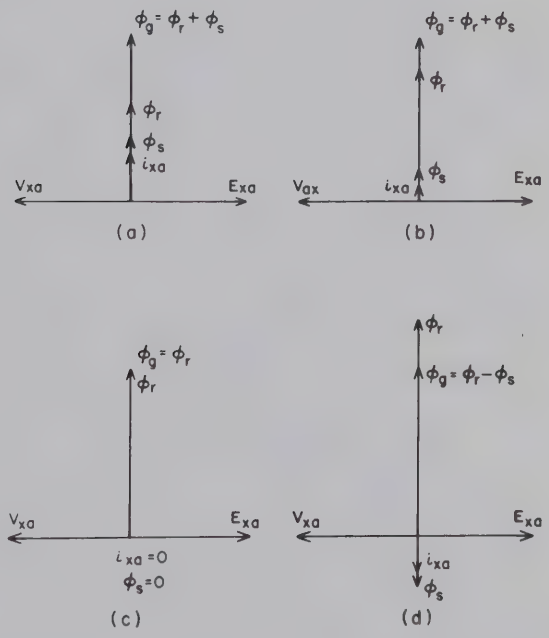

Fig. 5.14 Phasor diagrams for a synchronous motor with no-load showing how stator current is affected by rotor excitation. a) under excitation. b) under excitation. c) normal excitation. d) over excitation.

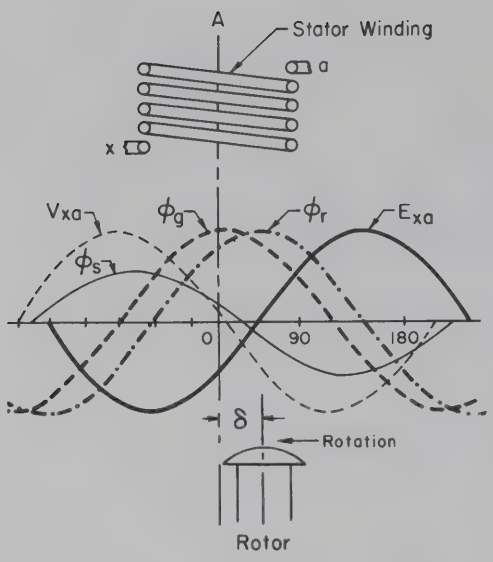

Fig. 5.15 Flux and voltage relations in one phase of a synchronous motor with load producing the torque angle δ.

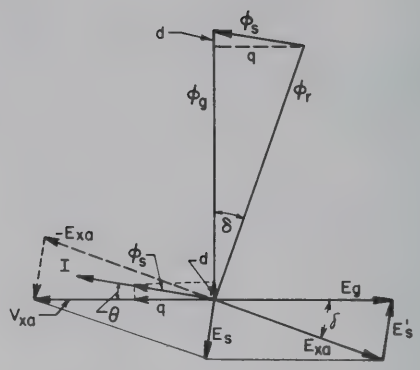

Fig. 5.16 Phasor diagram for one phase of a synchronous motor with load.

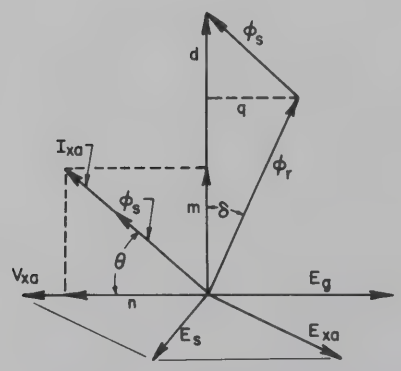

Fig. 5.17 Same as Fig. 5.16 with reduced rotor excitation.

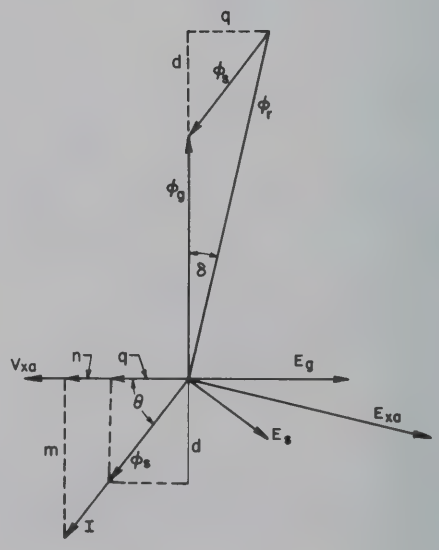

Fig. 5.18 Phasor diagram for one phase of a synchronous motor with the same load as for Fig. 5.16 with over excitation.

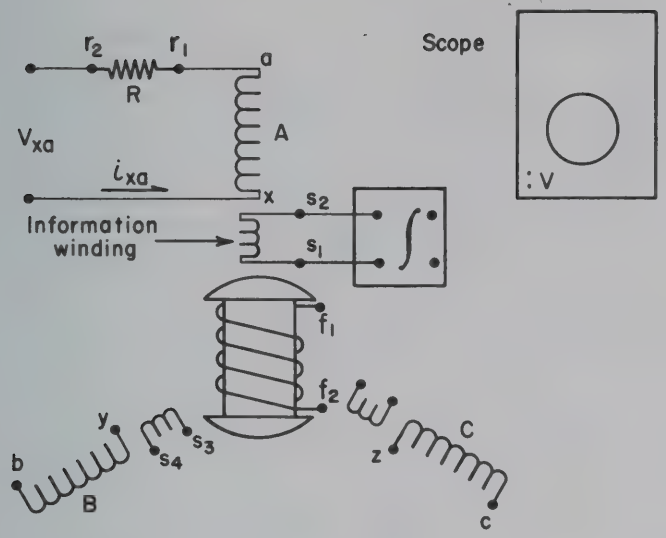

Fig. 5.19 Diagram for measuring stator flux.

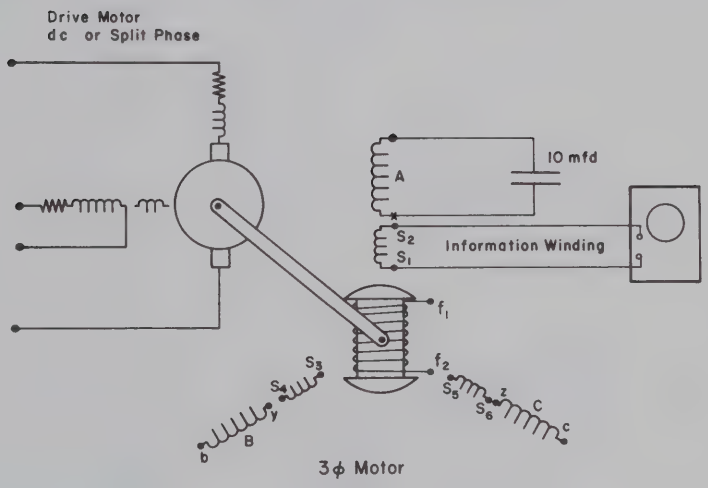

Fig. 5.20 Diagram for observing the effect of a capacitor load on the stator flux.

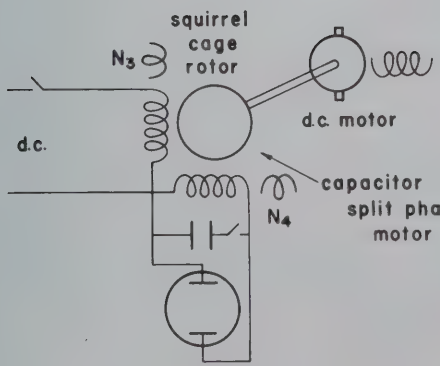

Fig. 5.21 Diagram for establishing self excitation in an induction motor.

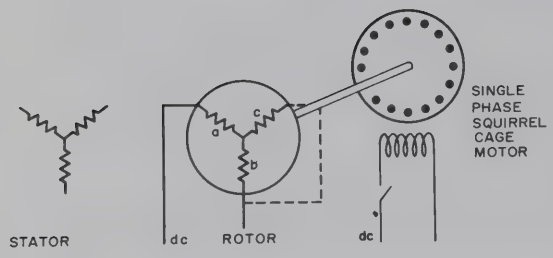

Fig. 5.22 Schematic diagram for using a 3-phase wound rotor induction motor as a synchronous motor.

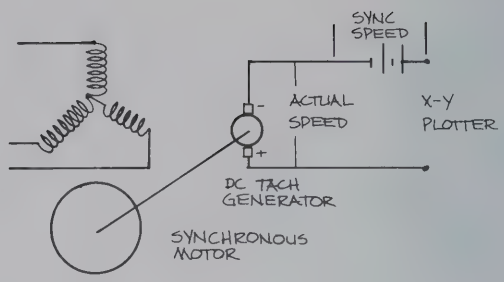

Fig. 5.23 Diagram for recording instantaneous speed.

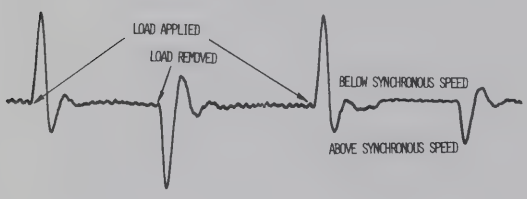

Fig. 5.24 Instantaneous change of rotor speed when load is repeatedly applied and removed.

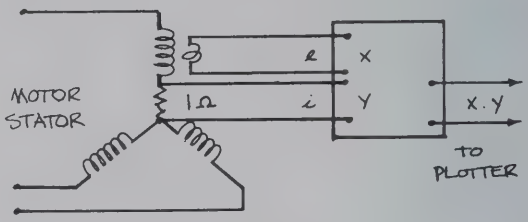

Fig. 5:25 Diagram for recording instantaneous power.

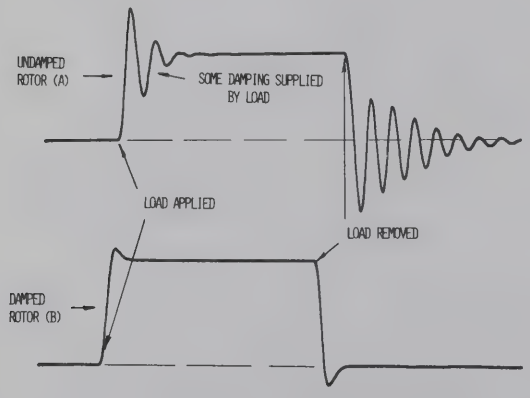

Fig. 5.26 Transient power in synchronous machine when load is suddenly applied and removed. a) low rotor dumping. b) high rotor dumping.

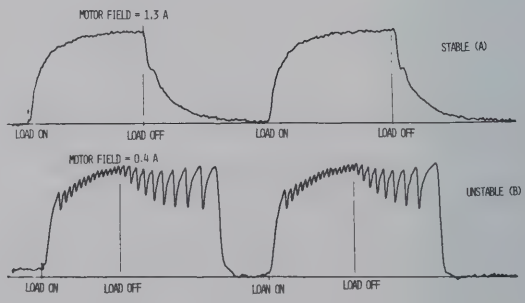

Fig. 5.27 Effect of field excitation on transient power. a) high field excitation. b) low field excitation.

NOMENCLATURE FOR CHAPTER 6

V_f - Voltage applied to the motor field.

e - Induced voltage in the field.

e_g - Generated voltage in the armature.

E_a - Terminal voltage of the armature.

i - Field current.

i_a - Armature current.

r_f - Resistance of the field winding.

r_a - Resistance of the armature winding.

R - Resistance shunted across the field terminals.

L_f - Inductance of the field winding.

L_a - Inductance of the armature winding.

τ_f - Time constant of the field circuit.

ϕ - Flux established by the field current.

$\mathfrak{R}$ - Reluctance of the magnetic circuit to the field flux.

N - Number of turns in the field winding.

K_a - Armature constant.

ν - Rotational speed of the armature.

T_L - Torque available for the load.

T_w - Torque required to supply the losses, windage and friction.

T - Torque developed in the armature.

J - Moment of inertia.

Δ - Incremental quantities.

(′), (″), and subscripts $_1$, $_2$ denote successive quantities.

CHAPTER 6

DC Machines

The dc generator cannot compete with the solid state rectifier as an economic source of dc power. The generator therefore is becoming less important in the study of electrical machines. The dc motor, on the other hand, is more broadly applied than ever. This chapter deals with the transient and dynamic behavior of the dc machine and applies, in general, to either the generator or motor.

6.1 The Field Circuit and the Transient Build-Up of Flux

The equivalent circuit for the field circuit consists of the winding resistance in series with the winding inductance as shown in Fig. 6.1. The winding inductance is frequently determined from the saturation curve, as explained later. Therefore, the leakage inductance need not be considered as a separate quantity, as in the transformer. The differential equation for this circuit is

$$V_f = r_f\, i + L_f\, di/dt.$$

A more preferable equation for this analysis is

$$V_f = r_f\, i + N\, d\phi/dt \qquad 6.1$$

In studying the internal behavior of the flux build-up equal intervals of time are used, each equal to one time unit, u

$$\Delta t_o = \Delta t_1 = \Delta t_2 = \cdots = \Delta t_n = u$$

The voltage V_f is applied to the circuit at t_o. During the equal time intervals the corresponding build-up of flux is

$$\Delta\phi_o,\ \Delta\phi_1,\ \Delta\phi_2, \cdots\cdots,\ \Delta\phi_n$$

The successive currents necessary to produce the fluxes are

$$\Delta i_o,\ \Delta i_1,\ \Delta i_2, \cdots\cdots,\ \Delta i_n$$

The relation between the incremental quantities and the finite quantities is given in the following equations:

$$t_1 = 0 + \Delta t_o \qquad 6.2$$

$$t_2 = t_1 + \Delta t_1 \text{ etc.}$$

$$i_1 = 0 + \Delta i_o = \Delta i_o \qquad 6.3$$

$$i_2 = i_1 + \Delta i_1 \quad \text{etc.} \tag{6.4}$$

$$\phi_1 = 0 + \Delta\phi_o = \Delta\phi_o$$

$$\phi_2 = \phi_1 + \Delta\phi_1 \quad \text{etc.} \tag{6.5}$$

In terms of incremental quantities Eq. 6.1 can be written

$$V_f = N\,\Delta\phi/\Delta t + r_f i \tag{6.6}$$

At $t = 0$, Eq. 6.6 becomes

$$V_f = N\,\Delta\phi_0/\Delta t_o + r_f\, i_o$$

or, when $i_o = 0$

$$\Delta\phi_o/\Delta t_o = V_f/N \tag{6.7}$$

Eq. 6.7 represents the initial slope of the flux build-up at the instant when the voltage is applied. At the end of the first interval of time

$$t_1 = 0 + \Delta t_o = \Delta t_o$$

The new slope of the flux build-up is

$$\Delta\phi_1/\Delta t_1 = V_f/N - r_f i_1/N \tag{6.8}$$

From Eq. 6.3

$$\Delta\phi_1/\Delta t_1 = V_f/N - r_f\,\Delta i_o/N \tag{6.9}$$

and from Eq. 6.7

$$\Delta\phi_1/\Delta t_1 = \Delta\phi_o/\Delta t_o - r_f\,\Delta i_o \tag{6.10}$$

Thus the slope of the build-up at the end of the first interval is less than the initial slope, that is $\Delta\phi_1/\Delta t_1 < \Delta\phi_o/\Delta t_o$.

Most circuit analyses are based on linearized assumptions. From Ohms Law of the magnetic circuit the reluctance is $\mathcal{R} = NI/\phi$, and it is assumed to be constant, that is, the relation between the magnetizing force and the flux is linear. This relationship is shown by the dotted curves in Fig. 6.2. In reality this is incorrect. The actual relations are shown by the saturation curve in Fig. 6.2 and the realistic reluctance curve with reluctance plotted as a function of flux is also shown. The reluctance curve is obtained by using successive incremental quantities in the equation $\mathcal{R} = \Delta NI/\Delta\phi$.

A linear analysis is given below. This is followed by an indication of

how the non-linear analysis can be made and where errors are involved in the linear analysis. From the magnetic circuit relations, the current change necessary to produce the flux change, assuming constant reluctance, is

$$\Delta i_o = \Delta\phi_o \mathcal{R}/N \qquad 6.11$$

Substituting $\Delta\phi_o$ from Eq. 6.7 in Eq. 6.11

$$\Delta i_o = V_f \Delta t_o \mathcal{R}/N^2 \qquad 6.12$$

At the time $t_2 = t_1 + \Delta t_1 = \Delta t_o + \Delta t_1$

$$\Delta\phi_2/\Delta t_2 = V_f/N - r_f i_2/N \qquad 6.13$$

Substituting Eq. 6.4 in Eq. 6.13

$$\Delta\phi_2/\Delta t_2 = V_f/N - r_f\, i_o/N - r_f \Delta i_1/N \qquad 6.14$$

Substitute Eq. 6.9 in Eq. 6.14, thus

$$\Delta\phi_2/\Delta t_2 = \Delta\phi_1/\Delta t_1 - r_f \Delta i_1/N \qquad 6.15$$

therefore

$$\Delta\phi_2/\Delta t_2 < \Delta\phi_1/\Delta t_1$$

The next incremental current is

$$\Delta i_1 = \Delta\phi_1 \mathcal{R}/N \qquad 6.16$$

Substituting Eq. 6.8 in 6.16

$$\Delta i_1 = (V_f/N - r_f i_1)\, \Delta t_1 \mathcal{R}/N \qquad 6.17$$

$$= V_f \Delta t_1 \mathcal{R}/N^2 - r_f i_1 \Delta t_1 \mathcal{R}/N \qquad 6.18$$

Substituting Eq. 6.12 in 6.18, remembering that $\Delta t_1 = \Delta t_o$

$$\Delta i_1 = \Delta i_o - r_f i_1\, \Delta t_1 \mathcal{R}/N \qquad 6.19$$

Thus $\Delta i_1 < \Delta i_o$. If this process is continued to t_n we find that

$$\Delta\phi_n < \Delta\phi_{n-1} < \ldots\ldots < \Delta\phi_2 < \Delta\phi_1 < \Delta\phi_o \qquad 6.20$$

and

$$\Delta i_n < \Delta i_{n-1} < \ldots\ldots < \Delta i_2 < \Delta i_1 < \Delta i_o \qquad 6.21$$

The general shape of the flux and current build-up curves is shown in Fig. 6.3.

The internal induced voltage from Eq. 6.7 is

$$e_o = N\Delta\phi_o/\Delta t_o = V_f \qquad 6.22$$

This means that at the instant of application of the voltage the induced voltage balances the entire applied voltage. The next value of induced voltage at t_1 is

$$e_1 = N\Delta\phi_1/\Delta t_1 \qquad 6.23$$

From Eq. 6.20 and Eq. 6.23 we have $e_1 < e_o$ and continuing the process we get

$$e_n < e_{n-1} < \ldots\ldots < e_2 < e_1 < e_o \qquad 6.24$$

The decay curve of induced voltage is shown in Fig. 6.3.

By accumulating the individual increments of current, the total current curve and the resistance drop, $r_f i$, curve can be plotted. By subtracting the $r_f i$ drop curve from the constant applied voltage we can get the induced voltage decay curve also shown in Fig. 6.3. If the increments are sufficiently small these curves become the familiar exponential curves.

The non-linear mathematical analysis is quite complex, but the incremental method is essentially no more complex than for the linear method. It is only necessary to use values of reluctance from Fig. 6.2 in the incremental current equations similar to Eq. 6.12 corresponding to the accumulated value of flux. The general incremental current equation becomes

$$\Delta i = \Delta\phi\,\mathcal{R}/N \qquad 6.25$$

The value of reluctance in this equation must correspond to some average value of flux at which the increment $\Delta\phi$ occurs, as shown in Fig. 6.2.

Notice that the value of $\mathcal{R}$ continually increases as the flux increases to saturation. Each incremental value of current calculated from incremental equations similar to Eq. 6.11 is greater than for the linear case because of the greater values of $\mathcal{R}$. The actual time-current build-up curve is shown in Fig. 6.4 with the linearized curve from Fig. 6.2 shown for comparison with the area of error indicated.

The exponential equation for the current build-up is

$$i = \frac{V_f}{r_f}\left(1 - \varepsilon^{-t/\tau_f}\right) \qquad 6.26$$

where τ_f is the time-constant of the field

$$\tau_f = L_f/r_f \qquad 6.27$$

In the linearized analysis the inductance and the time-constant are assumed to remain constant over the range of flux. In the realistic case however the time-constant must be considered as a variable.

Inductance is defined as flux linkages per unit of current. Thus

$$L_f = N\ \phi/i \qquad 6.28$$

For an incremental change current we can define incremental inductance as

$$\Delta L = N\ \Delta\phi/\Delta i \qquad 6.29$$

Along a linear portion of the saturation curve in Fig. 6.5 the inductance is constant. However, along the curved portion the $\Delta\phi$ becomes progressively less for successive values of Δi. At very high values of saturation the curve becomes essentially linear again and the inductance constant but lower in value. The inductance vs current curve is therefore non-linear and its general shape is shown in Fig. 6.5.

The time constant τ_f of the field is a non-linear variable but its value ($\tau_f = L_f/r_f$) becomes less, that is, shorter in time, as the field builds up. Therefore, we should expect the actual current to reach a given value in a shorter time than calculated from Eq. 6.26. The actual current build up can be predicted more accurately by using actual values of τ_f as illustrated in Fig. 6.5. This effect is the same as in Fig. 6.4.

6.2 Transient Induced Voltages in Field

When a switch is closed connecting a dc field of a machine to a power source, the rate of change of flux can never be great enough to produce an induced voltage higher than the supply voltage. See Eq. 6.1.

When the switch is opened the situation may be different. If the switch is opened and the terminals of the field simultaneously shorted, the induced voltage equals the supply voltage. The transient decay curves will be the inverse of the build-up curves because the time constant τ_f remains the same. However, if the field is connected to a high resistance, instead of being shorted, the total value of R is higher, τ becomes shorter, and the current and flux decays faster. Hence the $d\phi/dt$ may be high.

Let the field winding be energized and held in its steady state condition before the switch is opened to disconnect the supply voltage (Fig. 6.6a). At the instant before the switch is opened.

$$\begin{aligned} V_f &= ir_f + L_f\ di/dt \\ &= ir_f + N\ d\phi/dt \\ &= ir_f + 0 \end{aligned} \qquad 6.30$$

At the instant the switch is opened let the terminals of the winding be shorted as in Fig. 6.6(b); the current remains for an instant at its steady state value. Thus, at t = 0

$$V_f = 0 = ir_f + N\, d\phi/dt$$

or

$$-e = N\, d\phi/dt = -\, ir_f \qquad 6.31$$

The initial rate of flux decay is

$$d\phi/dt = -\, ir_f/N \qquad 6.32$$

In this case, when the terminals are shorted the maximum value of induced voltage is $ir_f = V_f$.

Now let the terminals of the field be connected to a high resistance at the instant of disconnecting the supply voltage, as in Fig. 6.6(c).

$$V_f = 0 = i\,(r_f + R) + N\, d\phi/dt$$

or

$$-e = N\, d\phi/dt = -\, i\,(r_f + R) \qquad 6.33$$

and the initial slope of the flux decay is

$$d\phi/dt = -\, i\,(r_f + R)/N \qquad 6.34$$

If the external resistance is very high as would be the case if there was no resistance across the terminals in Fig. 6.6(c), the induced voltage could be very high. This voltage occurs across the terminals of the field and may be high enough to damage the insulation in the field winding. For this reason a field discharge resistor is connected across the field if its supply voltage must be interrrupted. This greatly reduces the arcing at the contacts of the switch circuit breaker.

6.3 The Armature Circuit and the Transient Build-Up of Voltage at No-Load in a Generator

Fig. 6.1 shows the armature circuit of a dc machine having an ideal armature with external armature inductance and resistance. The inductance is quite low and may be neglected except for rapid armature current changes.

Let us consider the machine as a dc generator driven at a constant speed ν. Since the armature inductance and resistance are both inside the motor, the terminal voltage E_a is the only voltage available for measurement. At no-load $e_g = E_a$, and the latter may be used as a measure of the internally generated voltage.

The generated voltage is directly proportional to the field flux and to

the speed of rotation of the armature. Thus

$$E_a = e_g = K_a \phi \nu \qquad 6.35$$

K_a is an armature constant and dependent on the number of turns in the armature and on the geometry of the winding. The generated voltage is, at all times, directly proportional to the field flux when the speed is held constant.

When the field switch s in Fig. 6.1 is closed, there is a time-flux build up as shown in Fig. 6.4. The generated voltage-time build-up has identically the same shape as the flux; its value can be determined by multiplying the flux-time curve by $K_a \nu$.

The exponential equation 6.26 can be re-written as

$$i = \frac{V_f - V_f \varepsilon^{-t/\tau_f}}{r_f} \qquad 6.36$$

This equation can be represented by a block diagram Fig. 6.7(a) which represents the flow of current into the field. Initially the exponential term is equal to V_f when the current is zero. The exponential term soon dies out leaving the current $i = V_f/r_f$. The current creates a field flux according to the saturation curve Fig. 6.7(b) and both require identical times to arrive at their steady state values. The flux multiplied by the armature constant and speed gives the generated voltage Fig. 6.7(c).

Because of the linearity between the flux and generated voltage, the latter is frequently used as a measure of flux.

6.4 Transient Build-Up of Speed in Motor at No-Load

The differential equation for the armature circuit of the motor in Fig. 6.8 is

$$E_a = K_a \phi \nu + L_a di_a/dt + r_a i_a \qquad 6.37$$

$$= e_g + L_a di_a/dt + r_a i_a$$

The differential equation for the torque is

$$T_L = K_a \phi i_a - J \, d\nu/dt - T_w \qquad 6.38$$

Where

T_L is the torque available for the load.

$K_a \phi i_a$ is the torque developed in the armature.

$J \, d\nu/dt$ is the inertia torque, or torque required to change the speed of the rotor.

T_w is the torque necessary to overcome the losses.

Let the field be energized at steady state from a separate source as Fig. 6.8.

At t = 0, let the armature circuit be energized with the following assumptions

1) L_a is usually quite small and can be neglected but its effect is considered.
2) The load torque T_L is zero.
3) The losses T_w are negligible.

At t = 0 the velocity ν is zero and Eq. 6.37 becomes

$$E_a = K_a\phi\ \nu + L_a di_a/dt + r_a i_a$$

$$= \quad 0 \quad + \quad 0 \quad + r_a i_a \qquad 6.39$$

The initial current therefore is

$$i_a = E_a/ra \qquad 6.40$$

At a small increment of time Δt_o later some incremental velocity will be established. Thus, from Eq. 6.38

$$0 = K_a\ \phi\ i_a - J\ \frac{\Delta \nu_o}{\Delta t_o} - 0 \qquad 6.41$$

Thus all of the torque developed in the armature is expended in accelerating the rotor. From Eq. 6.41, the initial slope of the speed-time curve is

$$\Delta\nu_o/\Delta t_o = K_a\ \phi i_a/J \qquad 6.42$$

and

$$\Delta\nu_o = \Delta t\ K_a\ \phi i_a/J \qquad 6.43$$

At the end of the first interval of time the finite velocity is

$$\nu_1 = 0 + \Delta\nu_o \qquad 6.44$$

The generated voltage term in Eq. 6.39 becomes a finite value. Hence the new equation at the end of Δt_o is

$$E_a = K_a\phi\ \nu_1 + r_a i'_a \qquad 6.45$$

from which

$$i'_a = (E_a - K_a\phi\ \nu_1)/r_a \qquad 6.46$$

which is smaller than i_a.

If the inductance of the armature L_a is now included, Eq. 6.46 would be

$$i'_a = \frac{E_a - K_a\phi\, \nu_1 - L_a \frac{\Delta i_a}{\Delta t}}{r_a} \qquad 6.47$$

and the actual value of i'_a at this instant would be less than that calculated from Eq. 6.46.

The next increment of time, by similarity to Eq. 6.42,

$$\Delta\nu_1/\Delta t = K_a\phi\, i'_a/J \qquad 6.48$$

and

$$\Delta\nu_1 = K_a\, \phi\, i'_a\, \Delta t_1/J \qquad 6.49$$

hence, $\Delta\nu_1/\Delta t_1 < \Delta\nu_o/\Delta t_o$ and if the effect L_a is included the actual value of $\Delta\nu_1/\Delta t_1$ will be less than that calculated from Eq. 6.48.

At the end of the second period of time the velocity is

$$\nu_2 = \nu_1 + \Delta\nu_1 \qquad 6.50$$

Eq. 6.45 now becomes

$$E_a = K_a\phi\, \nu_2 + r_a i''_a \qquad 6.51$$

From which

$$i''_a = (E_a - K_a\phi\, \nu_2)/r_a \qquad 6.52$$

and this value of current is less than i'_a, because $\nu_2 > \nu_1$. Thus

$$i''_a < i'_a < i_a$$

From Eq. 6.43 and 6.49

$$\Delta\nu_2 < \Delta\nu_1 < \Delta\nu_o$$

The speed-time build-up and the current-time decay are plotted in Fig. 6.9. Also indicated on the curve is the effect of including the inductance.

6.5 Steady State Load on DC Motor

Equation 6.37 and 6.38 are repeated below

$$E_a = K_a\phi\, \nu + L_a\, di_a/dt + r_a i_a$$

and

$$T_L = K_a\phi\, i_a - J\, d\nu/dt - T_w$$

Let the motor be operating at constant speed, constant excitation and no load. Under these conditions, $L_a\ di_a/dt$ and $J\ d\nu/dt = 0$, hence

$$E_a = K_a\phi\nu + r_a i_a \qquad 6.53$$

and

$$i_a = E_a - K_a\phi\nu/r_a \qquad 6.54$$

also

$$T_L = K_a\phi i_a - T_w \qquad 6.55$$

from which

$$i_a = T_w/K_a\phi \qquad 6.56$$

Equations 6.54 and 6.56 show that the speed is such that the difference between the applied voltage E_a and generated voltage $E_g = K\ \phi\ \nu$ is just enough to allow a current to flow to balance the torque necessary to supply the losses (friction and windage).

In block diagram form equation 6.54 is represented in Fig. 6.10. The non-linear curve shown is the speed-torque curve for the motor.

Thus, like the transformer, the motor has self adjusting phenomenon which acts as a valve to control the flow of current into the motor. The only way in which more current can flow into the motor when load is added is by a drop in speed (with line voltage and flux assumed constant).

When the motor is supplying a constant load, Eq. 6.55 becomes, with $Jd\nu/dt = 0$

$$T_L = K_a\phi i_a - T_w \qquad 6.57$$

or

$$i_a = (T_L - T_w)/K_a\phi = T/K_a\phi \qquad 6.58$$

Where $T = T_L + T_w$

Combining equations 6.54 and 6.58 we get

$$i_a = (E_a - K_a\phi\ \nu)/r_a = T/K_a\phi$$

and

$$= E_a/K_a\phi - Tr_a/\ (K_a\phi)^2 \qquad 6.59$$

Eq. 6.59 is represented by the block diagram of Fig. 6.11. From 6.59 it is

obvious that the speed drops as the torque is increased.

6.6 Sudden Application of Constant Load

The incremental analysis is useful in understanding and predicting the torque-speed transient due to a sudden load.

Equations 6.37 and 6.38 are repeated again for convenience

$$E_a = K_a\phi\, \nu + L_a\, di_a/dt + r_a i_a$$

$$T_L = K_a\phi\, i_a - J\, d\nu/dt - T_w$$

Assume the motor is operating at a constant speed, constant line voltage, constant excitation, at no-load, and that L_a may be temporarily neglected. At $t = 0$; $L_a\, di_a/dt = 0$; $T_L = 0$; and $J\, d\nu/dt = 0$. Then

$$E_a = K_a\phi\nu + r_a i_a \qquad 6.60$$

and

$$K_a\phi i_a - T_w = 0 \qquad 6.61$$

Now let the load of T_L be applied at $t = 0$. At $t = 0+$ no additional current has been able to flow into the motor. Hence all of the added torque must be supplied by a slowing down of the rotating mass of the motor rotor. Thus at $t = 0+$

$$T_L = K_a\phi i_a - J\, \Delta\nu/\Delta t - T_w$$

and since $K_a\phi i_a$ just balanced T_w before the load was added, we can state that

$$T_L = -\, J\, \Delta\nu/\Delta t \qquad 6.62$$

or

$$\Delta\nu/\Delta t = -\, T_L/J \qquad 6.63$$

This is the initial slope of the drop in speed curve. Assuming a unit of time for Δt we can determine $\Delta\nu$. Thus

$$\Delta\nu = -\, \Delta t\, T_L/J \qquad 6.64$$

When $t = 0 + \Delta t$, equation 6.60 becomes,

$$E_a = K_a\phi\, (\nu - \Delta\nu) + r_a\, (i_a + \Delta i_a) \qquad 6.65$$

$$E_a = K_a\phi\nu - K_a\phi\Delta\nu + r_a i_a + r_a \Delta i_a$$

$$\Delta i_a = (E_a - K_a\phi\nu)/r_a - i_a + (K_a\phi\Delta\nu)/r_a \qquad 6.66$$

From 6.60

$$i_a = (E_a - K_a\phi\nu)/r_a \qquad 6.67$$

Substituting 6.67 in 6.66

$$\Delta i_a = i_a - i_a + K_a\phi\Delta\nu/r_a \qquad 6.68$$

or

$$\Delta i_a = K_a\phi\Delta\nu/r_a$$

The new current

$$i'_a = i_a + \Delta i_a \qquad 6.69$$

The new torque equation becomes,

$$T_L = K_a\phi\, i'_a - J\,\Delta\nu_1/\Delta t \qquad 6.70$$

$$\Delta\nu_1/\Delta t = -T_L/J + K\phi\, i'_a/J \qquad 6.71$$

and

$$\Delta\nu_1 = \Delta t\,(-T_L/J + K\phi\, i'_a/J) \qquad 6.72$$

Hence

$$\Delta\nu' < \Delta\nu$$

Likewise

$$\Delta i'_a = K_a\phi\Delta\nu_1/r_a < \Delta i_a \qquad 6.73$$

The incremental process can be repeated and each time $\Delta\nu$ and Δi will be less than the preceding value. Thus the curve becomes an exponential decay of speed and an exponential increase in current is illustrated in Fig. 6.12.

This discussion is based on the assumption of stable non-oscillatory condition. It is quite likely that a sudden application of load may cause some speed oscillations because of overshooting of the rotor due to its inertia. This analysis is valid for the understanding of the general shape of the current and speed curves.

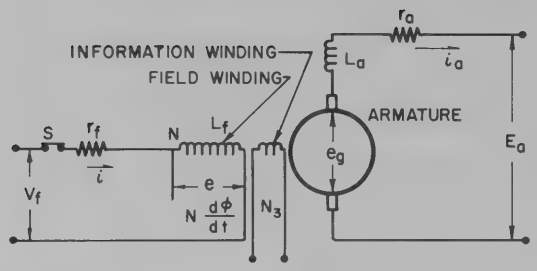

Fig. 6.1 Field and armature circuits for a dc machine showing the location of information winding.

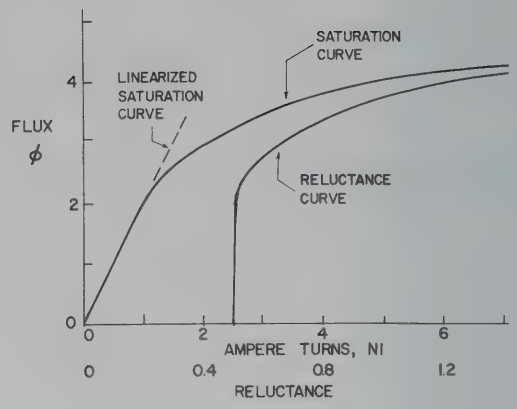

Fig. 6.2 Saturation and reluctance curves for a magnetic material.

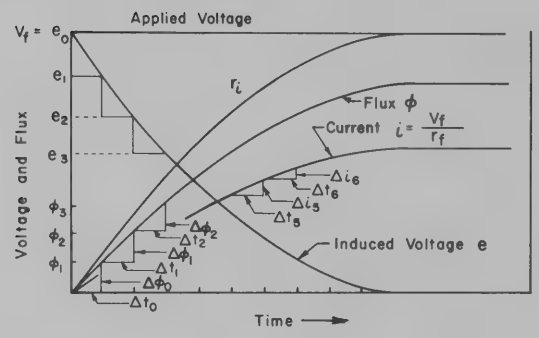

Fig. 6.3 Predicted build-up curves of current and flux in a field winding.

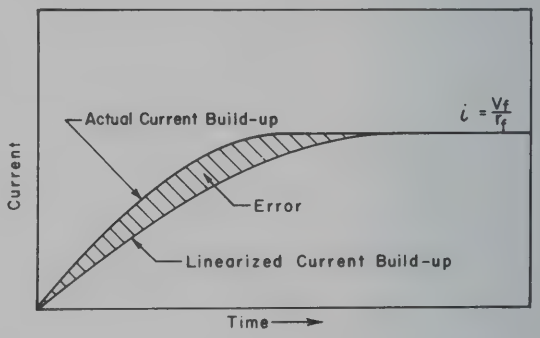

Fig. 6.4 Comparison of current build-up curve by linear and non-linear analysis.

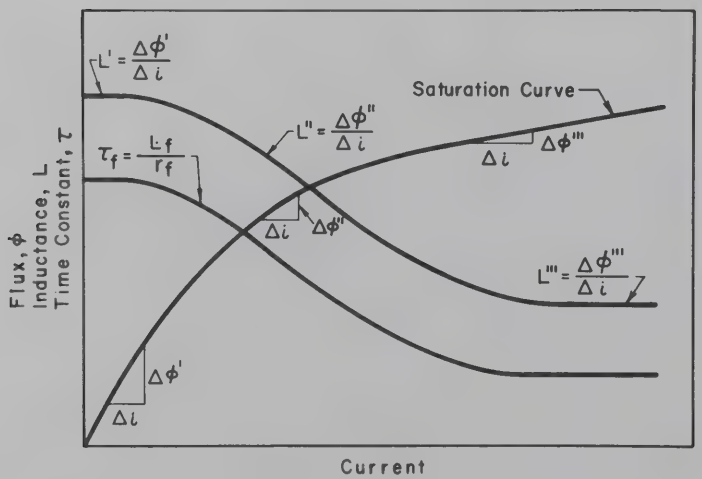

Fig. 6.5 Non-linear shapes of inductance and time constant curves.

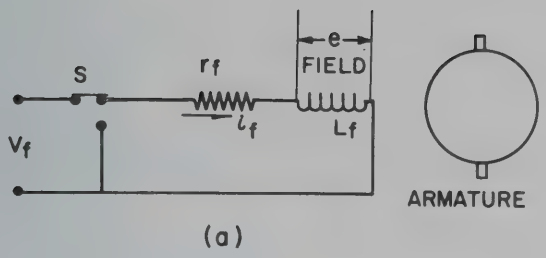

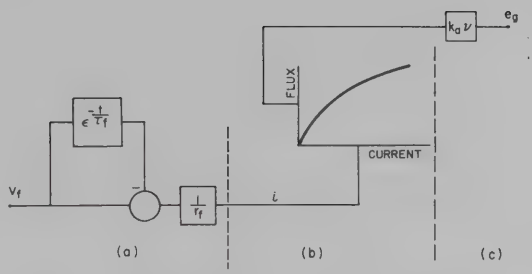

Fig. 6.7 Block diagram for dc generator.

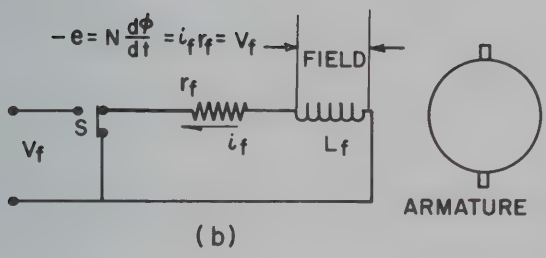

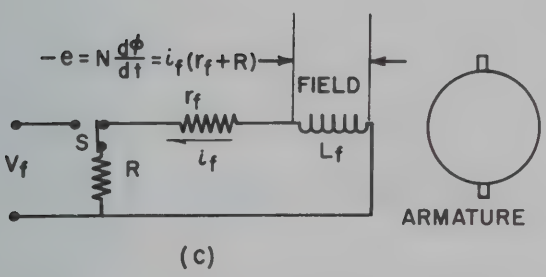

Fig. 6.6 Induced voltage caused by opening the field switch S under different situations.

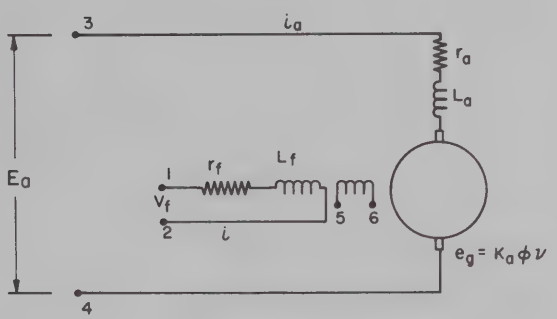

Fig. 6.8 The separately excited dc motor.

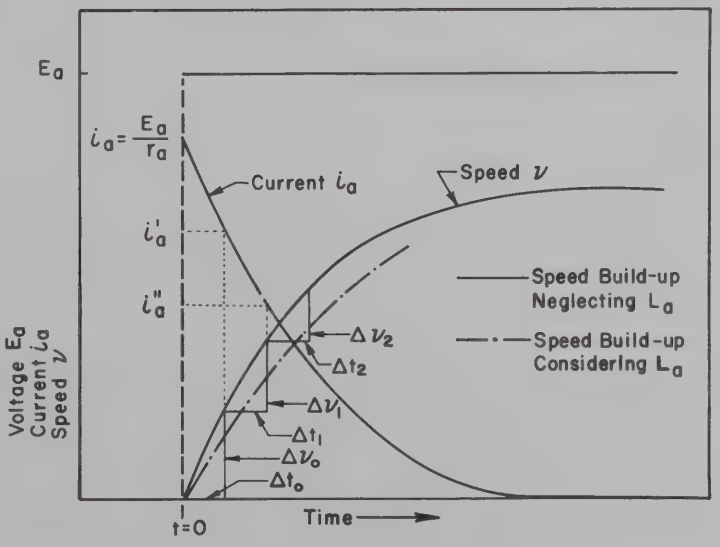

Fig. 6.9 General shape of the build-up curve for speed.

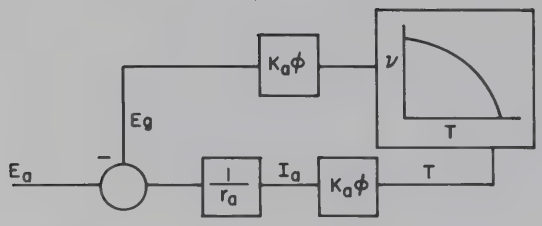

Fig. 6.10 Block diagram for dc motor.

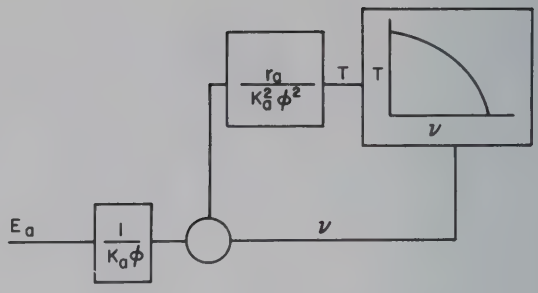

Fig. 6.11 Block diagram for motor speed.

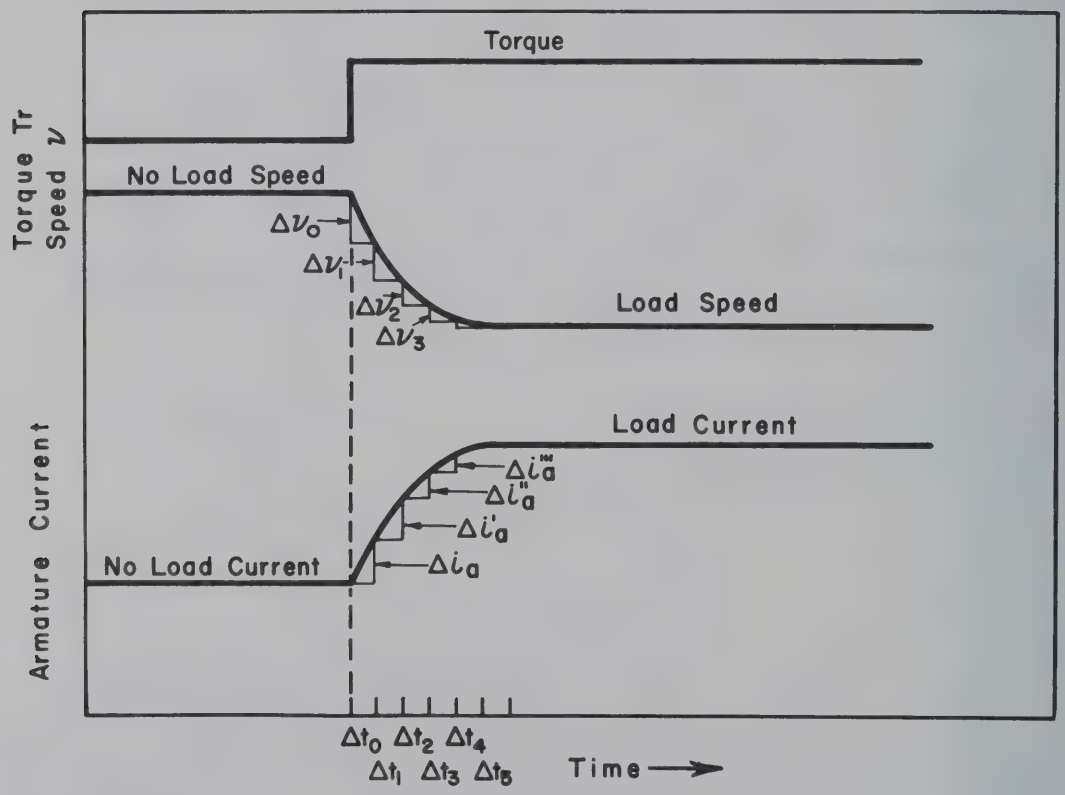

Fig. 6.12 Predicted changes in torque and current caused by a sudden application of load.

U.S. Textbooks used in a one semester, 3 credits course on electrical machines:

Electromagnetic and Electromechanical Machines, L. W. Matsch, Intext Educational Publishers, Scranton, Pa., 1972.

Electric Machinery, Third edition, A. E. Fitzgerald, Chas. Kingsley, A. Kusko, Mc Graw Hill Book Co., New York, N.Y., 1971.

Magneto Electric Devices, G. R. Slemon, John Wiley and Sons, New York, N.Y., 1966.

D-C and A-C Machines, Based on Fundamental Laws, M. Liwschitz-Garik, R. T. Weil, D. Van Nostrand Co., New York, N.Y., 1952.

Alternating-Current Machines, Third edition, A. F. Puchstein, T. C. Lloyd, A. G. Conrad, John Wiley and Sons, New York, N.Y., 1954.

A classic in laboratory engineering:

Experimental Electrical Engineering, Vols. I and II, Fourth edition, V. Karapetoff, B. C. Denison, John Wiley and Sons, New York, N.Y., 1941.